1995-09-01

Cloning and Cell Cycle Analysis of NuMA, a Phosphoprotein That Oscillates Between the Nucleus and the Mitotic Spindle

Cynthia A. Sparks
University of Massachusetts Medical School

CLONING AND CELL CYCLE ANALYSIS OF NUMA, A PHOSPHOPROTEIN THAT OSCILLATES BETWEEN THE NUCLEUS AND THE MITOTIC SPINDLE

A Dissertation

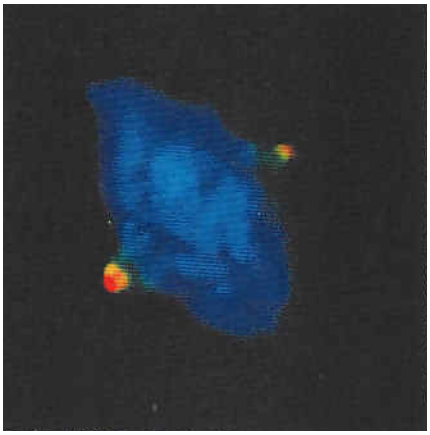

Presented to the Faculty of the University of Massachusetts Graduate School of Biomedical Sciences

in partial fulfillment of the requirements for

the Degree of

DOCTOR OF PHILOSOPHY IN CELL BIOLOGY

by

Cynthia Ann Sparks

September 1995

CLONING AND CELL CYCLE ANALYSIS OF NUMA, A PHOSPHOPROTEIN THAT OSCILLATES BETWEEN THE NUCLEUS AND THE MITOTIC SPINDLE

A DISSERTATION PRESENTED BY

CYNTHIA A. SPARKS

Approved as to style and content by:

Jeanne B. Lawrence	Chairperson of Committee Co-Dissertation Advisor
Sandy C. Marks	Member of Committee
Yicktung T. Ip	Member of Committee
Robert S. Lahue	Member of Committee
Michael Snyder	Member of Committee

Edward G. Fey	Dissertation Advisor
Thomas B. Miller	Dean of Graduate School of Biomedical Sciences

Department of Cell Biology
September 1995

COPYRIGHT NOTICE

Parts of this dissertation have appeared in separate publications:

1. Sparks, C.A., C.A. Vidair, and S.J. Doxsey. (1995) Centrosome assembly: Role of Pericentrin. Manuscript in preparation.

2. Sparks, C.A., E.G. Fey, C.A. Vidair, and S.J. Doxsey (1995) Phosphorylation of NuMA occurs during nuclear breakdown and not mitotic spindle assembly. J.Cell Sci. In press.

3. Bangs, P.L., C.A. Sparks, P.O. Odgren, and E.G. Fey. (1995) The product of the oncogene-activating gene TPR is a phosphorylated protein of the nuclear pore complex. J. Cell Biochem. In press.

4. Sparks, C.A., P.L. Bangs, G.P. McNeil, J.B. Lawrence, and E.G. Fey (1993) Assignment of the Nuclear Mitotic Apparatus Protein NuMA Gene to Human Chromosome 11q13. Genomics 17: 222-224.

5. Fey, E.G., P. Bangs, C. Sparks, and P. Odgren (1991) The nuclear matrix: defining structural and functional roles. Crit.Rev.in Euk.Gene Exp. 1:127-143.

Dedication

This dissertation and the years that are represented in this work are dedicated to Trish Lutke, my closest and dearest friend, without whom this achievement would not have been realized.

ACKNOWLEDGMENTS

I would like to begin my acknowledgments by thanking the members of my advisory committee: Drs. Jeanne B. Lawrence, Edward Fey, Rob Singer, Janet Stein, Sandy Marks, Tony Ip and Bob Lahue for their suggestions in my thesis work. By far, my sincerest gratitude goes to Dr. Jeanne B. Lawrence, my chairperson and co-advisor. Jeanne was the first scientist that I had ever met and I have met no better. The fact that she is also a woman, a mother and a wife made her destined to be my role model. The most important gift that Jeanne has given me is the restoration of my belief that one can succeed in science while holding to the highest levels of integrity in the face of every conceivable adversity. Jeanne, I thank you for renewing this in me.

I am greatly indebted to my fellow graduate student, Peter Bangs, for his support and friendship as well as contributions to my thesis work. Peter is now and will always be one of my closest friends. We worked together as well as any two people can. I can not imagine a time when I will be working without him nearby to offer advice or make me laugh, although I guess that time will come. Peter never let me be intellectually lazy and always taught as he went along. It was a privilege to be a recipient to this kind of attention. Peter also convinced me that there is never a good reason to be unkind to another person, a standard of living that I will always try to uphold in my own life. Much thanks to you, Peter.

I had the great fortune to collaborate with Dr. Stephen J. Doxsey. In the end, he became my mentor. I would like to express my utmost appreciation for his time and patience in training me as a scientist and a critical thinker. Steve was solely responsible for encouraging my interests in Cell Biology and securing my scientific ardor. It was a turning point in my career and my life. I will be forever grateful. Steve was the first scientist to demonstrate a confidence in me that, in turn, gave me greater confidence in

myself. He taught me to speak and write in a professional manner, an often thankless job. He taught me to work everyday with a critical eye. Your experiment is only as good as your controls. I can say this in my sleep. At the end of a thesis, students are often asked if they would choose the same mentor. Without hesitation, I would. His unbridled enthusiasm is contagious and working with him has made it all worthwhile.

I would like to end the acknowledgments with expressing my sincerest thanks to my friends and family, whose support and love made this work endurable if not pleasurable.

ABSTRACT

CLONING AND CELL CYCLE ANALYSIS OF NUMA, A PHOSPHOPROTEIN THAT OSCILLATES BETWEEN THE NUCLEUS AND THE MITOTIC SPINDLE

Cynthia A. Sparks

University of Massachusetts Graduate School
of Biomedical Sciences
1995

The overall objective of this study was to identify novel proteins of the nuclear matrix in order to contribute to a better understanding of nuclear structure and organization. To accomplish this, a monoclonal antibody specific for the nuclear matrix was used to screen a human λgt11 expression library. Several cDNAs were isolated, cloned, sequenced, and shown to represent NuMA, the nuclear mitotic spindle apparatus protein. Further characterization of the gene and RNA was undertaken in an effort to obtain information about NuMA. The NuMA gene was present at a single site on human chromosome 11q13. Northern and PCR analysis of NuMA mRNA showed a major 7.2 kb transcript and minor forms of 8.0 and 3.0 kb. The minor forms were shown to be alternatively spliced although their functional significance is not yet understood. Immunofluorescence microscopy demonstrated that NuMA oscillates between the nucleus and the microtubule spindle apparatus during the mitotic cell cycle. NuMA appeared as a 200-275 kDa protein detectable in all mammalian cells except human neutrophils. To determine whether NuMA's changes in intracellular distribution correlated with post-translational modifications, the protein's phosphorylation state was examined through the cell cycle using highly synchronized cells. NuMA was a phosphoprotein in interphase and underwent additional phosphorylation events in mitosis. The mitotic phosphorylation events occurred with similar timing to lamin B (G_2/M transition) and were concomitant with NuMA's release from the nucleus and its association with the mitotic spindle. However, the mitotic phosphorylation occurred in the absence of spindle formation. Dephosphorylation of NuMA did not correlate with reassociation with the nuclear matrix but occurred in two distinct steps after nuclear reformation. Based on the timing of these events, phosphorylation may play a role in nuclear processes. In conclusion, the work in this dissertation identified NuMA, a nuclear matrix protein and showed that it is phosphorylated during the cell cycle and may be important for nuclear events such as nuclear organization, transcription, or initiation of DNA replication at G_1/S.

TABLE OF CONTENTS

LIST OF FIGURES

LIST OF FIGURES - CONT. PAGE

LIST OF TABLES

LIST OF ABBREVIATIONS

bp, base pairs

BSA, Bovine serum albumin

^{o}C, degrees Celsius

CHEF, Chinese hamster embryonic fibroblasts

CHO, Chinese hamster ovary

CSK, cytoskeletal buffer

DAPI, 4'-6 diamidino-2-phenylindole

DMEM, Dulbecco's minimal essential media

DNA, deoxyribonucleic acid

cDNA, complementary DNA

EDTA, disodium ethylene diaminetetracetic acid

EGTA, ethylene glycol-bis(β-aminoethyl ether)N, N, N', N'-tetracetic acid

FITC, fluorescein isothiocyanate

FBS, fetal bovine serum

HEPES, N'-2-hydroxyethylpiperazine-N'-ethanesulfonic acid

hnRNA, heterogeneous nuclear RNA

HSTF1, oncogene for FGF-related factor 4

INT2, oncogene for FGF-related factor 3

kb, kilobase

kDa, kilodalton

MARs, matrix attachment regions

MPF, maturation promoting factor

NM, nuclear matrix

nm, nanometer

NuMA, nuclear mitotic spindle apparatus

NP-40, nonidet P-40

PAGE, polyacrylamide gel electrophoresis

PCR, polymerase chain reaction

PBS, phosphate buffered saline (pH 7.4)

PMSF, Phenyl methyl sulfonyl fluoride

RNA, ribonucleic acid

mRNA, messenger RNA

RNP, ribonucleoprotein particle

rt-PCR, reverse transcriptase PCR

SDS, sodium dodecyl sulfate

SP-H, human autoantigen identified to be NuMA

SP-N, spindle-pole nucleus

SSC, sodium citrate, sodium chloride

TBE, Tris borate EDTA

TBS, Tris buffered saline

TPR, translocated promoter region

UCSF, University of California, San Franscico

ug, microgram

CHAPTER 1

INTRODUCTION

A. Specific Aims

The overall objective of this dissertation was to contribute to our understanding of the nuclear matrix. This study was based on the fundamental principle that structure is important for biological function. For example, the specialized architecture of the nuclear matrix may affect the highly regulated and essential functions of the mammalian nucleus. The goal of this work was to identify and analyze a specific nuclear matrix protein component. When the identity of the nuclear matrix protein examined in this study was revealed to be NuMA, the overall objectives were expanded to encompass the role of this protein in another highly specialized structure, the mitotic spindle. The specific goals of this study were:

1. To identify the protein that reacts with a nuclear matrix antibody by isolating cDNAs and obtaining sequence information
2. To obtain information about the gene and mRNA including:
    - -Characterize the gene for size and complexity
    - -Map the position of this novel gene in the human genome
    - -Characterize the mRNA in terms of size and relative abundance
    - -Identify mRNA isoforms
3. To obtain information about the protein including:
    - -Characterize the subcellular distribution through the cell cycle
    - -Determine the size and complexity of the protein
    - -Determine if the protein is phosphorylated

4. To obtain specific information about the protein through the cell cycle that may relate to its function including:

-Changes in subcellular localization

-Changes in phosphorylation state

-Changes in solubility

The objectives of this dissertation are best appreciated after examining what is known about the nuclear matrix, NuMA, and mitosis. The next three sections respectively will review these areas of investigation.

B. The nuclear matrix.

The nuclear matrix is defined as a fibrillogranular network including the nuclear lamina and an interior protein scaffold that resists extraction with detergents, digestion with nucleases, and extraction with elevated ionic strength [1-9]. The nuclear matrix was first described by Berezney and Coffey [1, 10] as the residual nuclear structure in rat liver cells remaining after sequential extraction with non-ionic detergents, digestion with DNase I, and extraction with 2 M NaCl. These extractions removed most proteins, lipids, and nucleic acids, yet from examination at the level of the electron microscope, the remaining structure retained the original nuclear shape and size characteristics. Further investigations supported these observations although methodologies varied and structures were assigned a variety of names (nuclear scaffold - [11], nucleoskeleton - [12]). Nevertheless, these nuclear substructures contained essentially the same components: the nuclear lamina, the nuclear pore proteins, and an intranuclear fibrillogranular network composed of protein and RNA (Figure 1, [6]). The structures and their variations have been reviewed [13-16].

FIG 1. Nuclear matrix electron micrograph. Nuclear matrix observed using resinless electron microscopy. (a) The nuclear matrix-intermediate filament scaffold is imaged as a whole mount. (b) When the interior of the nuclear matrix is examined under conditions that preserve hnRNA, the RNP-containing nuclear matrix is shown to be a network of filaments. Taken from Fey et al. J. Cell Biol. 102:1654 (1986).

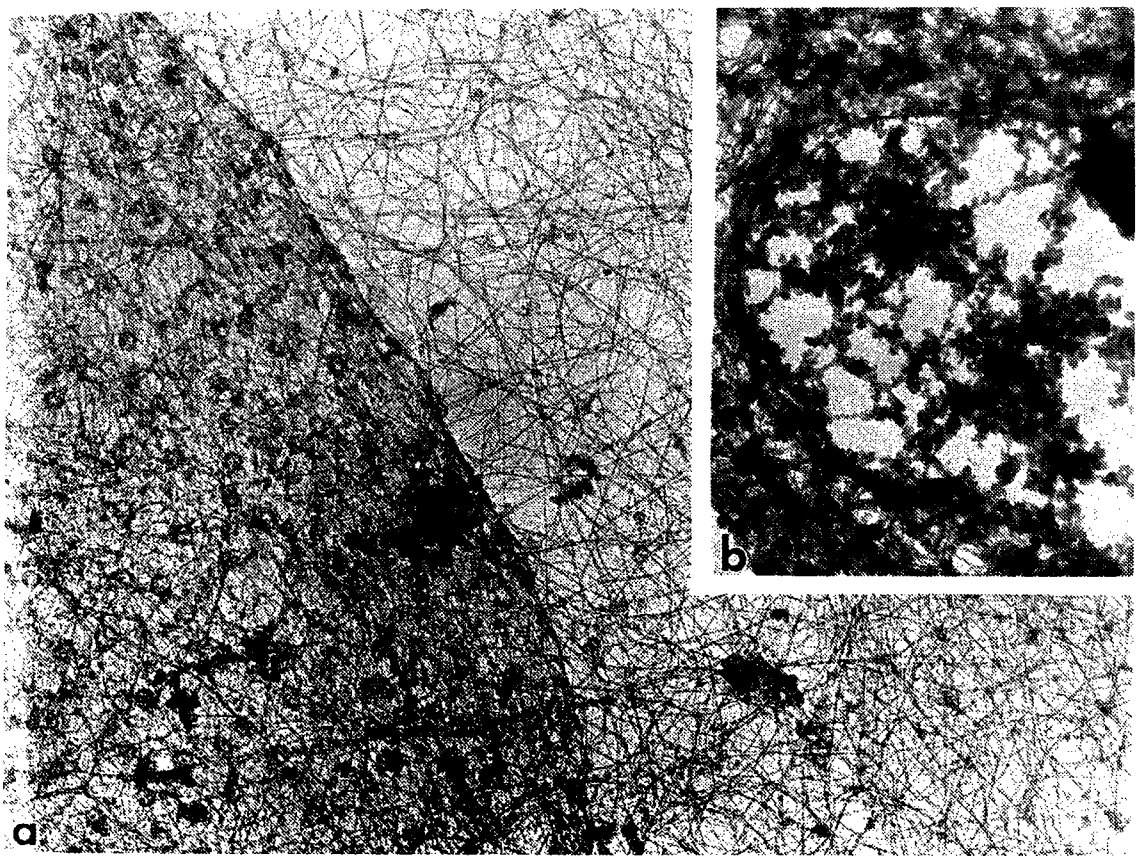
a
b

Extensive studies have suggested roles for the nuclear matrix in nuclear functions. Most of these studies demonstrated association of particular molecules or biological activities with the nuclear matrix. The role of the nuclear matrix in the function of these molecules or activities was then hypothesized based on a physical association. These investigations have indicated a variety of roles for the nuclear matrix in nuclear functions, reviewed in [13-19]. The nuclear matrix appeared to be a site for binding DNA via matrix attachment regions (MAR) to loops of DNA [11, 20]. The sites for DNA replication were found in association with the nuclear matrix [21-26]. HnRNA was associated with the nuclear matrix [5, 6, 27, 28], and the matrix acted as a site for the efficient splicing of mRNA [29]. These results were somewhat controversial. One report had most of the active RNA polymerase associated with the nucleoskeleton [12] while another report had contradictory results [30]. It is possible that the harsh treatment used to isolate the nuclear matrix (such as high salt extraction) caused artifactual association of some molecules [17, 31].

Despite a number of studies indicating a relationship between the nuclear matrix and nuclear functions, the significance of this relationship remains in question. Advances are hampered by the nebulous definition of the nuclear matrix based on isolation procedures. The field would benefit greatly by approaching the functions of the nuclear matrix at the molecular level. The proteins and RNAs that comprise the nuclear matrix need to be identified and evaluated for direct roles in nuclear processes, perhaps based on interactions with nuclear compartments such as DNA replication sites or splicing domains. One of the difficulties in studying these proteins is their relatively low abundance. The lamins and nuclear pore proteins comprise more than half of the total nuclear matrix proteins [1]. The remaining components of the interior matrix are present in low abundance making standard biochemical techniques problematic.

Monoclonal and polyclonal antibodies to nuclear matrix proteins have been developed at Matritech, Inc (Cambridge, MA). One of the monoclonal antibodies, 204.41, was the initial tool used to identify a novel nuclear matrix protein. It was the fundamental goal of this dissertation to identify a nuclear matrix protein and provide information about its relationship to the nucleus and nuclear function. The nuclear matrix protein identified in this study was NuMA.

C. NuMA

NuMA was first identified in 1980 by Lydersen and Pettijohn using antisera raised against HeLa cell non-histone chromosome proteins [32] and was characterized in several subsequent studies [33-36]. It was found to be a single 240 kDa protein in human cells but also was present in many other species [34, 37]. By analyzing cells at different stages of the cell cycle by immunofluorescence microscopy, NuMA appeared as granular staining in the nucleus at interphase, associated with the spindle poles at metaphase, and returned to the reforming nucleus in telophase (For a review, see [38])[32, 34, 37 , 39-43], and this study) regardless of the fixation method used [39]. In many of the earlier studies, this protein was described using different names (centrophilin [39], SPN [37], SPH [40]). Immunofluorescence experiments with metaphase chromosomes suggested that NuMA may associate with centromeres, although not consistently from experiment to experiment [34, 36, 39, 44].

NuMA is a highly antigenic protein [45] as evidenced by its ability to illicit an immune response when prepared from fractions as varied as kinetochores [39], crude nuclear preparations [37], nuclear matrix protein preparations (this study), non-histone chromosome proteins [32], chromosome scaffolds [41], and epithelial cell nuclei [43].

Interestingly, some patients with autoimmune diseases have antibodies directed against the NuMA protein [33, 40, 42, 46]. The full length cDNA has been cloned by several groups [42-45], and the amino acid sequence predicts a large coiled-coil protein flanked by non-coiled ends [42].

Northern analysis revealed a 7.2 kb mRNA and at least two other minor RNA isoforms (this study, [43]). Overexpression of the protein encoded by the minor mRNA isoforms in mammalian cells showed localization of the protein to the centrosome [47]. A different study proposed that NuMA isoforms may participate in organization of pre-mRNA splicing domains based on data obtained with a specific antibody [48]. The nuclear localization signal was found in the C-terminus of the protein [45, 47, 49], specifically at amino acid residues 1972-2007 [47]. A larger region was found to be responsible for spindle localization, at amino acid residues 1516-1667 by expression studies with NuMA deletion constructs [47].

The function of NuMA is unknown. Most studies have concluded that NuMA may have a role in stabilizing the mitotic spindle. These results have been summarized in Table 1. It is known that intact microtubules are required for NuMA's spindle association. Treatment with microtubule depolymerizing agents such as nocodazole disrupts the spindle and NuMA disperses throughout the cell, see Figure 21 [32, 37, 39]. If you wash away the drug, NuMA will concentrate at the microtubule nucleation sites [39]. Taxol-induced microtubule asters contain NuMA at the minus end of the microtubules [40, 50]. NuMA will co-sediment with purified microtubules in vitro [40, 50]. Thus, there appears to be a physical relationship between NuMA and spindle microtubules.

TABLE 1 - Summary of NuMA Studies. Various features and functions of NuMA are summarized with experimental procedures used and references to which groups did each study to date.

Table 1 - Summary of NuMA Studies

NuMA Feature	Based on	Ref.
1. Cloned and sequenced		[42-45], this study
2. Forms α-helical coiled-coil	Prediction from cDNA sequence	[42, 45]
3. NuMA RNA is alternatively spliced	Cloning and PCR analyses	[43], this study
4. Single protein > 200 kDa	Western blot	[34, 37, 39, 40, 42-45, 51, 52], this study
5. Two forms of protein	Western blot	[39, 48]
6. NuMA is a phosphoprotein	ortho-phosphate labeling and immunoprecipitation	[34, 53], this study
7. Binds microtubules	Co-sedimentation with purified microtubules	[37, 40]
8. Localization to centers of taxol asters	Immunofluorescence microscopy	[39, 40, 50]
9. Cell cycle-dependent localization	Immunofluorescence microscopy	[32, 34, 37, 39, 40, 42-44, 50], this study
	Electron microscopy	[39, 54]
10. Microtubule-dependent localization at mitosis	Immunofluorescence microscopy after depolymerization with drugs	[32, 39, 40, 50] this study
11. Centrosome localization	Expression studies with cDNA constructs	[47]
	Immunofluorescence microscopy	[39], this study
12. NuMA is an autoantigen	Immunofluorescence microscopy	[33, 40, 42]

TABLE 1 - CONT.

13. Component of nuclear matrix	Biochemical fractionation	[32, 37, 54], this study
14. Nuclear localization sequence in c-terminus	Expression studies with cDNA constructs	[43, 45, 49]
15. Spindle binding domain in c-terminus	Expression studies with cDNA constructs	[43, 45, 49]
16. Role in spindle assembly/stability	Micronucleation result of:	
	-Overexpression of n-terminus deleted construct	[49]
	-Overexpression of c-terminus deleted construct	[49]
	-RCC1 mutation rescued by NuMA full-length	[49]
	-antibody microinjection	[37, 52]
	Spindle malformation	
	-antibody microinjection	[37, 51, 52]
17. Role in nuclear reformation	Antibody microinjection	[34, 44]
18. No role in nuclear reformation	Antibody microinjection of anaphase cells	[51]

NuMA may also have a functional relationship with the mitotic spindle. In contrast, it has also been suggested that there may be no function for NuMA at the spindle except to redistribute the protein efficiently to each daughter cell [41]. NuMA antibody microinjection studies resulted in blocking the formation of or collapse of the spindle apparatus [34, 37, 51] and concluded that NuMA is required for spindle integrity in the early phases of the mitotic cell cycle. Another result showed that microinjection of a monoclonal antibody could reverse taxol-induced aster formation in Ptk2 cells. Non-taxol treated cells in this study had normal mitoses but formed micronuclei after completing mitosis [52]. A study using a polyclonal antibody microinjected into cells entering early mitotic stages showed that these cells were unable to form a spindle, but in later stages (anaphase or beyond), the antibody had no effect on cells [51]. These and other functional studies have been summarized in a recent review [38]. From these studies, it appears that NuMA may have a role in the formation and stability of the mitotic spindle.

Examination of NuMA's distribution through the cell cycle shows that NuMA leaves the spindle poles in late anaphase/early telophase when the nucleus reforms leading to a second hypothesis that NuMA may play a role in this process [34]. In support of this, microinjection studies have often resulted in the formation of micronuclei, a phenotype that some groups have characterized as a nuclear reformation defect [44, 49, 52]. Overexpression of truncated forms of NuMA lacking the n- or c-terminal globular domains also resulted in this phenotype [49]. One study showed that overexpressed human NuMA can rescue the micronucleation phenotype induced in the hamster cell line tsBN2 carrying a mutation in the nuclear chromosomal binding protein RCC1 [49]. Together with the knowledge that NuMA is a nuclear matrix

protein (see below), these studies indicate that NuMA may have a role in nuclear reformation.

NuMA is a component of the nuclear matrix (this study, [32 , 37, 41]). NuMA appears to be a component of the fibers that form the core filament/network of the nucleus, as shown by immuno-gold electron microscopy [54]. This localization of NuMA in the fibrillogranular network complements the functional data suggesting a role in stabilizing the nucleus and mitotic spindle. Some important questions remaining from these observations include how NuMA contributes to the stabilization of these structures and the identity of the proteins or RNAs that interact with NuMA. In addition, the mechanism for NuMA's movement between the nucleus and spindle is not understood.

D. Mitosis and the Spindle

The process of cell division can be broken into 6 linear stages applicable to eucaryotic organisms: prophase, prometaphase, metaphase, anaphase, telophase, and cytokinesis (an exception to the linear arrangement, cytokinesis overlaps with anaphase and telophase). These stages together are termed *mitosis* (see reviews [55, 56]). This process ensures that all proteins, RNA, and DNA are properly segregated into each daughter cell. At mitosis, there is a dramatic rearrangement of cellular components such as the cytoplasmic microtubules, which reorganize to form the mitotic spindle apparatus. This microtubule reorganization is largely due to the centrosome, the principal microtubule organizing center of the cell, which duplicates and separates to opposite poles by prometaphase. At mitosis, biological activities are altered such as protein synthesis drops to approximately 25%, and RNA synthesis stops.

The mitotic spindle is the machinery responsible for the segregation of chromosomes. At prophase, the duplicate chromosomes condense, and various types of microtubules begin assembling the spindle. In higher eucaryotes, the nucleus and nuclear envelope break down at prometaphase, allowing the spindle microtubules to capture the chromosomes and align them to form a "metaphase plate". At anaphase, sister chromatids separate and move via molecular motors along the microtubules to the poles. At telophase, the nuclear envelope begins to reform around the chromosomes which decondense, and the nucleus assembles [57].

Segregation of cellular components occurs in many ways. Many organelles are divided into each cell by simply doubling in amount or breaking up into vesicles and associating with the mitotic spindle. The association with the spindle may guarantee equal distribution into daughter cells. Segregation of nuclear matrix proteins may occur using several different pathways. Some nuclear matrix proteins have been observed in the structures of mitotic chromosomes [58], whereas NuMA appears to be segregated by association with the spindle pole [44].

Entry of eucaryotic cells into mitosis is regulated by a cascade of kinase activities. Phosphorylation of MPF, a complex of cyclin B and cdc2 kinase, initiates mitosis (see [59]). Activation of cdc2 kinase by binding to cyclin B is followed by initiation of nuclear envelope breakdown and DNA condensation. As cells enter telophase, the final stage of mitosis, nuclear reformation is accompanied by degradation of cyclin B, deactivation of MPF, and dephosphorylation of many proteins. [60-64]. Several substrates for cdc2 have been proposed, of which lamin B is the best characterized. Lamin B is phosphorylated in prophase, leading to the disassembly of the nuclear lamina. Lamin B dephosphorylation

drives its reassembly into reforming nuclei beginning in late anaphase continuing through early G_1 [65-70].

There is evidence that phosphorylation may regulate the function or localization of NuMA in the cell. A basal level of NuMA phosphorylation has been demonstrated using HeLa cells [34, 53]. NuMA from mitotic cells is also phosphorylated (this study, [53]). Analysis of the amino acid sequence of NuMA predicts over 24 phosphorylation sites for a variety of kinases [42] including four sites for cdc2 kinase, all at the C-terminus. Site-directed mutagenesis of these four sites results in failure in spindle localization and aberrant spindle formation [53]. Although NuMA is demonstrated to be a phosphoprotein in that study, a direct role for phosphorylation in the aberrant localization has not been demonstrated. This may be the result of secondary effects of the point mutations such as misfolding of the protein. Furthermore, given the basal level of phosphorylation, the regulation of NuMA may be quite complicated.

SUMMARY

In summary, the nuclear matrix is operationally defined as the fibrillogranular network that remains following sequential extraction with detergents, digestion with nucleases, and extraction with high salt. The nuclear matrix has been implicated in many nuclear processes including DNA replication, transcription, and chromatin organization. This investigation identified perhaps the first protein component unique to the interior of the nuclear matrix, NuMA. With the identity known for one nuclear matrix protein, the door has been opened to finding other components based on their interaction with NuMA. This study is only a beginning to the understanding of how the proteins of the nuclear matrix form this structure and contribute to nuclear functions.

At mitosis, NuMA redistributes from the nucleus to the spindle pole. The protein has been examined during mitosis for changes in biochemical properties. The discovery of mitosis-specific changes in NuMA phosphorylation has been pivotal in permitting one to examine how the protein is regulated in a cell cycle-specific manner and if these changes directly affect properties such as subcellular localization. To begin to answer these questions, the effects of phosphorylation on other properties of NuMA, such as solubility, were examined in this dissertation. While one study will not answer every question, it is hoped that this work will contribute to a better understanding of the mechanisms by which the cell regulates proteins participating in such complex tasks as nuclear organization and cell division. What remains to be answered by future studies includes the identity of binding partners and the identification of the signal transduction pathways involved in the cell cycle-specific regulation through defining the kinases and phosphatases acting on NuMA.

CHAPTER 2

MATERIAL AND METHODS

A. Cells, Cell lines and Tissue Culture

Chinese hamster ovary (CHO) cells, ME180 human cervical cells, HL-60 human premyeloblastic cells, NIH3T3 mouse fibroblast cells, and MCF7 human breast carcinoma cell lines (ATCC, Rockville, MD) were maintained in a 5% CO_2 incubator at 37^{o}C in Dulbecco's minimal essential media (DMEM, Gibco-BRL/Life Technologies, Gaitherburg, MD) supplemented with 10% fetal calf serum or iron-supplemented calf serum (Hyclone, Logan, UT), 50 ug/ml streptomycin, and 50 U/ml penicillin prior to use in immunofluorescence experiments, and purifications of RNA, protein, and DNA . Purified

Purified human granulocytes were generously provided by Dr. Richard Jack (Harvard University, Cambridge, MA).

B. Antibodies

Lamin B monoclonal, NuMA monoclonals 204.41, 107.7, and 302.22, NuMA polyclonal, and TPR monoclonal antibodies were obtained from Matritech Inc. (Cambridge MA). Other antibodies were obtained from the following: tubulin monoclonal antibody from Sigma Chemical (DM1α, St. Louis, MO), lamin B polyclonal antibodies from Dr. H. Worman [71], pericentrin monoclonal antibodies from Drs. S. Doxsey and J. Burkhart (UCSF), and polyclonal pericentrin antibodies from Dr. S. Doxsey [72].

C. Cloning and sequencing cDNAs

The 204.41 antibody was used to screen a λgt11 human cervical cDNA expression library (Clontech, Palo Alto, CA). Library screening was performed essentially as described in Sambrook [73]. The cDNA inserts from each clone were amplified by PCR [74] and used for mapping and sequencing experiments. Amplified DNA inserts were visualized on 1% agarose/TBE gels to determine the size of the inserts in each λgt11 clone. Double stranded PCR products were digested with a number of restriction enzymes (Boehringer Mannheim Biochemical (BMB), Indianapolis, IN), and individual clones were aligned. The cDNA sequences were obtained using a Taq polymerase sequencing system (Promega, Madison, WI) with a thermal cycler (MJ Research, Watertown, MA). Primers to the λgt11 cloning site were used to initially sequence double stranded cDNA clones. Internal restriction fragments were subcloned into pBluescript SK+ (Stratagene, LaJolla, CA). Single stranded DNA from subclones was prepared according to manufacturer's instructions and both single and double stranded clones were sequenced with pBluescript SK+/-specific primers. In some cases,

synthetic oligonucleotide primers were designed using the Oligo software (National Biosciences, Inc., Plymouth, MN) and used as sequencing primers to obtain a complete sequence of individual clones. Sequence analysis was done by searching the Genbank database using the TFASTA program [75].

D. Northern and Southern blots

ME180 total or Poly A+ RNA was isolated using cesium chloride procedures described in Sambrook [73] or using the Fastrack RNA isolation kit (Invitrogen, San Diego, CA) according to manufacturer's instructions. RNA was separated by electrophoresis in 1% agarose/formaldehyde/MOPS gels, blotted, and probed with cDNA probes radiolabeled by PCR direct incorporation or random-primed ^{32}P-dCTP incorporation using standard methods [73]. Blots were exposed to autoradiographic film for 1-21 days at -70^{o}C with an intensifying screen.

For Southern blot analysis, cDNA probes were labeled by random primed incorporation with digoxygenin dUTP. Total cellular DNA was prepared from ME180 cervical carcinoma cells, digested with a variety of restriction enzymes (BMB), separated on 0.8% agarose/TBE gels, and blotted onto nylon membranes essentially as described in Sambrook [73]. Results were visualized using the Genius system (BMB).

E. Fluorescence In Situ Hybridization

Two cDNA clones encompassing approximately 2.5 kb of the NuMA sequence at positions 3428 - 5450 [42] were used as templates for digoxygenin probe synthesis. Hybridizations were performed essentially as described by Lawrence [76]. Metaphase spreads were prepared from normal peripheral blood lymphocytes using standard

procedures and stored at -80°C. Slides were baked at 65°C for 5 hours, rinsed in 2 X SSC, and denatured in 70% formamide, 2 X SSC for 2 minutes at 70°C followed by dehydration in graded ethanol series and air drying. 50 ng of NuMA cDNAs were labeled by nick translation in the presence of digoxygenin dUTP (BMB), denatured and mixed with hybridization buffer (2:1:1:1 - 50% dextran sulfate, 10 mg/ml BSA, 20XSSC, double distilled deionized water). Labeled probe was added to the slides and incubated overnight at 37°C. Slides were washed in 2 X SSC/50% formamide for 30 minutes, 2 X SSC for 30 minutes, 1 X SSC for 30 minutes, then incubated with an anti-digoxygenin antibody conjugated directly to fluorescein or rhodamine (1:500, BMB). Slides were counterstained with DAPI to identify individual chromosomes and banding patterns. Slides were mounted in 90% glycerol, 0.1% phenyline diamine and viewed by fluorescence microscopy. Photography was done using Kodak (Rochester, NY) Ektachrome 400 slide film exposing for 1-5 minutes or with Ektar 1000 print film at 0.5-2 minute exposure times.

F. PCR Analyses

ME180 Poly A+ RNA was oligo dT-primed and reverse transcribed into cDNA using the cDNA cycle system (Invitrogen). This cDNA was used as a template in PCR reactions using a variety of primers to NuMA. Alternatively, genomic DNA was prepared as described above and analyzed with PCR and similar primers. Results were visualized on 1% agarose/TBE gels stained with ethidium bromide. Various PCR products were subcloned into pCR vectors with the TA cloning system (Invitrogen) and sequenced.

G. Immunofluorescence

Cells were grown or cytospun onto poly-l-lysine coated coverslips or at 30 x g. for 10 minutes. Coverslips were washed in PBS (137 mM NaCl, 2.7 mM KCl, 10 mm

Na_2HPO_4, 1.8 mM KH_2PO_4, pH 7.4), fixed and extracted at the same time in 3.7% formaldehyde in cytoskeletal (CSK) buffer (0.5% Triton X-100, 100 mM NaCl, 300 mM sucrose, 10 mM Pipes pH 6.8, 3 mM $MgCl_2$, 1 mM EGTA) for 15 minutes at room temperature or in -20°C methanol for 15 minutes. In some cases, cells were extracted for 5 minutes at room temperature then fixed in -20°C methanol for 15 minutes. Isolated centrosomes were prepared as previously described [72]. All subsequent steps were done at room temperature in a humid chamber. Coverslips were washed twice with PBS, and blocked in PBSAT (0.5% Bovine Serum Albumin-BSA and 0.1% Triton X-100 in PBS) for 5 minutes. Primary antibodies were diluted in PBSAT and incubated for 30 minutes. Coverslips were washed 3X in PBSAT and incubated in secondary antibodies, goat anti-mouse, rabbit, or rat conjugated to fluorescein or rhodamine (Jackson ImmunoResearch Labs, West Grove, PN) for 20 minutes. Coverslips were washed for one minute twice in PBSAT, once in PBS, once in PBS with DAPI (2 ug/ml, Sigma) to detect DNA, twice in PBS and mounted in glycerol with phenyline diamine (100 ug/ml, Sigma). Microscopy was done on an Axioplan immunofluorescence microscope (Carl Zeiss, Oberkochen, Germany) with a Photometrics 200 series CCD camera (Tuscon, Az) or an Axioscope immunofluorescence microscope (Carl Zeiss).

H. Preparation of Protein Extracts

i. Total Protein

Protein extracts were prepared from various cell lines by lysing in a modified RIPA buffer (180 mM NaCl, 1% NP-40, 0.5% Deoxycholate, 0.1% SDS, 50 mM Tris, pH 8.0) containing protease and phosphatase inhibitors (0.15 ug/ml phenyl methyl sulfonyl fluoride - (PMSF); 10 ug/ml each - aprotinin, leupeptin, chymostatin; 5 mM EDTA; 2.5 mM beta-glycerol phosphate; 100 uM sodium vanadate) for ten minutes at

4°C [77]. In some cases, phosphatase inhibitors were omitted (Figure 17A). Lysates were cleared by spinning at 50,000 x g for 5 minutes at 4°C. Relative protein concentrations were determined using a Coomassie assay (Biorad Labs, Hercules, CA) according to manufacturer's instructions with BSA as a standard. Alternatively, cells were lysed in a buffer containing 8M urea, 2% nonidet P40, and 2% β-mercaptoethanol.

ii. ^{35}S and ^{32}P labeling

CHO cells or ME180 cells were grown in T-175 cm^2 flasks, washed twice in phosphate-free DMEM with 10% dialyzed serum, and incubated for 4 hours in phosphate-free DMEM with 10% dialyzed serum and ^{32}P-orthophosphoric acid (2 mCi/ml, Dupont/NEN Boston, MA). These cells were washed twice in cold PBS, and lysed at 4°C as described above. To obtain ^{32}P-labeled mitotic cells, cultures were treated with 5 ug/ml nocodazole for 4 hours, collected by mitotic shake-off, rinsed in cold PBS, and protein extracts were prepared from them as described above. An average of 10^4-10^5 mitotic cells was obtained as determined by cell counts done on unlabeled populations of CHO cells.

iii. Synchronized Cell Extracts

Mitotic CHO cells were prepared using two methods. For most experiments described in this study, mitotic (M) cells were obtained by Dr. Charles Vidair, UCSF, using a drug-free manual shake-off protocol described in detail elsewhere [78] that typically produces populations with mitotic indices between 97-99% (data not shown). These mitotic populations were frozen and stored according to the method of Borrelli [79]. Cells frozen in this way show no significant reduction in viability following thawing and plating and progress rapidly and synchronously through the cell cycle. It should be

noted that the electrophoretic mobility of NuMA was unaffected by this procedure (Figure 23B, lane I*). A second method used to obtain mitotic cells involved arresting them at mitosis with nocodazole (5 ug/ml) for 4 hours and collecting them by shaking manually. The nocodazole-blocked (N) mitotic cells consist of >90% prometaphase cells (data not shown and [80]).

Asynchronous CHO cells were grown to 95% confluency (5 x 10^6 cells per 100 mm plate) then washed three times in PBS to remove mitotic cells leaving > 95% interphase (I) cells (see below). To obtain cells in various stages of the cell cycle, mitotic (M) cells (above) were thawed rapidly at 37^0C, gently spun through 5 ml of ice-cold PBS at 30 x g, plated into 37^0C media, and pelleted at various periods of time after release (anaphase -10 minutes, telophase -25 minutes, G_{1E}- 60 minutes, and G_{1L}- 240 minutes). 5 x 10^6 cells from each time point were pelleted and lysed in a modified RIPA buffer (above). Populations of G_2 Chinese hamster cells were a generous gift of Dr. V. Prem Reddy, UMMC, Worcester MA.

iv. Cell fractionation

For isolation of soluble fractions, cells were extracted with a Triton buffer (CSK). The remaining protein was solubilized in the modified RIPA buffer (above) or in a buffer containing 8M urea, 2% nonidet P40, and 2% β-mercaptoethanol and used as an insoluble fraction. Nuclear matrix-intermediate filament extracts were prepared as previously described [5]. For nuclear matrix immunofluorescence, cells on coverslips were extracted 3X for 5 minutes with CSK buffer on ice, then extracted in digestion buffer (CSK with only 50mM NaCl, plus 100 ug/ml Dnase I, Sigma) for 20 minutes at room temperature. Coverslips were extracted with CSK containing 0.25M $(NH_4)_2SO_4$, washed with CSK buffer, fixed in -20^0C methanol, and processed as described above.

I. Immunoprecipitation and Western blot analysis

Cell lysates (above) were cleared of non-specific binding by preincubation with 20 ul of Protein A agarose beads (Gibco BRL) for 30 minutes at 4°C in an orbital shaker. After preclearing, 3 ug of each polyclonal antibody was added to 250 ul of a cell extract and incubated for one hour in the cold in an orbital shaker. Immune complexes were collected by incubation with 30 ul of Protein A or G beads for 3 hours in the cold and pelleting the bead-protein complex by centrifugation at 10,000 x g for 15 seconds. Beads were washed three times with lysis buffer then resuspended in 30 ul of SDS sample buffer.

Polyacrylamide gels were run according to the method of Laemmli [81]. In order to detect mitotic shifts (Figures. 18-20, 23), 5% polyacrylamide gels were run on 11-12 cm resolving gels until the 200 kDa myosin marker reached the bottom of the gel. SDS-PAGE was followed by transfer to Immobilon-P nylon (Millipore Corporation, Bedford, MA) using a semi-dry blotting apparatus (Owl Scientific, Cambridge, MA). Blots were incubated in 5% blocking agent (Biorad Labs) in TBS (20 mM Tris.HCL pH 7.5, 0.5M NaCl) then exposed to antibodies (final IgG concentration 1-3 ug/ml) for one hour in TBS containing 1% blocking agent and 1% BSA at room temperature. After three washes in TBST (TBS, 0.05% Tween 20), blots were incubated in secondary antibodies (goat anti-mouse or goat anti-rabbit alkaline phosphatase conjugate, Biorad Labs) for one hour at room temperature. Blots were washed 3X in TBST, once in TBS then incubated for 5 minutes in Immunlite chemiluminescent substrate (Biorad Labs) and exposed to reflection film (Dupont /NEN) for 5 minutes to 3 hours at room temperature.

J. Phosphatase Treatment

After immunoprecipitation, bead pellets were washed three times in phosphatase buffer (20 mM Hepes, pH 7.4, 100 mM NaCl, 1 mM DTT, 1 mM $MgCl_2$, 0.1 mM $ZnCl_2$) then incubated with 96 units of calf intestinal alkaline phosphatase (Sigma) at 37°C for 30 minutes [82]. The pellets were washed three times in phosphatase buffer then resuspended in SDS sample buffer and analyzed by immunoblotting.

CHAPTER 3

Identification and Characterization of the NuMA gene and mRNA

To begin to understand the nature and function of the nuclear matrix, this study has been designed to identify protein components by molecular cloning. From the time of its first description [1], the nuclear matrix has been the subject of numerous studies suggesting that it may play a functional role in fundamental nuclear processes such as DNA replication, transcription, and chromatin organization. Several comprehensive reviews of these investigations have been written [13-16]. Despite extensive evidence in support of a nonchromatin nuclear structure that is important in nuclear function, the nuclear matrix is somewhat controversial. The main criticism is that it has not been confirmed in the intact cell and therefore the structure identified after extractions may not accurately reflect the in vivo structure of the nuclear interior [17]. The components of the nuclear matrix that have been identified could have been trapped by the stringent methodologies used to prepare the samples. Identification of a resident protein component of the fibrillogranular network of the nuclear matrix and localization to this structure both in vivo and in vitro will contribute greatly to its validation and the ability to examine a functional relationship with the nucleus.

In this chapter, a novel nuclear matrix protein was identified using a molecular cloning strategy. Antibodies to nuclear matrix preparations were used to isolate cDNAs. Once sequenced, these cDNAs were used as tools to examine the gene and messenger RNA. The rationale for this strategy was that monoclonal antibodies raised against nuclear matrix fractions would provide specific tools that would allow for isolation of a nuclear matrix cDNA and thereby, identification of a novel protein component of the nuclear matrix. Once identified, the cDNAs and antibodies would be used for an examination of the gene and mRNA in the hopes of obtaining basic information about the structure and function of the molecule and thereby better understand the nuclear matrix. This characterization should provide insight into specific properties of the protein. The sequence information should allow for prediction of the secondary and tertiary structure that could provide clues to the molecular structure of components of the nuclear matrix. The sequence data would also provide insight into nuclear localization signals, binding motifs, and regulatory sites. In addition, mapping the position of the gene in the human genome would possibly provide a link to a genetic disease and allude to a function for the protein. Examination of RNA expression patterns may lead to mechanisms used to transcriptionally regulate the levels of the protein. In summary, the objective of this chapter is to clone, sequence and characterize a novel protein at the level of the gene and mRNA in the hopes of advancing our understanding of the structure and function of the nuclear matrix.

RESULTS

A. cDNA isolation and identification of a novel nuclear matrix protein

The 204.41 nuclear matrix antibody was used to screen several human λgt11 expression libraries. The screenings resulted in the isolation of 3 major clones

encoding polypeptides that react strongly with the 204.41 antibody. Two clones, NMP4 and NMP8 were initially isolated by a rotating student (G.P.McNeil). Analysis of these clones began with amplification of the inserts using the PCR and λgt11 primers to assess clone size. DNA was purified from a variety of sources (phage - single or double stranded, PCR products or subcloned plasmids) and digested with several restriction endonucleases (not shown). The individual insert restriction maps were compiled. The cloned fragments of the cDNAs were sequenced using the Taq sequencing system (Promega, Madison, WI). Using this kit, up to 500 bp of sequence from purified lambda DNA were routinely obtained. Results from these analyses identified overlapping sequences between each clone. Using the data obtained from restriction mapping and sequencing, the clones were aligned. This work has been summarized in Figure 2. As sequences became available, regular searches were conducted on Genbank for homologous sequences. Initially, all cDNA sequence was found to be unique and not homologous to any nucleic acid sequence yet reported.

The full sequence of the clones was obtained by subcloning the inserts into several different plasmid vectors (Table 2). Larger clones required digestion with Pst I, and cDNA fragments were subcloned. Oligonucleotide primers were made in order to complete the sequencing of the larger inserts. The sequencing of these overlapping cDNA clones was completed at the same time that the sequence became available in Genbank. The cloned cDNA sequences revealed 98% identity to NuMA [42, 44]. Figure 3 represents the sequence of the cDNA clones from this study aligned to the sequence of NuMA at bases 3428-5813 [42].

FIG. 2. Cloning summary. Schematic summarizing cloning work. Three major clones were isolated from library screenings, A4, NMP4, and NMP8. The clones were used as probes to identify a 7.2 kb mRNA on Northern analysis. The clones were restriction digested and sequenced to align them to each other. A map shows the restriction sites identified in the cDNA. The clones were sequenced and this information was used to obtain the identity of the protein.

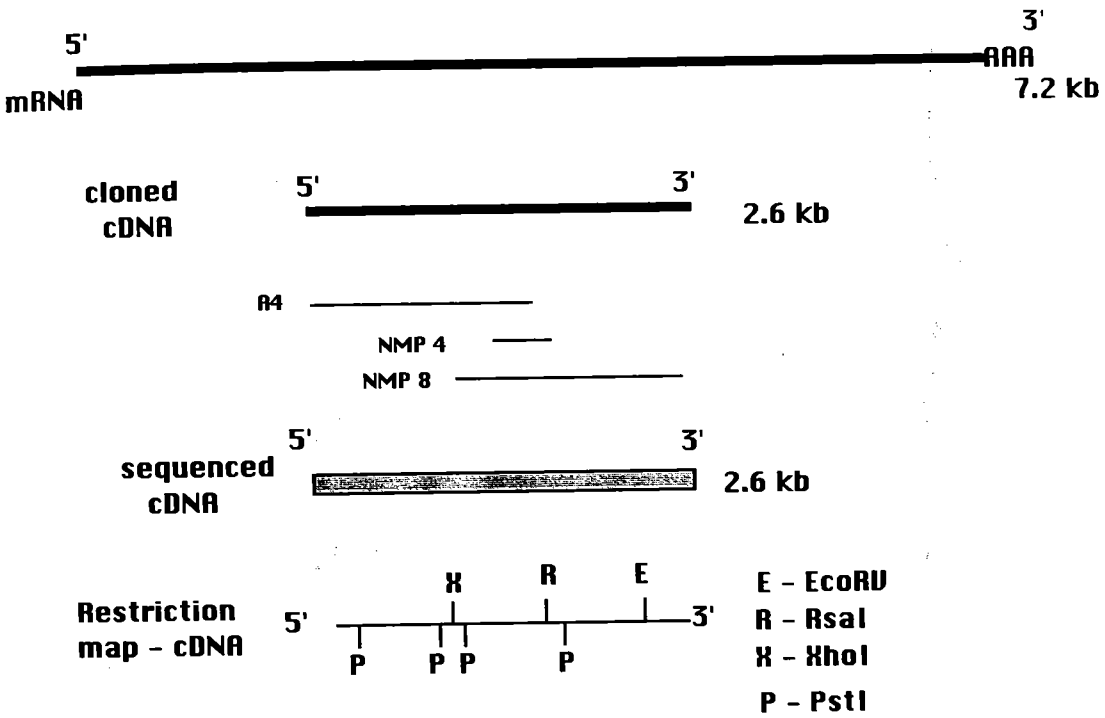
5'
3'
AAA
mRNA
7.2 kb
cloned
cDNA
5'
3'
2.6 kb
A4
NMP 4
NMP 8
5'
3'
sequenced
cDNA
2.6 kb
Restriction
map - cDNA
5'
3'
X
R
E
P
P
P
P
E - EcoRV
R - RsaI
X - XhoI
P - PstI

Table 2 - NuMA cDNA Subclones

Clone	Vector	Insert(bp)	T7 orientation	Position in 204.41
pCS1	pCR1000	277	(-)	2171-2448
pCS2	pCRII	508	(-)	1826-2334
pCS3	pCR1000	859	(+)	5039-5898(Yang)
pCS4	pCR1000	859	(-)	5039-5898(Yang)
pCS6	pCR1000	508	(+)	1826-2334
pCS7	pCRII	630	(-)	1826-2334(+120)
pCS8	pCR1000		(-)	1826-2334
pCS9	pCR1000			1826-2334
pCS10	pCR1000			1826-2334
pCS14	pCR1000	277	(-)	2171-2448
pCS17	pCR1000	277	(-)	2171-2448
D9	pSK+	194	(-)	88-282
SC-12	pSK+	620	(-)	4200-4820(Yang)
SC-10	pSK+	620	(+)	4200-4820(Yang)
C1	pSK+	194	(+)	88-282
C2	pSK+	78	(-)	282-370

TABLE 2. Various sections of cDNAs were subcloned into different vectors for the sequencing project. These tools were then used in subsequent molecular analyses. The table gives the clone name, then the vector used, followed by the insert size in bp, then the orientation of the insert relative to the T7 promoter common to all vectors, and lastly the position of the clone in the 204.41 cDNA unless otherwise indicated ("Yang" indicates the position in the sequence published by Yang and Snyder, 1992 [51].

FIG. 3. NuMA sequence. The sequence obtained from the 204.41 cDNA clones in alignment with sequence to NuMA, the nuclear mitotic apparatus protein, at positions 3420-5820 [42].

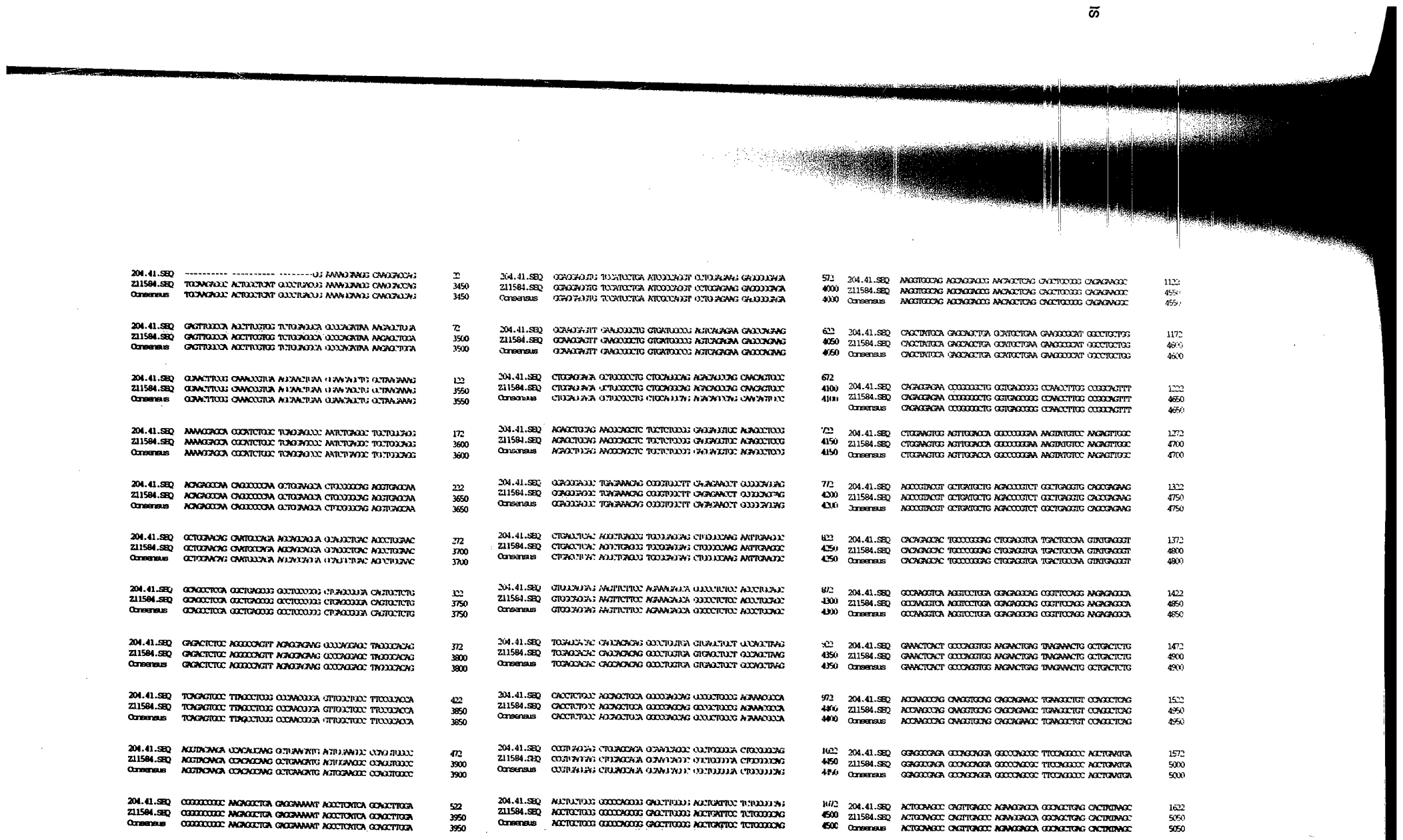

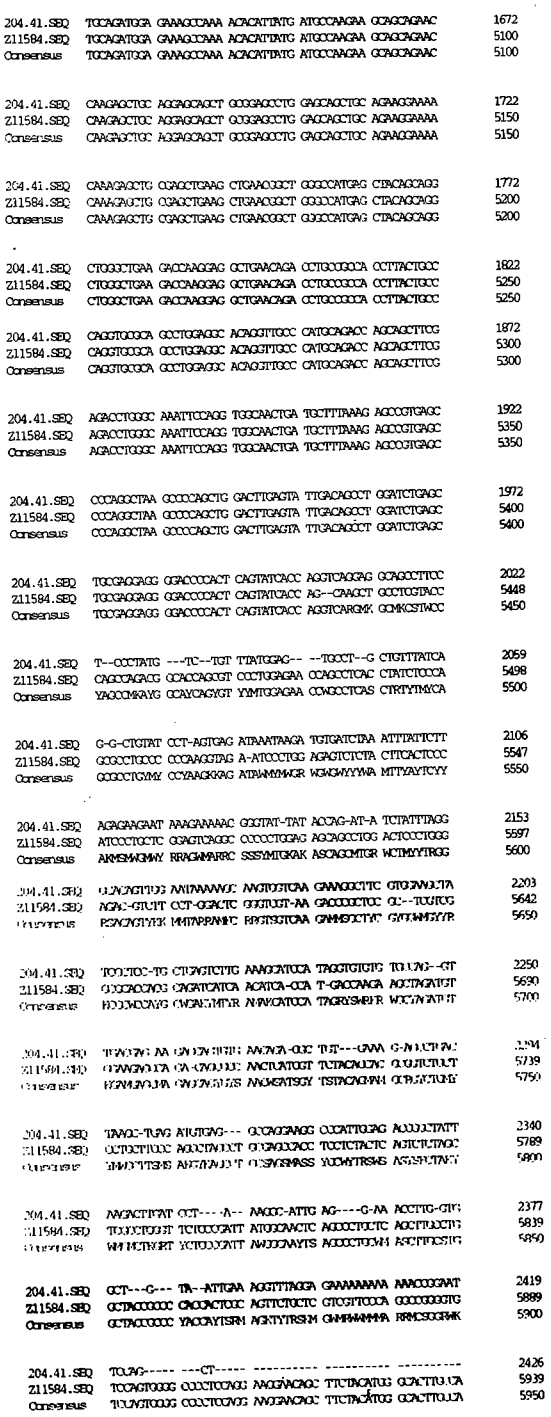

FIG. 3. NuMA sequence (cont.)

B. Characterization of NuMA mRNA

In order to assess the size of the mRNA, Northern blot analysis was performed. Total or poly A+ RNA from ME180 cells was isolated and separated on 1% agarose-formaldehyde-MOPS gels, and transferred onto nylon membranes. Blots were probed with cDNA clones radiolabeled with ^{32}P-dCTP by PCR direct incorporation in most cases. This analysis resulted in the detection of two low abundance mRNAs for NuMA (Figure 4 , middle lane, see Figure 11 also). The major form was at 7.2 kb with a minor form at approximately 8.0 kb. Another study described similar results but estimated the sizes to be a major 8.0-8.5 kb thick band and a minor 9.2 kb band [43]. As a control, Northern blots were done with another probe. A probe to the nuclear pore protein, TPR, detected a large ~8.5 kb band (Figure 4, left lane). 28s and 18s ribosomal RNAs served as markers and positions are indicated by arrowheads. Thus, the NuMA mRNAs consist of several forms including a major 7.2 kb form and a minor 8.0 kb form.

C. Analysis of the NuMA gene

As a first characterization of the gene for NuMA, we wanted to map its position in the human genome. This analysis may provide insight into a function for NuMA (if it mapped to a disease position). This technique may also provide insight into whether NuMA was a single copy gene or the member of a multi-gene family. Two approaches were used to examine this, Southern blot analysis and fluorescence in situ hybridization. Southern blot analysis was conducted to determine the size and complexity of the NuMA gene as well as to provide a physical map of the restriction sites within the gene. High resolution in situ hybridization was used to assess position of the NuMA gene in the human genome and copy number.

FIG. 4. NuMA Northern blot. ME180 cervical carcinoma cell poly A+ RNA (20ug/well) was probed with clones TPR-NMP1(left) and NuMA-NMP4 (right) radiolabeled with ^{32}P-dCTP by PCR direction incorporation. Position of 28s and 1 ribosomal RNA are indicated by the upper and lower arrows respectively.

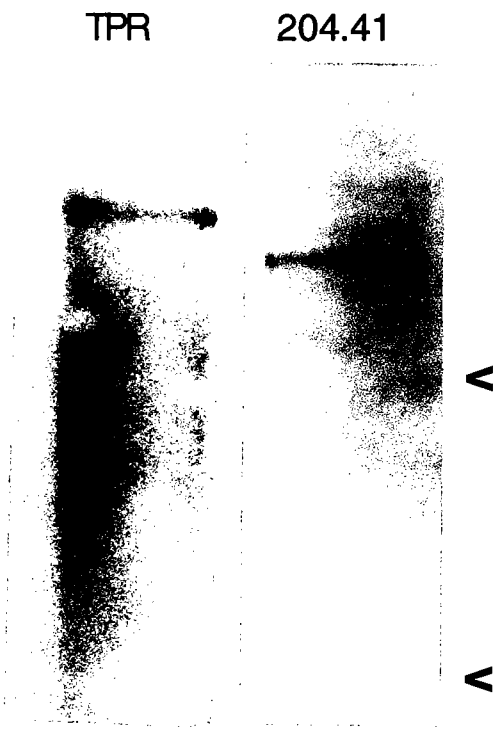
TPR
204.41

Genomic Southern blot analysis with NuMA cDNA probes A4 and NMP8 resulted in a simple pattern of one or two bands ranging from 7 to 13 kb in size using high stringency post-hybridization washing conditions (0.5XSSC/0.5%SDS final wash) consistent with the presence of a single copy gene (Figure 5, [43]). The number of sites cut for each restriction enzyme such as XbaI were in agreement with the sites predicted by the published cDNA sequence. Eco RI and Bam HI digests each produced two bands(seen better on long exposure) however, indicating restriction sites in the gene which are not in the cDNA. Therefore, intervening sequences are probably present in the region of the NuMA gene recognized by the cDNA probes indicating splicing of a primary transcript.

High resolution in situ hybridization was performed with the NuMA cDNA and human metaphase chromosomes. The NuMA cDNA was found to hybridize consistently at a single locus on a metacentric C-group chromosome (Figure 6A,B). Both sister chromatids generally showed label, confirming bona fide hybridization. Hybridization of this relatively small (2.5 kb) probe was detected without amplification or image processing. The majority of cells showed one labeled chromosome, and approximately one-third of cells showed two labeled homologous chromosomes. Signal was not observed on any other chromosomes. Cells in interphase most often gave single hybridization signals (data not shown). Within the limits of resolution of this technique, these results indicate that NuMA is a singe copy gene.

To identify the chromosome and regional position of the gene, banding analysis was employed using DAPI staining. The NuMA gene was localized to chromosome 11 based on screening 62 banded metaphase spreads (2 examples shown in Figure 6A,B). The position of the NuMA gene was determined by evaluating 25 chromosomes for signal

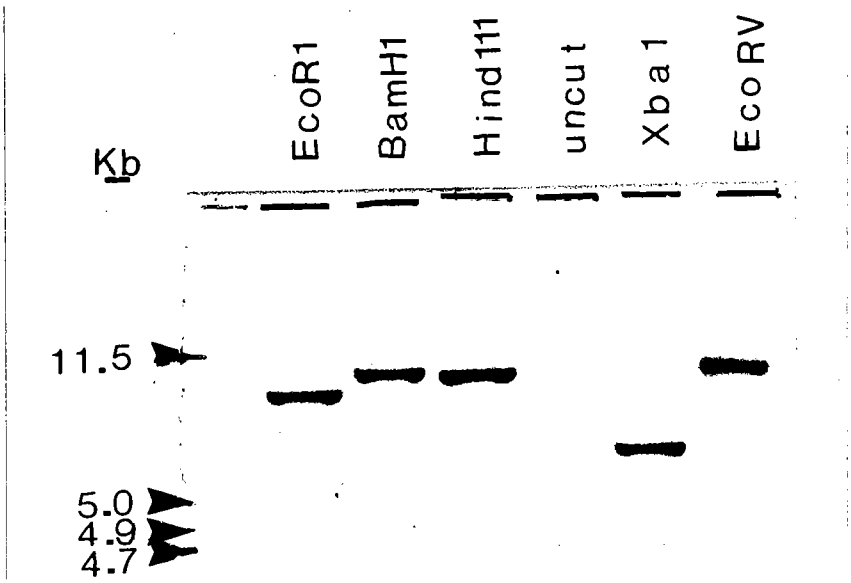

FIG. 5. Southern blot. For analysis of the NuMA gene in total genomic DNA, ME180 cervical carcinoma cell DNA (10ug/well) was restriction digested with various enzymes and Southern blotted. Probes were labeled by random primed DNA synthesis with incorporation of digoxygenin dUTP. Results were visualized by non-isotopic chemiluminescence (BMB).

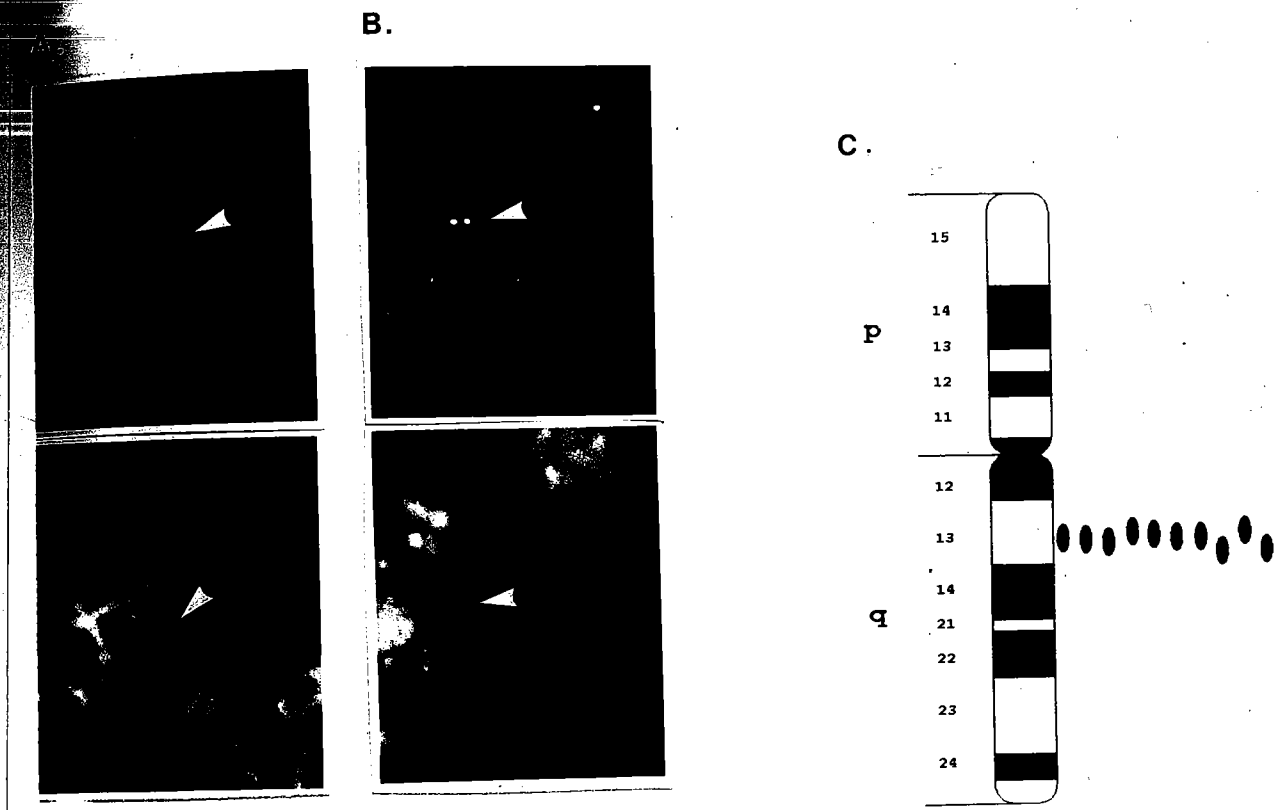

FIG. 6. Localization of the NuMA gene by fluorescence in situ hybridization. (A,B) Two examples of the NuMA cDNA hybridized to human chromosome 11. The FITC signal is on the top and the DAPI banded chromosome is on the bottom. Arrow indicates location of signals and corresponding chromosomes. (C) Idiogram of human chromosome 11 showing placement of the NuMA gene in 11q13 based on analysis of 10 banded metaphase chromosomes. Measurement of signal placement in 15 additional metaphase spreads agreed with this localization.

placement with respect to chromosome bands as well as total chromosome length (Figure 6A,B,C). These results indicated that the NuMA gene is localized to band q13 on chromosome 11. The results from ten evaluations were summarized on the idiogram in Figure 6C. Taken together, the Southern analysis and in situ hybridization demonstrated that the gene for NuMA appears to be a single locus gene located on human chromosome 11q13 [83].

D. Identification of alternatively spliced mRNA isoforms

The cDNA probes for NuMA reacted with multiple mRNA bands in Northern analysis. In situ hybridization and Southern analysis detected a single NuMA gene indicating that these forms of mRNA may be transcribed from the same gene. Further evidence for spliced mRNA isoforms was as follows. In the course of library screening, one cDNA clone was isolated that contained a potential splice site followed by novel sequence information (Figure 7A). The clone NMP 8 when sequenced at the 3' end revealed 408 bp of novel sequence with a translational termination site that could account for a truncated version of the NuMA protein with 23 novel amino acids in the C-terminus (Figure 7B). The point of divergence between the published sequence and the novel sequence was at a consensus splice sequence (AG'GT, Figure 7A). The 408 bp sequence was searched against Genbank and shared no homology to any known sequence. A restriction map for NMP 8 also revealed an Eco RV site in this region which was not present in the published NuMA sequence (data not shown, Figure 7A, 204.41.seq position 2103). Another interesting splice sequence was isolated during PCR analysis (Figure 7C, discussed below).

To confirm the presence of alternatively spliced mRNA in the total mRNA from human cells, PCR analysis was done with NuMA primers (Figure 8) and RNA or DNA from

FIG. 7. Sequence of RNA isoforms. (A) The 3' end of NuMA's clone NMP 8 was aligned to the published full length cDNA from Yang [42] revealing a novel 408 bp sequence. A consensus splice sequence is at Yang position 5432. (B) Analysis of the predicted amino acid sequence of NMP 8 demonstrates that this isoform would translate 24 novel amino acids. (C) Sequence of clone pCS7, another putative alternatively spliced mRNA.

```
204.41.SEQ   TGCGAGGAGG GGACCCCACT CAGTATCACC AGGTCAGGAG GCAGCCTTCC   2022
Z11584.SEQ   TGCGAGGAGG GGACCCCACT CAGTATCACC AG--CAAGCT GCCTCGTACC   5448
Consensus    TGCGAGGAGG GGACCCCACT CAGTATCACC AGGTCARGMK GCMKCSTWCC   5450

204.41.SEQ   T--CCCTATG ---TC--TGT TTATGGAG-- --TGCCT--G CTGTTTATCA   2059
Z11584.SEQ   CAGCCAGACG GCACCAGCGT CCCTGGAGAA CCAGCCTCAC CTATCTCCCA   5498
Consensus    YAGCCMKAYG GCAYCAGYGT YYMTGGAGAA CCWGCCTCAS CTRTYTMYCA   5500

204.41.SEQ   G-G-CTGTAT CCT-AGTGAG ATAAATAAGA TGTGATCTAA ATTTATTCTT   2106
Z11584.SEQ   GCGCCTGCCC CCCAAGGTAG A-ATCCCTGG AGAGTCTCTA CTTCACTCCC   5547
Consensus    GCGCCTGYMY CCYAAGKKAG ATAWMYMAGR WGWGWYYYWA MTTYAYTCYY   5550

204.41.SEQ   AGAGAAGAAT AAAGAAAAAC GGGTAT-TAT ACCAG-AT-A TCTATTTAGG   2153
Z11584.SEQ   ATCCCTGCTC GGAGTCAGGC CCCCCTGGAG AGCAGCCTGG ACTCCCTGGG   5597
Consensus    AKMSMWGMWY RRAGWMARRC SSSYMTGKAK ASCAGCMTGR WCTMYYTRGG   5600

204.41.SEQ   GCWCWGTTGG AATAAAAWGC AWGTGGTCAA GAAWGGCTTC GTGCAWGCTA   2203
Z11584.SEQ   AGAC-GTCTT CCT-GGACTC GGGTGGT-AA GACCCGCTCC GC--TCGTCG   5642
Consensus    RSWCWGTYKK MMTWRRAWYC RRGTSGTCAA GAMMGGCTWC GYGCWMGYYR   5650

204.41.SEQ   TCGCTCC-TG CTGWGTCTTG AAAGCATCCA TAGGTGTGTG TCTCAG--GT   2250
Z11584.SEQ   GCGCACCAGG CAGATCATCA ACATCA-CCA T-GACCAAGA AGCTAGATGT   5690
Consensus    RCGCWCCAYG CWGAWGMTAR AWAYCATCCA TAGRYSMRYR WSCTWGATGT   5700

204.41.SEQ   TTWCTGW AA GWCWGWGTG AWCWGA-CGC TGT---GAA G-WCTCTWC   2294
Z11584.SEQ   CTAAGWCTA GA-GWCTGCC AACTCATGGT TCTACAGCWC GCGTCTCTCT   5739
Consensus    RGWWTWCTWA GWCWGSTGS AWCWSATSGY TSTACWGWAW GCRTCTCTMT   5750

204.41.SEQ   TAAGC-TGAG ATGTGAG--- GCCAGGAAGG CCCATTGCAG ACCCCTATT   2340
Z11584.SEQ   CCTCCTTCCC AGCCTACCCT GCGAGCCACC TCCTCTACTC AGTCTCTAGC   5789
Consensus    WMWCCTTSWS ARGTWACCYT CCSWGSWASS YCCWYTRSWS ASTSTCTAKT   5800

204.41.SEQ   AAGACTTTAT CCT----A-- AAGCC-ATTG AG----G-AA ACCTTG-GTG   2377
Z11584.SEQ   TCCCCTGGGT TCTCCCGATT ATGCCAACTC ACCCCTGCTC AGCTTCCCTG   5839
Consensus    WHTCCTKGRT YCTCCCGATT AWGCCWAYTS ACCCCTGCWH ASCTTCCSTG   5850

204.41.SEQ   GCT---G--- TA--ATTGAA AGGTTTAGGA GAAAAAAAA AAACCCGAAT   2419
Z11584.SEQ   GCTACCCCCC CACCACTCGC AGTTCTGCTC GTCGTTCCCA GCCCCGGGTG   5889
Consensus    GCTACCCCCC YACCAYTSRN AGKTYTRSKM GAMRMMMMA RRMCSCGRMK   5900

204.41.SEQ   TCCAG----- ---CT----- ---------- ---------- ----------   2426
Z11584.SEQ   TCCAGTCCCG CCCCTCCAGG AAGGAACAGC TTCTACATGG GCACTTCCCA   5939
Consensus    TCCAGTCCCG CCCCTCCAGG AAGGAACAGC TTCTACATGG GCACTTCCCA   5950
```

B.

```
        10         20         30         40         50
1234567890 1234567890 1234567890 1234567890 1234567890
GTCAGGAGGC AGCCTTCCTC CCTATGTCTG TTTATGGAGT GCCTGCTGTT   50
V R R Q  P S S  L C L  F M E C  L L F
 S G G  S L P P  Y V C  L W S  A C C L
  Q E A  A F L  P M S V  Y G V  P A V

TATCAGGCTG TATCCTAGTG AGATAAATAA GATGTGATCT AAATTTATTC  100
 I R L  Y P S E  I N K  M . S  K F I L
  S G C  I L V  R . I R  C D L  N L F
Y Q A V  S . .  D K .  D V I .  I Y S

TTAGAGAAGA ATAAAGAAAA ACGGGTATTA TACCAGATAT CTATTTAGGG  150
  R E E  . R K  T G I I  P D I  Y L G
L E K N  K E K  R V L  Y Q I S  I . G
 . R R  I K K N  G Y Y  T R Y  L F R A

CACAGTTGGA ATAAAAAGCA AGTGGTCAAG AAAGGCTTCG TGGAAGCTAT  200
H S W N  K K Q  V V K  K G F V  E A I
 T V G  I K S K  W S R  K A S  W K L S
  Q L E  . K A  S G Q E  R L R  G S Y

CGCTCCTGCT GAGTCTTGAA AGCATCCATA GGTGTGTGTG CCAGGTTGAC  250
 A P A  E S .  K H P .  V C V  P G . R
  L L L  S L E  S I H R  C V C  Q V D
R S C .  V L K  A S I  G V C A  R L T

GAGAAGAGCA GTGTGAACAG AGGCTGTGAA AGAGCCTGAC TAAGCTGAGA  300
  E E Q  C E Q  R L .  K S L T  K L R
E K S S  V N R  G C E  R A .  L S .  D
 R R A  V . T E  A V K  E P D  . A E M

TGTGAGGCCA GGAAGGCCCA TTGGAGACCG GCTATTAAGA CTTGATCCTA  350
C E A R  K A H  W R P  A I K T  . S .
 V R P  G R P I  G D R  L L R  L D P K
  . G Q  E G P  L E T G  Y . D  L I L
```

C.

GTAAGAATTT GGCTGGCAGA CTCACCTCAC TCCTATTCCA CTGGACCCCT 50

GTGCCCTCTS CTCCTAGGCC ACTGCTGCCT TAGGCTTTTC TTCACTCTCC 100

CCCTGGCCCT CTCCTTCT

FIG. 7. Sequence of RNA isoforms (cont.)

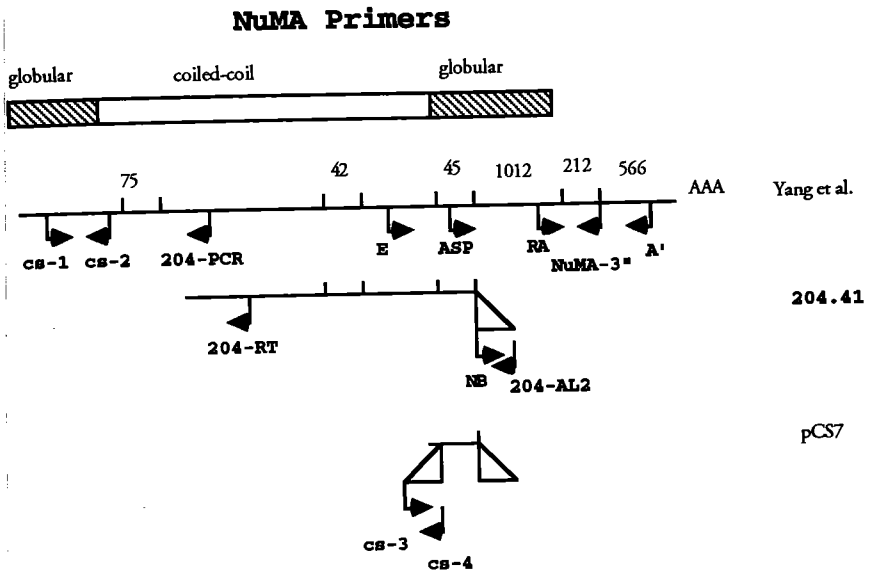

Primer name	Position(Yang)	Sequence
cs-1	273	AGAGCTGGAACTGGCGAAGAT
cs-2	596	GGAGAAGCTGGAGAACCTGAG
204-PCR	3256	GGCAAACCGTGAAGCAACTGAAGGA
204-RT	3613	GCAAGGCTGAAGATGAGTGGAAGGC
E	4594	GGCAGAAACTCACTGCCCAGGTGG
ASP	5039	TGCGCAGCCTGGAGGCACAG
RA	5761	GAGCCTGAGCAGCTGGATGA
NUMA-3'	5880	GACCCCCAAGAGACCCTGCG
A'	6113	ACCAGGCCAGGGTGCGGGCA
NB	2171(204.41)	AGCAAGTGGTCAAGAAAGGC
204AL2	2327(204.41)	AAGGCCCATTGGAGACCGGC
cs-3	9(PCS7)	TTGGCTGGCAGACTCACCTC
cs-4	84(pCS7)	AGGGGGAGAGTGAAGAAAAG

FIG. 8. Oligonucleotide primers for NuMA. This schematic illustrates the position on the cDNA and sequence of all primers used in sequencing and subsequent PCR analysis.

human cells. ME180 poly A+ mRNA was oligo dT primed and reverse transcribed into cDNA. This cDNA was used as a template in PCR amplification using primers (ASP/204AL2, Figure 8) that bracket the potential splice site described in Figure 7. The amplification resulted in the expected band of 510 bp based on the sequence in Figure 7 and an upper band of 630 bp (Figure 9A, lane 3). These PCR products were subcloned into a TA cloning vector and sequenced. The sequence of the smaller band (lane 3) was identical to the 3' end of the NMP8 clone (lane 1), confirming the presence of the RNA isoform in cells. This subclone was termed pCS2.

The larger amplification product contained 120 bp of novel sequence on the 5' end, bracketed by a consensus splice sequence (lane 3 and Figure 7C). This construct was named pCS7. To test whether the pCS7 sequence was part of the gene or an artifact, the same PCR primer pair, ASP/204AL2, was used to amplify a band from total human genomic DNA. This resulted in a 630 bp product corresponding to the pCS7 insert (lane 9). Amplification of RNA by rt-PCR using primers that bracket the C-terminus of NuMA produced 3-4 bands suggesting that at least 3 mRNA isoforms may exist (Figure 9B). This was confirmed by other studies [43]. The alternatively spliced mRNA data were summarized in schematic form in Figure 10.

As a final confirmation of the presence of alternatively spliced forms of NuMA RNA and to obtain further insight into how the spliced mRNA is produced, the cloned splice sequences were labeled and used in Northern analysis with ME180 poly A+ RNA (Figure 11). The splice sequence detected the upper band of approximately 8.0 kb and a lower 3.0 kb band, while a probe to a conserved region detected the 8.0 kb band as well as the major 7.2 kb band. These experiments demonstrated that the splice sequence may be derived from the lower abundance 8.0 kb transcript and perhaps a smaller 3.0 kb

FIG. 9. PCR analysis of RNA isoforms. (A) ME180 poly A+ RNA was reverse transcribed into cDNA and amplified with primers bracketing the potential splice site or primers to the sequence at the 3' end of NMP 8. PCR products were separated on ethidium bromide stained gels and photographed. (B) PCR amplification of total cDNA's with primers bracketing the 3' end of NuMA.

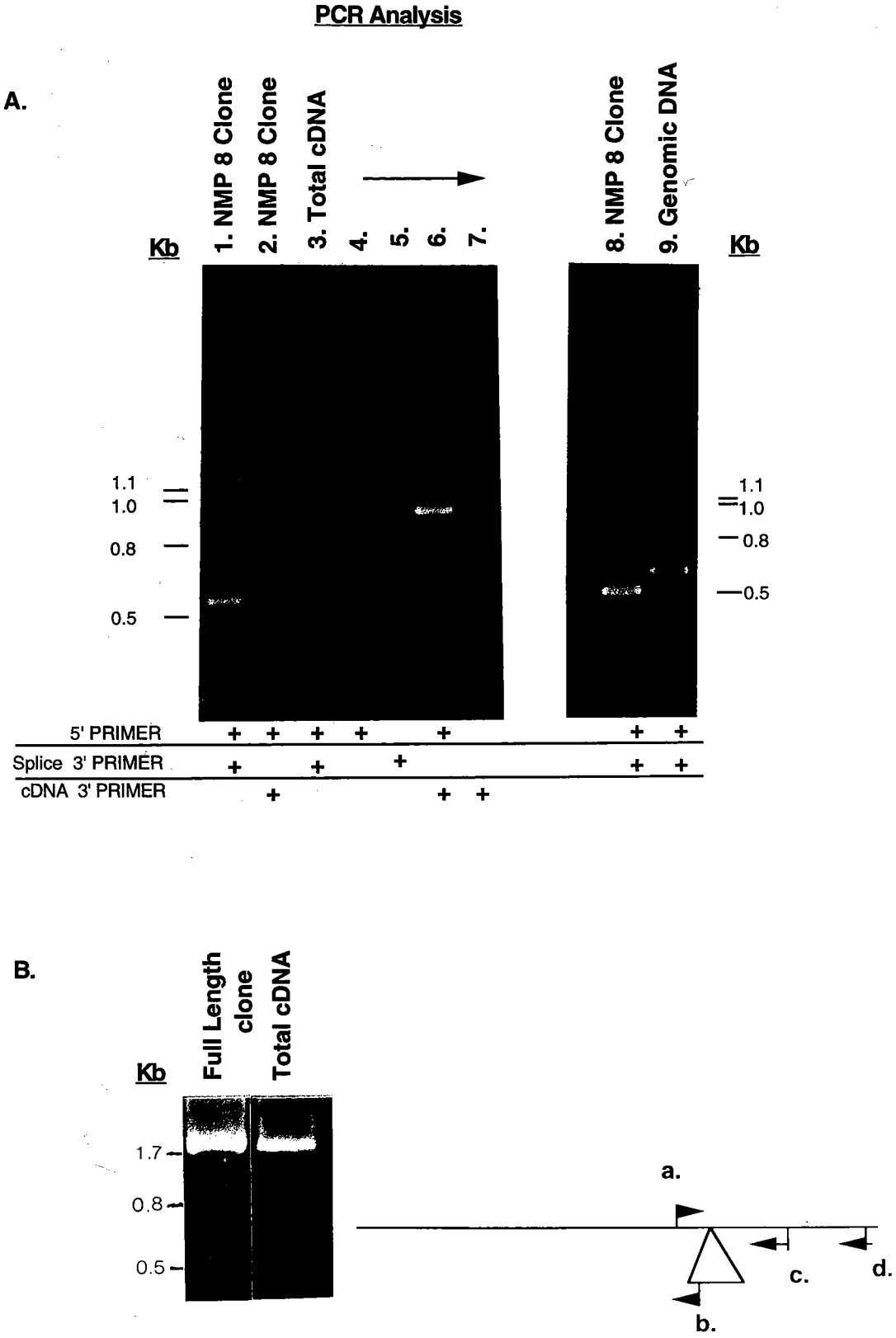
PCR Analysis
A.
Kb
1. NMP 8 Clone
2. NMP 8 Clone
3. Total cDNA
4.
5.
6.
7.
8. NMP 8 Clone
9. Genomic DNA
Kb
1.1
1.0
0.8
0.5
1.1
1.0
0.8
0.5
5' PRIMER
Splice 3' PRIMER
cDNA 3' PRIMER
B.
Kb
Full Length clone
Total cDNA
1.7
0.8
0.5
a.
b.
c.
d.

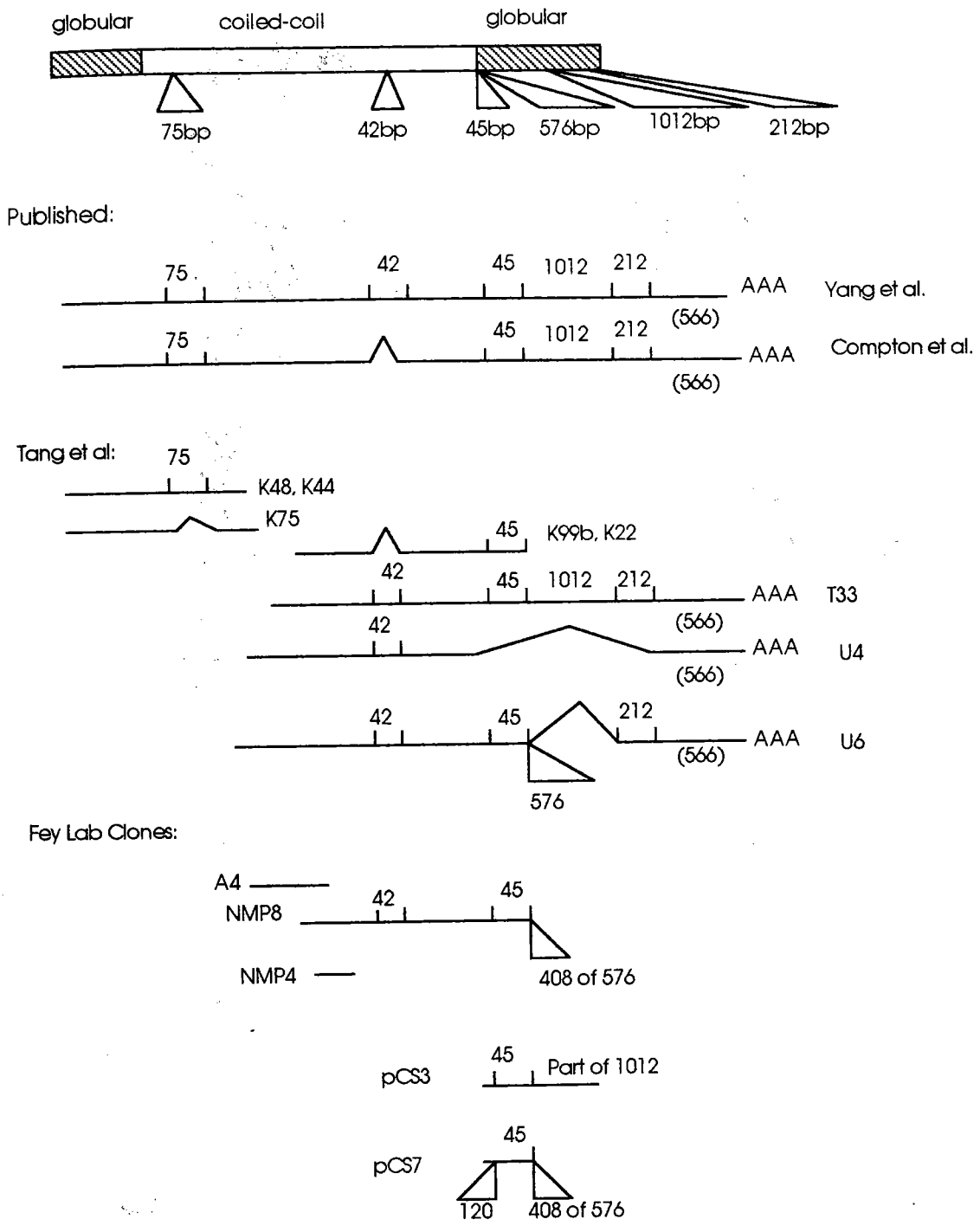

FIG. 10. Summary of RNA isoform analysis. Schematic of all NuMA sequences identified thus far. Variable regions are excised out as triangles and sizes are in base pair.

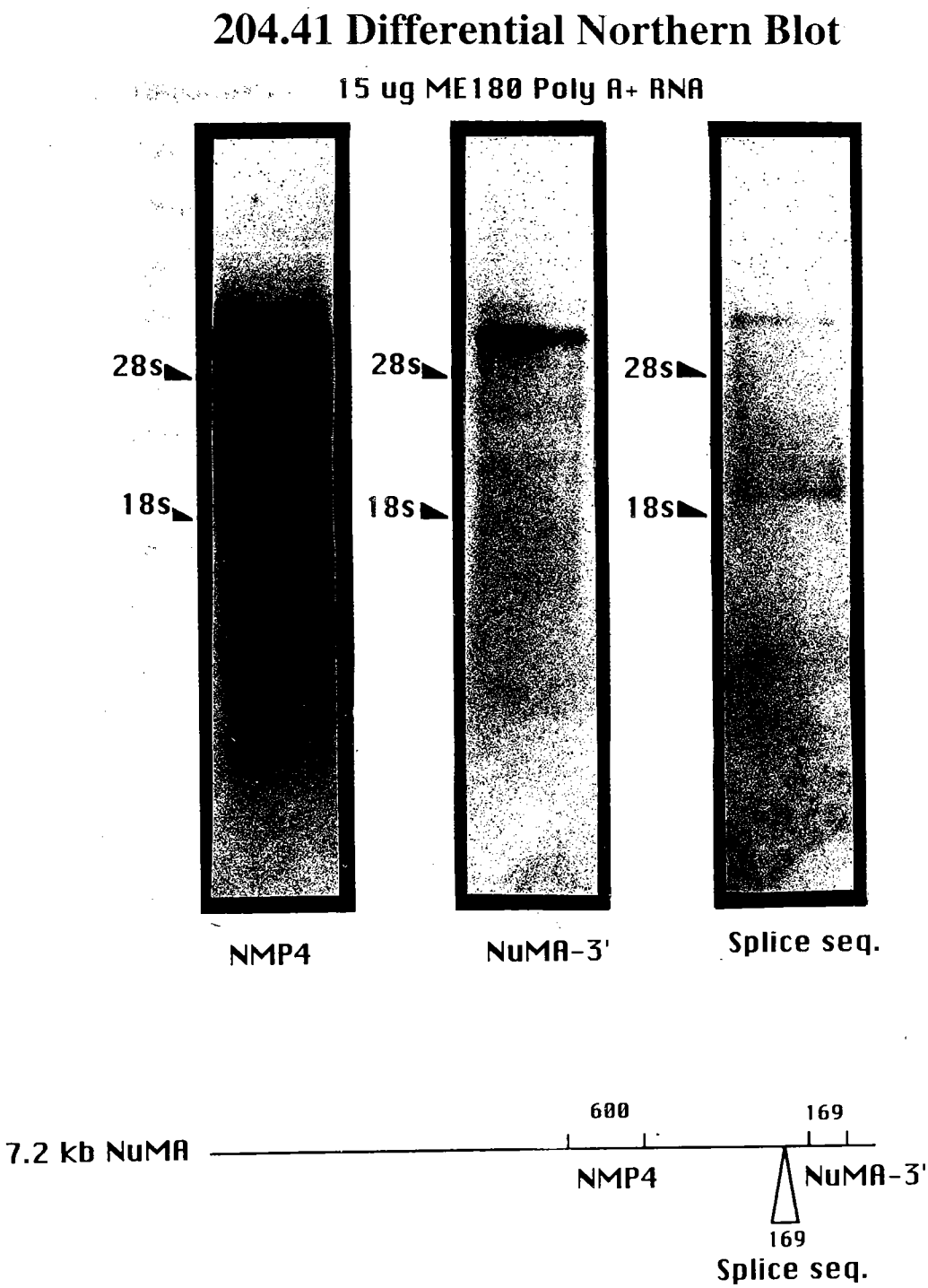

FIG. 11. Northern analysis of RNA isoforms. 15 ug of ME180 Poly A+ RNA was probed with radiolabeled probes to various regions of the NuMA cDNA. Left lane - probe is to a conserved region, NMP4; Middle lane - probe is to the 3' end of the published NuMA cDNA; Right lane - probe is to the novel splice sequence. The splice sequence detects the low abundance larger RNA isoform.

form but not the major 7.2 kb transcript. In summary, there was one major NuMA transcript of 7.2 kb that was represented in the published cDNA sequence. In addition, several NuMA mRNA isoforms were expressed in the cell. One isoform was represented in an 8.0 kb transcript.

E. Discussion

The goal of this study was to identify a resident protein component of the nuclear matrix using molecular cloning techniques to isolate and sequence the corresponding cDNA. Once NuMA was discovered, the cDNA became a molecular tool to probe the gene and mRNA to obtain information about the nature of this nuclear matrix protein. From the amino acid sequence, the protein was predicted to be a 1485 amino acid coiled-coil dimer that would form a 200 nm central rod domain [42]. With this in mind, a pressing question is whether NuMA can form these filamentous structures and whether these structures contribute to the fibrillogranular network of the nuclear matrix seen in electron microscopy (Figure 1).

While these are difficult questions to answer, there are several pieces of evidence that support this hypothesis. First, immunogold electron microscopy localized NuMA to the fibrillogranular network of the nuclear matrix [54]. Second, negative stain electron microscopy of purified full length fusion protein gave a filamentous structure [84]. Third, an in depth computer analysis suggested the possibility of head-to-tail aggregation of NuMA based on possible interaction of the acidic head domain with the basic tail domain after dimerization, thereby creating a loose meshwork not unlike the nuclear matrix [85]. How these conformations of NuMA would contribute to the structure and stability of the mitotic spindle is less clear.

During the cloning and characterization of NuMA, several significant observations were made about the gene and messenger RNA. First, using the sensitive technique of in situ hybridization, the NuMA gene was localized to human chromosome 11q13 (Figure 6). Cancer related aberrations in chromosome 11q13 site have been described and are varied, ranging from deletions and translocations to DNA amplifications [86]. Chromosome 11q13 has long been recognized as a folate-sensitive fragile site, FRA11A [87], a site that in response to environmental factors can be damaged leading to tumorigenesis. Cyclin D, INT2, and HSTF1 have been mapped to 11q13 and have been linked to esophageal and breast cancer, defined by a general amplification of the DNA in that area [88]. These observations have led to the idea that chromosome 11q13 may contain cell cycle genes involved in tumorigenesis in certain cancer types [89]. Although NuMA may not participate in this proposed mechanism for tumorigenesis, the observation that the NuMA gene localizes to chromosome 11q13 raises some interesting possible roles for the protein. For example, overexpression of NuMA could contribute to the acceleration of proliferation if it were normally found in limiting quantities in the cell.

NuMA has a complex mRNA expression profile with interesting functional implications. Northern analysis with a 600 bp partial cDNA detected a major transcript of 7.2 kb and a less abundant transcript of ~8.0 kb. As previously discussed, these transcripts appeared to arise from a single gene. While screening libraries, one of the cDNA clones was found to contain a variation in the sequence at the 3' end (Figure 7A). This variation was not a library artifact (common in λgt11 libraries) but an actual isoform of NuMA mRNA based on the following evidence. First, the sequence variation began with a consensus AG'GT splice site and a EcoRV restriction site (Figure 7)not found in the published cDNA but confirmed by Southern blot analysis (Figure 5). Second, the PCR

analysis showed that this isoform sequence exists in the mRNA of cells (Figure 9A, lane 3) and in the gene (Figure 9A, lane 9). Finally, Northern analysis using probes specific to spliced regions showed that the isoform is likely to be the larger and low abundance 8.0 kb NuMA mRNA (Figure 11, right lane). It must be noted that the 8.0 kb message may be unspliced RNA. Unspliced RNA for some messages can be carried in a poly A+ RNA selection procedure that starts with total RNA. NuMA pre-mRNA may be present and future studies should attempt to resolve this issue by examining cytoplasmic RNA or specific proteins produced from the alternatively spliced transcripts to validate these transcripts. The results, however, suggest that there is an isoform of NuMA mRNA that is produced by alternative splicing from one NuMA gene and is expressed as an 8.0 kb transcript.

The expression profile for NuMA mRNAs is summarized in Figure 10. There are three variations in the 3' end of NuMA mRNA identified thus far. T33 was the proposed 3' end of the major 7.2 kb transcript. U6/NMP8 was the 3' end of the ~8.0 kb transcript and U4 was a third variation. Tang and co-workers predicted that the U4 and U6 isoforms produce truncated versions of the protein at sizes of 194 and 196 kDa respectively, based on proteins detected in immunoprecipitation experiments [43]. These may be overinterpretations for the following reasons. The first is that there has been no analysis of variations of NuMA mRNAs in the 5' end. In fact, there has been little analysis of the first 5000 bases of NuMA mRNA. There is no information about the sequence of the NuMA gene other than the minor PCR analysis done in this study. This study indicates that there are other varied regions (Figure 7C) not detected by Tang and colleagues. Without information about the full length transcripts for the isoforms and the gene that encoded them, definitive statements can not be made about what the proteins will be if produced from them. Secondly, it is unclear whether the U4/U6

isoforms produce proteins of 194 and 196 kDa detected by Tang and colleagues [43] or whether they are due to protein degradation. There are degradation products that plague most NuMA protein analyses (which will be discussed further in Chapter 4) and can lead to misinterpretation of the NuMA protein profile.

Without the ability to correlate the RNA isoforms with actual proteins, it is difficult to assess the functional significance of the alternative splicing. However, there was one subsequent observation from Tang et al. worth noting. These workers recently prepared expression constructs by fusing the variable 3' ends to the major transcript (assuming that this was the in vivo isoform) at the splice site (position 5155, [42]). Overexpression of the U4 and U6 constructs resulted in localization to interphase centrosomes. As NuMA oscillated between the nucleus and centrosome (see below, Chapter 4), this was an interesting result. Tang proposed that these are forms of NuMA that are resident centrosome components in normal cells. The significance of this observation will be discussed in Chapter 6.

CHAPTER 4

CHARACTERIZATION OF NUMA PROTEIN

Of all the antibodies raised to nuclear matrix proteins, the monoclonal antibody 204.41 was chosen as a research tool as it gave a distinctive distribution pattern in the cell by immunofluorescence microscopy. In most cells, it was predictably nuclear. But in dividing cells, it redistributed to the spindle poles. This was intriguing as it suggested that this nuclear matrix protein also functioned during cell division. In this chapter, NuMA was examined in greater detail at the protein level. The experimental strategy

was to use the NuMA antibodies to scrutinize the subcellular localization of NuMA in all phases of the cell cycle and to characterize the protein biochemically in a series of immunoprecipitation experiments. These experiments examined the nature of the protein with respect to its size, degree of conservation, and phosphorylation state. Obtaining this information about NuMA could enrich our understanding of the function of NuMA in the nucleus or the mitotic spindle and could contribute to our knowledge of mitotic and other nuclear processes.

The changes in NuMA's locations in the cell could be explained in several ways. It is possible that different isoforms of NuMA exist at different places in the cell. Alternatively, one protein may exist but be regulated by modifications such as phosphorylation. To address these possibilities, a biochemical characterization was performed to assess the size and phosphorylation state of the protein, as well as to identify any isoforms. In addition, these studies could potentially contribute to the our understanding of alternatively spliced RNA isoforms. There is more than one RNA isoform [43], so it was of interest to see if there are corresponding protein isoforms synthesized in the cell that were detectable with our antibodies.

There are other interesting properties of NuMA that could be examined biochemically. Whether NuMA is a highly conserved protein could be investigated by screening for the protein in Western blot analyses of protein preparations from various species. If the protein was highly conserved, then the function of the protein could be significant if not essential. The degree of conservation of the protein would also be useful in designing future experiments. For example, if cell cycle studies were to be conducted, some cell types would be easier to synchronize than others.

From these observations, several important questions could be asked about the nature of the protein. 1) What is the function of the protein through the cell cycle? 2) What specifies the localization of NuMA to the spindle pole? 3) What regulates the change in distribution? 4) What are its binding partners? 5) Are there cells that have no NuMA and what is that phenotype? Answering these questions may contribute to understanding the function of NuMA in the cell (e.g. if the function of a binding partner is known) and how it is regulated (phosphorylation).

Results

A. Subcellular distribution through the cell cycle

The antibody 204.41 was used in immunofluorescence staining experiments with several human cell lines. Results obtained with MCF-7, a human breast carcinoma line, are depicted in Figure 12. In interphase cells, NuMA is localized throughout the nuclear interior in a punctate pattern and was excluded from nucleoli (A,B). During early prophase, the nuclear staining gradually decreases (Panels D,F) until metaphase, where staining is observed at the polar region of the spindle apparatus (close to the centrosomes, Figure 12, Panels H and J). Centrioles are not stained as seen in panel H where an end-on view of the metaphase plate shows star-like staining with a clear center. The star-shaped spindle structure appears to be composed of approximately 10 separate microtubule arms. A side view of the metaphase plate indicates staining on both spindle poles (Panel J). As the cells divide, the proteins redistribute to the newly developing nuclei until telophase where the punctate intranuclear staining is restored (Panels L-P).

FIG 12. Distribution of NuMA during the cell cycle. Indirect immunofluorescence microscopy of MCF7 breast carcinoma cells was performed with the NuMA monoclonal antibody and an FITC conjugated secondary antibody. Corresponding DNA in each field is on the left stained with DAPI. Phases of the cell cycle were as follows: interphase (A,B), early prophase (C,D), late prophase (E,F), metaphase (G-J), anaphase (K,L), early telophase (M,N), late telophase (O,P). Cell G-H is an end on view of one spindle pole. Cell I-J is a side view of both spindle poles. Note the lack of NuMA staining at the centrioles indicated by the dark central hole (Panel H). Bar 5 um.

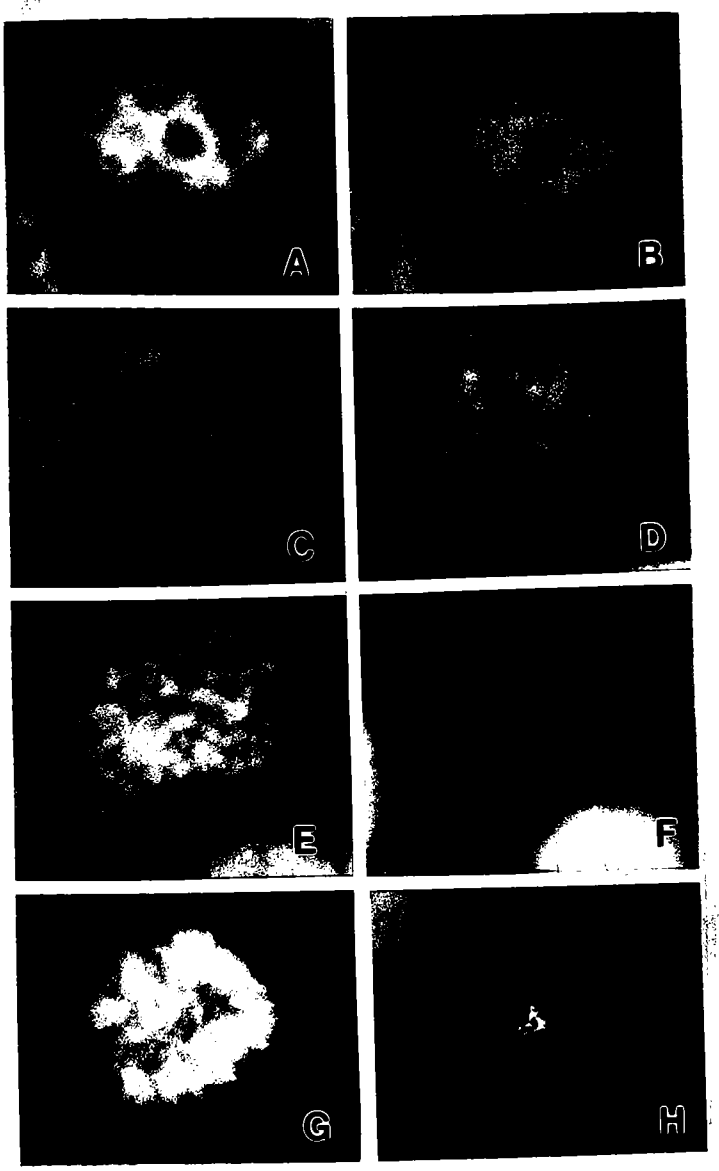
A
B
C
D
E
F
G
H

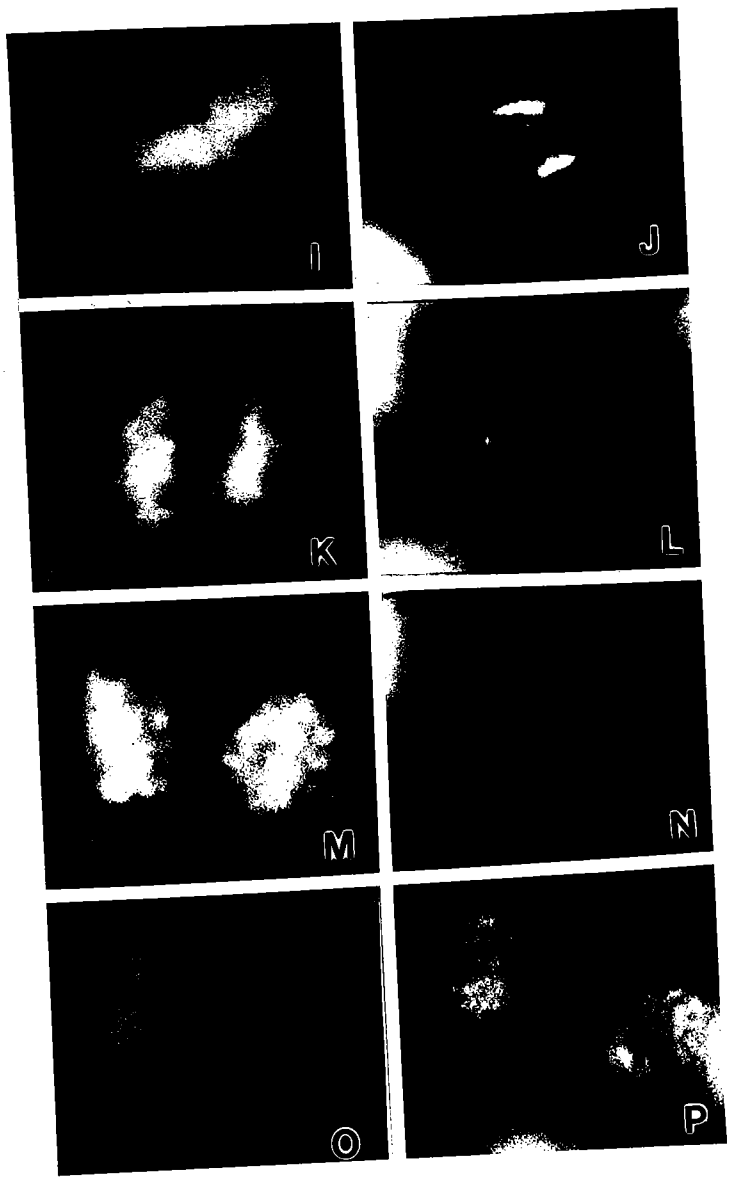

FIG 12. Distribution of NuMA during the cell cycle (cont.)

B. Variations on the distribution of NuMA

Most immunofluorescence experimental protocols used in this study involved extraction of a cell with Triton buffer before fixing the samples with paraformaldehyde or methanol. These methods removed much of the soluble protein and lipid prior to fixation and staining. To illustrate the variation in patterns of NuMA localization or background seen with NuMA antibodies, samples were prepared without extraction prior to fixation. Figure 13A is an ME180 cell that has been fixed in methanol without prior extraction. There is a diffuse cytoplasmic signal as well as the typical punctate nuclear staining. CHO cells have a faint, somewhat vesicular stain in the cytoplasm (Figure 13B). The CHO cell nuclei are also stained with DAPi to visualize the DNA.

In a preliminary study with Dr. Richard Jack at Harvard University, NuMA was examined in a terminally differentiated cell system, the human granulocyte system. First, the subcellular distribution of NuMA was examined in the progenitor cell, the premyeloblast. The tissue culture cell line HL-60 was employed as these cells are premyeloblasts and can be induced to form either monocytes or neutrophils with the appropriate agents. First the DNA was stained with DAPi to identify the nuclei (Figure 13C). Next, the HL-60 were stained with NuMA antibodies and gave the expected nuclear distribution of NuMA (Figure 13D) excluded from nucleoli. In neutrophils, the nuclei are condensed and multi-lobed, illustrated in Figure 13E using DAPi stain. In granulocyte cell preparations, which contain 99.5% neutrophils and eosinophils (R. Jack, personal communication), NuMA is absent from the nuclei (Figure 13F) although there is some cytoplasmic background signal. Eosinophils were found in the same preparation (not shown) and did not appear to contain any nuclear or cytoplasmic NuMA. This preliminary study shows that NuMA may be downregulated in the differentiation pathway of granulocytes.

FIG 13. Variations in NuMA subcellular distribution. Indirect immunofluorescence microscopy of cells with atypical NuMA staining patterns. (A) an unextracted, methanol fixed ME180 human cervical carcinoma cell and (B) an unextracted, methanol fixed CHO cell stained with the NuMA 204.41 antibody showing cytoplasmic background staining. The CHO cell is also stained with DAPi to show the DNA in the nucleus. (C,D) HL-60 human premyeloleukemic cells stained with DAPi to visualize DNA in blue (C) and NuMA antibody 204.41 to show NuMA distribution in the nucleus in green (D). These cells can be induced to differentiate into neutrophils (E,F, here purified from human blood) in which nuclei become multi-lobed (E, DAPi-blue) and appear to exclude NuMA (F, NuMA-green). Bar 5 um.

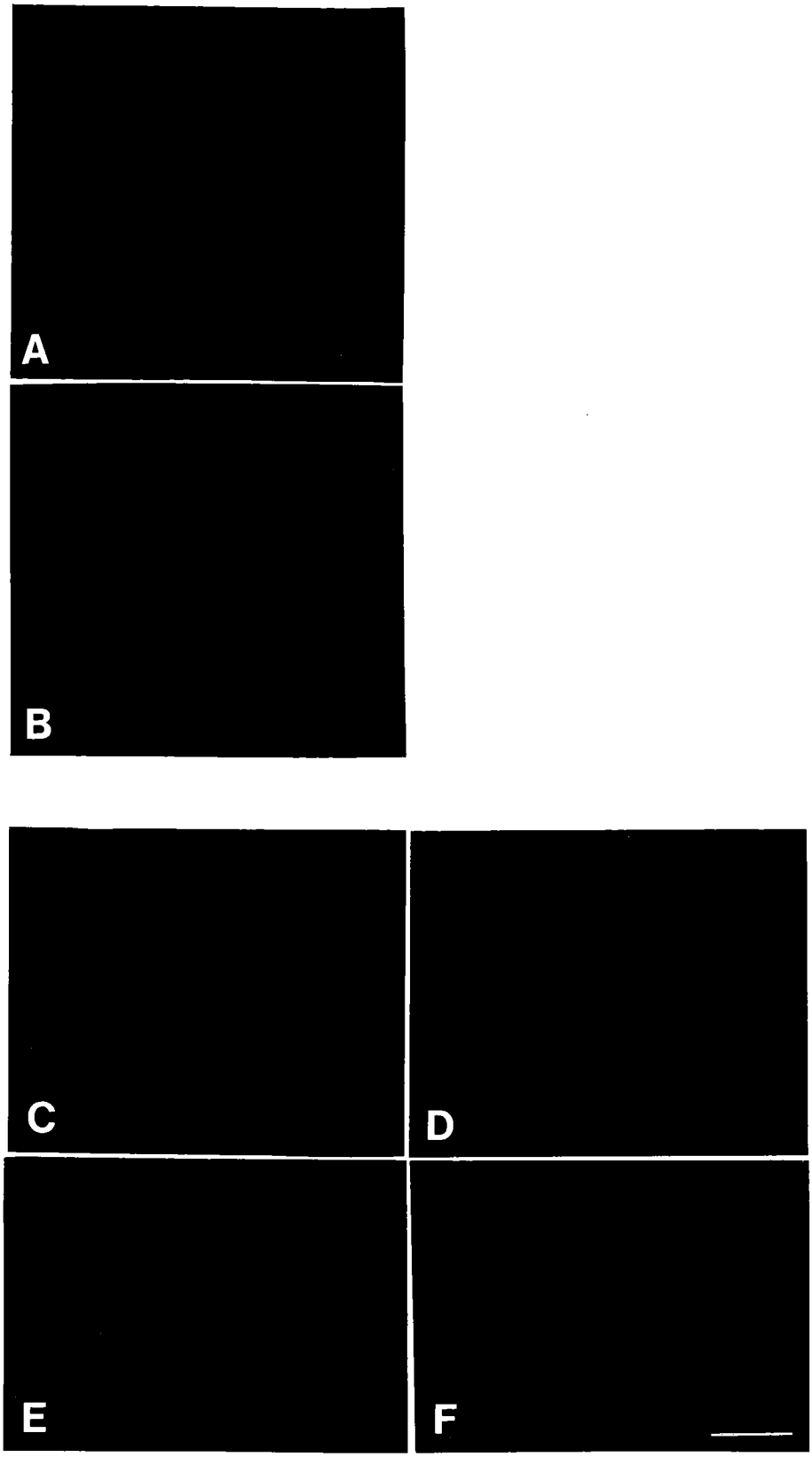
A
B
C
D
E
F

C. Biochemical characterization of the protein

The NuMA monoclonal antibody 204.41 was used in Western blot analyses and detected a protein of ~250 kDa molecular weight in total protein extracts from CHO cells (Figure 14). It was the only band detected using all NuMA antibodies. The same was true for NuMA in other mammalian species. There was one major band at approximately 250 kDa in mouse, hamster, and human (Figure 15). The protein was not detected in *Xenopus laevis* total protein extracts (Figure 15) with any of the NuMA antibodies (the 204.41 monoclonal shown here). In some samples, more than one band reacted with anti-NuMA antibodies but the lower molecular weight bands are most likely due to protein degradation (see discussion). In most of the biochemical analyses, antibodies to several different proteins were used as controls. The antibody used most often was to pericentrin, a highly conserved protein of the centrosome [72]. These studies were done in collaboration with Dr. Stephen Doxsey (UMass Medical Center, Worcester, MA). Pericentrin was readily detectable in extracts from most species examined. Pericentrin appeared to be a doublet of approximately 250 and 300 kDa of varied intensities in mammalian cells (Figure 15).

The next analysis of NuMA involved testing the monoclonal (204.41/107.7) and polyclonal antibodies for the ability to immunoprecipitate the protein from cell lysates. NuMA was immunoprecipitated cleanly as a single band from whole cell extracts (Figure 16A, right). Pericentrin antibodies immunoprecipitated two polypeptides (Figure 16A, left) similar to those seen in Western blots. The small bands at approximately 60 kDa were the rabbit immunoglobulin bands that were detected by the secondary antibodies (Figure 16, left). To test whether there were any co-precipitating proteins that were not detected by Western blot analysis,

FIG. 14. NuMA Western blot. 20 ug of CHO cell protein extract was subjected to SDS-PAGE on 5% gels and blotted onto Immobilon-P. Blots were probed with the NuMA monclonal antibody 204.41 and detected with a secondary goat anti-mouse alkaline phosphatase conjugated antibody followed by exposure to chemiluminescent substrate and autoradiography.

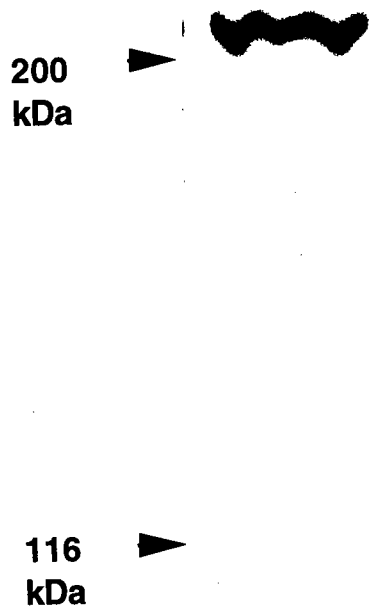
200
kDa
116
kDa

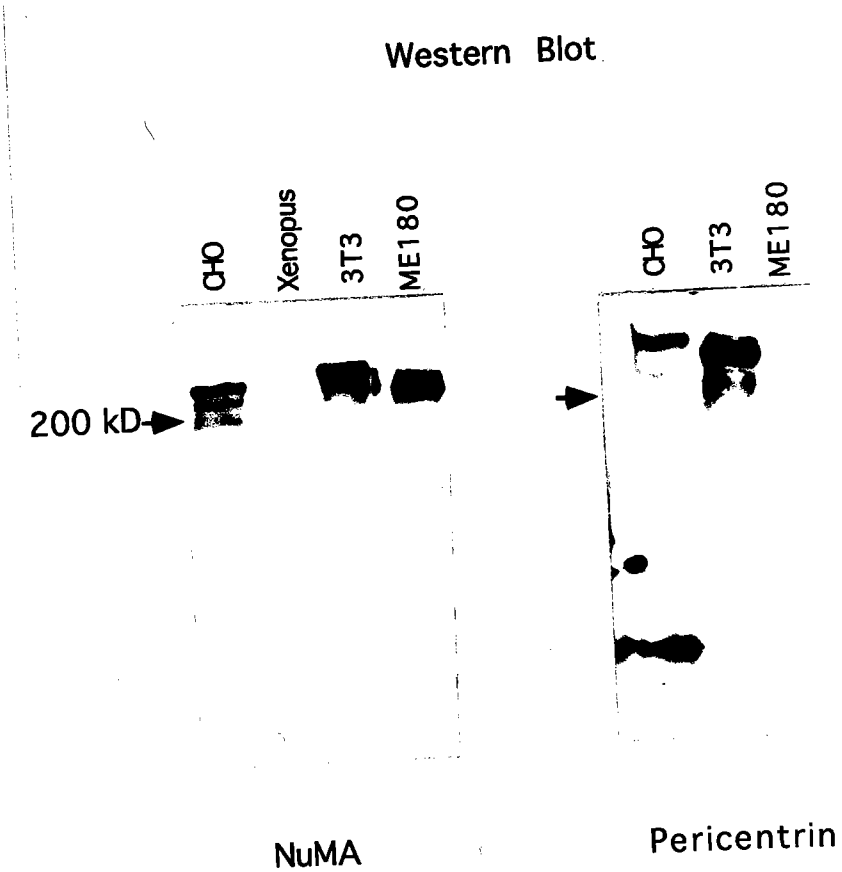

FIG. 15. NuMA Zoo Western blot. 20 ug of protein extract from hamster(CHO cells), Xenopus(oocytes), mouse (3T3 cells), and human (ME180 cells) was Western blotted and probed for NuMA with the 204.41 monoclonal antibody or with a pericentrin polyclonal antibody. Molecular weight markers are in kDa.

FIG. 16. NuMA immunoprecipitation. (A) NuMA and pericentrin were immunoprecipitated with polyclonal antibodies to each protein from total CHO or 3T3 protein extracts and analyzed by Western blot with the monoclonal antibody 204.41 for NuMA or the pericentrin polyclonal antibody. (B) NuMA was immunoprecipitated out of CHO extracts after metabolic labeling with ^{35}S-methionine and analyzed by SDS-PAGE. Gels were dried and autoradiographed. Lane 1 - total extract; lane 2 - beads alone; lane 3 - NuMA polyclonal immunoprecipitation; lane 4 - NuMA monoclonal immunoprecipitation.

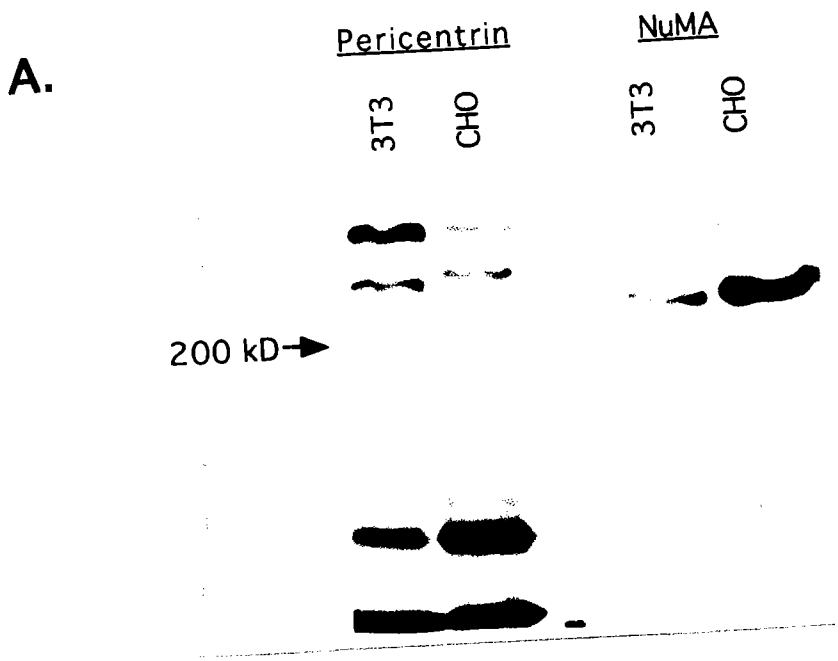
A.
Pericentrin
NuMA
3T3
CHO
3T3
CHO
200 kD

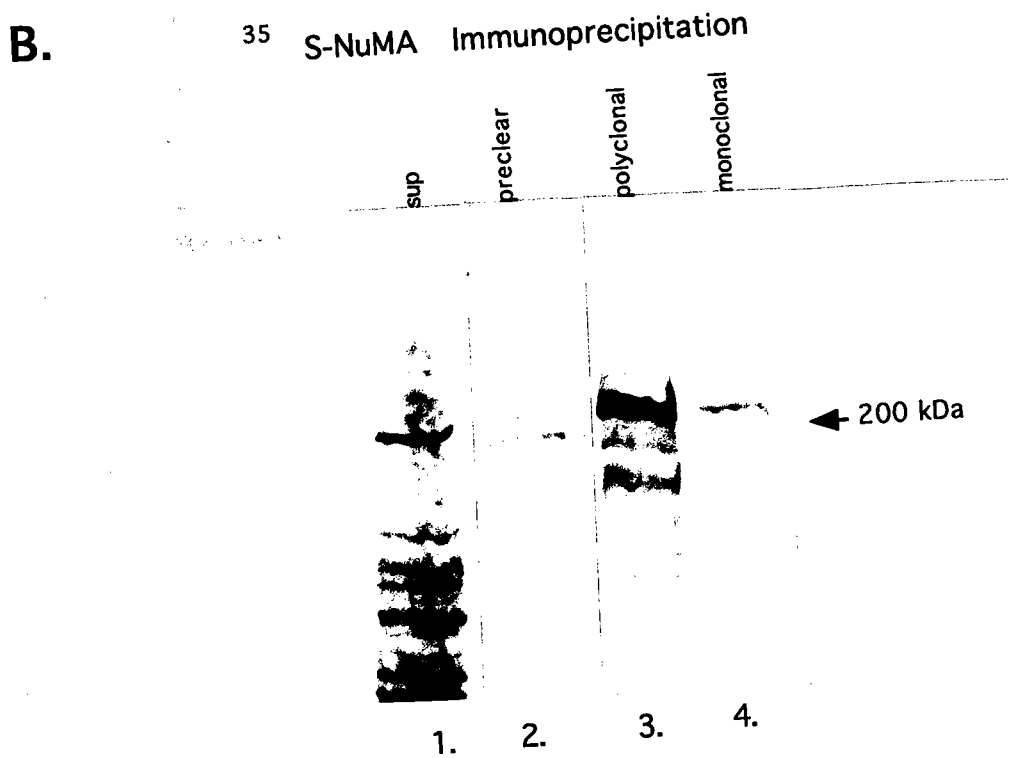
B.
35 S-NuMA Immunoprecipitation
sup
preclear
polyclonal
monoclonal
200 kDa
1.
2.
3.
4.

immunoprecipitations were done with extracts from cells that had been labeled with ^{35}S-methionine. NuMA antibodies precipitated a single, major protein (Figure 16B).

D. Phosphorylation of NuMA.

The phosphorylation state of NuMA was examined by immunoprecipitation from extracts of log-phase cells that were labeled for four hours with ^{32}P-orthophosphate. As shown in Figure 17 A, NuMA is immunoprecipitated as a single phosphoprotein band with the expected molecular weight of 250 kDa (lane 1). When a phosphatase inhibitor cocktail was included in the lysis buffer [90], a second phosphoprotein was detected (Figure 17B, lanes 4,5) at approximately 180 kDa in the NuMA immunoprecipitations. A similar co-precipitating protein was seen in pericentrin immunoprecipitates (lanes 2,3) but not in TPR immunoprecipitates (lane 1). NuMA's identity was confirmed by subsequent Western analysis of lane 4 from Figure 17B (Figure 17C, lane 1). In summary, this work demonstrated that NuMA and pericentrin are phosphorylated in log-phase cells and may interact with another phosphoprotein of 180 kDa whose identity is unknown.

E. Identification of an electrophoretic mobility shift in mitotic NuMA

The mitotic phosphorylation state of NuMA was initially determined in vivo by ^{32}P-orthophosphate labeling and immunoprecipitation. In interphase cells, the 250 kDa phosphoprotein was resolved on SDS-PAGE after autoradiography (Figure 18, lane I). In addition, the phosphoprotein of approximately 180 kDa coprecipitated with NuMA (Figure 18, asterisk). In mitotic cells labeled with ^{32}P-orthophosphate, NuMA appeared as a broader band of higher molecular weight than in interphase cells (lane M). Interestingly, the 180 kDa protein did not coprecipitate with NuMA in extracts prepared from mitotic cells.

FIG 17. NuMA is a phosphoprotein. (A.1) NuMA was immunoprecipitated with the polyclonal antibody from CHO extracts after labeling with ^{32}P, separated on 5% polyacrylamide gels, blotted and autoradiographed. Lane 2 is the supernatant. (B) Inclusion of specific phosphatase inhibitors resulted in the detection of a co-precipitating protein with NuMA (lanes 4,5) and pericentrin (lanes 2,3) that ran at ~180 kDa. This band was absent from an immunoprecipitation of TPR (lane 1) from ^{32}P-labeled ME180 protein extracts. Lanes 2 and 4 are immunoprecipitations from ^{32}P-labeled 3T3 protein extracts. Lanes 3 and 5 are immunoprecipitations from ^{32}P-labeled CHO protein extracts. Lane 6 is the supernatant from the ^{32}P-labeled 3T3 protein extracts. Lane 7 is the supernatant from the ^{32}P-labeled CHO protein extracts. (C) This 180 kDa band did not cross react with the NuMA antibody in subsequent Western blot analysis (lane 1). Lane C2 is the ^{32}P signal with a longer exposure of lane B.4. Molecular weight markers are in kDa.

Figure 17

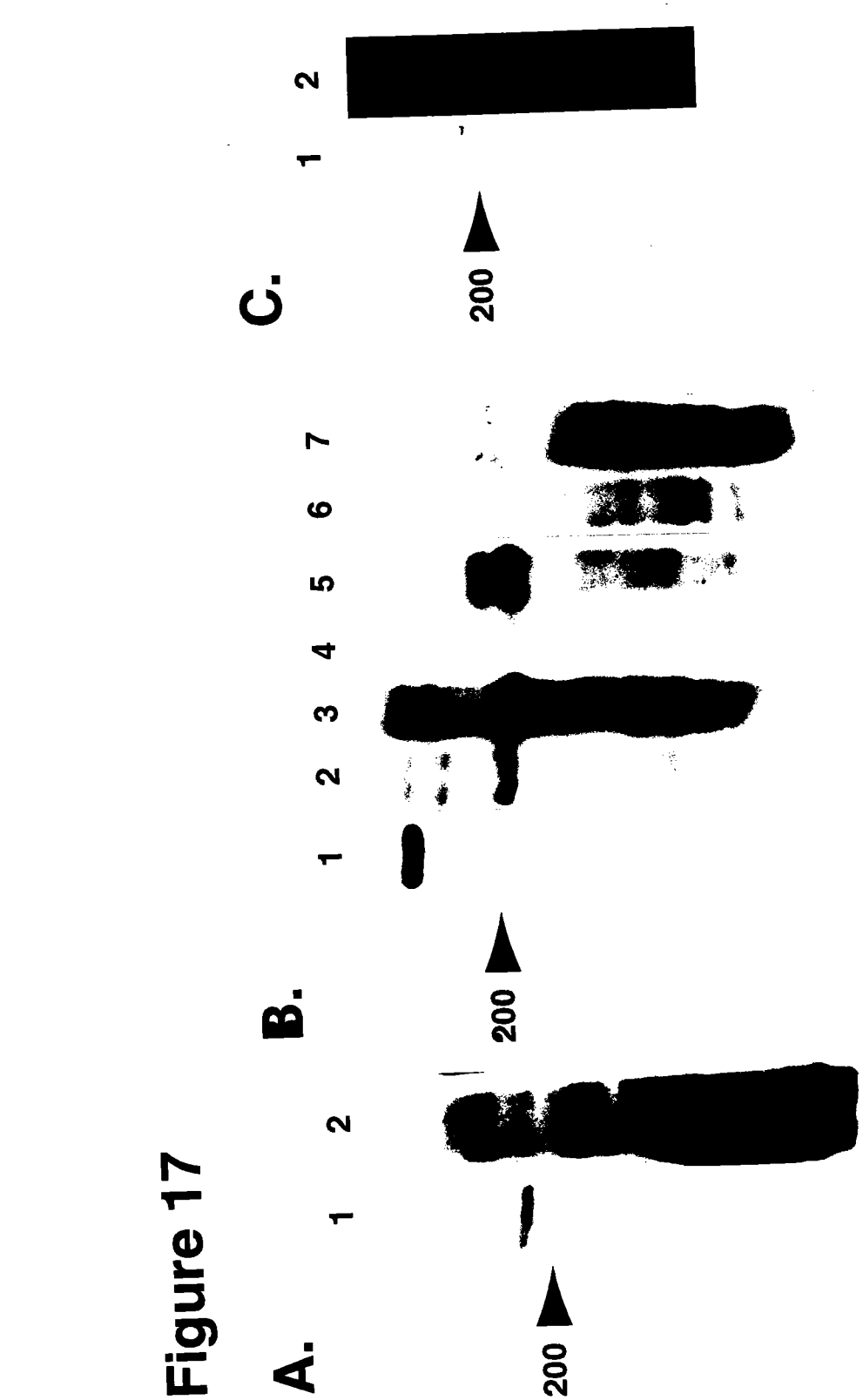

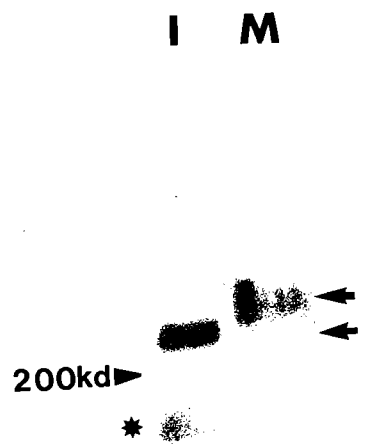

FIG. 18. Immunoprecipitation of NuMA from cells labeled with ^{32}P-orthophosphate. Protein extracts were prepared from interphase (I) and mitotic (M) CHO cells in the presence of ^{32}P-orthophosphoric acid. NuMA was immunoprecipitated, run out on 5% polyacrylamide gels, transferred onto Immobilon-P membranes and subjected to autoradiography. Arrows indicate electrophoretic shift in mobility of mitotic NuMA. Asterisk (*) indicates 180kd co-precipitating protein from interphase extracts. Molecular mass standards are indicated in kDa.

To determine whether the mobility shift seen in mitosis was due to phosphorylation, immunoprecipitates from unlabeled cells were treated with alkaline phosphatase and Western blotted (Figure 19). Following optimization of the gel system for the resolution of the high molecular weight species (see Materials and Methods), alkaline phosphatase treatment demonstrated that the shifted mitotic protein was reduced to interphase mobility (lanes 2 and 4). Inclusion of phosphatase inhibitors in the preparation prevented the shift down to interphase mobility (lane 6) and controlled for contaminating proteolytic activity in the phosphatase preparation. The phosphatase sensitivity of NuMA demonstrated that the change in the electrophoretic mobility was the result of phosphorylation. The fact that the electrophoretic mobility of interphase NuMA was unaffected it's phosphorylation state or subsequent phosphatase treatment (Figure 19, lanes 1 and 3) made it possible to study the mitosis-specific phosphorylation of NuMA in unlabeled cells in future experiments.

F. Discussion

The biochemical and morphological work on NuMA in this chapter defined some properties of the protein that may have major implications for its cellular function. Using the antibodies as probes, the protein was examined in the cell by indirect immunofluorescence microscopy through the cell cycle as well as in various biochemical analyses to characterize the size, conservation, subcellular distribution, and post-translational modifications. From these results, several observations have been made that contribute to our understanding of NuMA.

This immunofluorescence study identified a cell type that appeared to contain no NuMA in its nucleus(Figure 13F). These cells are human neutrophils that were fixed in methanol and stained with NuMA antibodies. Neutrophils arise from a well characterized

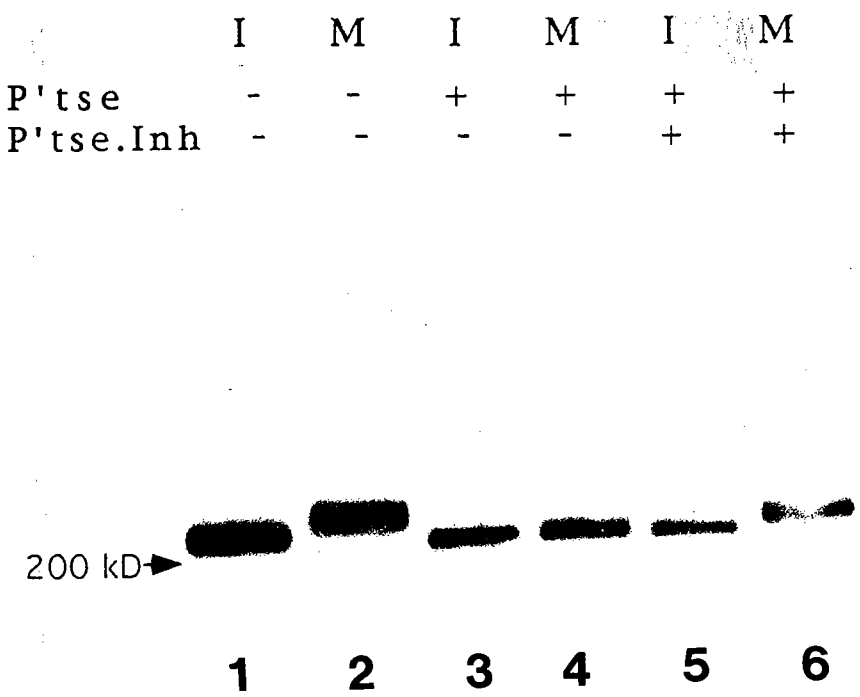

FIG. 19. Phosphatase sensitivity of NuMA. NuMA immunoprecipitates from interphase (I) and mitotic (M) CHO cells were treated under various conditions, run on SDS gels, transferred to Immobilon, and detected by chemiluminescence. Lanes 1 and 2, untreated samples; 3 and 4, alkaline phosphatase-treated; 5 and 6, treated with alkaline phosphatase in the presence of phosphatase inhibitors. Molecular mass standards are indicated in kDa.

differentiation pathway starting with premyeloblasts (dividing cells with round nuclei) and ending with terminally differentiated polymorphonuclear cells [91]. These cells had nuclei with distinctively lobed shapes. They were also most-mitotic. Given NuMA's proposed role in nuclear and spindle stability, it was interesting that a cell that had an unusual nuclear shape and no longer assembled mitotic spindles, would lack NuMA. It is possible that NuMA may be excluded from the final nuclei that reform during the last mitosis of these cells. An alternative explanation is that NuMA could be downregulated at a specific stage in the differentiation pathway for neutrophils. A system such as the HL-60 cell line [92] should prove useful for examining these changes in NuMA's distribution as well as the mechanisms by which these changes occur. These studies may provide insights into the function of NuMA.

Western blot analyses consistently showed NuMA to be a single band (Figure 14). However, two studies by other groups showed multiple bands on NuMA Western blots [39, 43]. One study claimed that a lower band was an isoform of NuMA that colocalized to domains enriched in splicing components [48]. It is possible that this "NuMA isoform" may be authentic, but to date, no other investigations could corroborate these findings. Another study claimed that the lower band may have been derived from alternatively spliced NuMA RNAs (see Chapter 6, [47]). This has not been directly demonstrated. Most studies found that the multiple bands would appear if the protein extract had undergone degradation (data not shown, [35, 37, 40 , 44, 47]).

Probing a Western blot of total protein from a variety of species resulted in detection of mammalian NuMA only (Figure 15). It is possible that there is no NuMA homologue in nonmammalian species such as Xenopus, but this is unlikely given that one group may have cloned the Xenopus homologue (Cleveland group, see [53]). It is more likely that

the antibodies used in this study do not crossreact with nonmammalian NuMA protein. It will be important to identify NuMA homologues in other species, especially ones amenable of genetic manipulations (such as yeast), in order to define a function for the protein.

NuMA was isolated as a phosphoprotein (Figure 17). What was surprising about this work was the co-precipitation of another phosphoprotein (Figure 17B, lane 4,5, [34]). This phosphoprotein was ~180 kDa and a similar protein appeared with pericentrin as well but was absent from the TPR lane. It was unlikely that the 180 kDa protein was a breakdown product of NuMA since this protein was not detected in Western analyses (Figure 17C, lane 1) or when phosphatase inhibitors were omitted (Figure 17A, lane 1). This work demonstrated that NuMA is a phosphoprotein in log-phase cells and leads into an examination of the phosphorylation of NuMA through the cell cycle (Chapter 5).

In examining NuMA from interphase and mitotic cells, there was a phosphorylation-induced shift in electrophoretic mobility in mitotic NuMA (Figures 18 and 19). The mitosis-specific phosphorylation events described here had previously gone unnoticed [40 , 43, 93], probably due to technical difficulties associated with detection of the phosphorylation-induced shift in electrophoretic mobility. Changes in the mobility of mitotic NuMA have been confirmed recently [53]. Such shifts in electrophoretic mobility occur in many [94, 95], but not all [65], phosphoproteins. Although it has been hypothesized that the addition of phosphate affects charge or tertiary structure, even under conditions of SDS-PAGE, the cause of the shifts remains unclear [94]. Other conditions can alter a proteins mobility on SDS-PAGE such as overloading a lane or

varying the salt concentration between lanes, however this study carefully avoided such conditions.

CHAPTER 5

CHARACTERIZATION OF PHOSPHORYLATION OF NUMA THROUGH THE CELL CYCLE

NuMA is a component of the nuclear matrix (Chapter 3) that redistributes to the spindle poles at mitosis (Chapter 4). While the function of NuMA is not known, it has been implicated in spindle organization during mitosis and nuclear reformation. Phosphorylation is thought to play a regulatory role in NuMA function [34, 42, 53]. In the work presented in Chapter 4, NuMA is shown to be a phosphoprotein that undergoes mitosis-specific phosphorylation events. The work in this chapter takes this observation and expands it by examining the phosphorylation of NuMA throughout the cell cycle using highly synchronized cells. The experimental strategy involves isolating populations of synchronized cells to obtain a careful temporal analysis of NuMA's phosphorylation state during its changing subcellular distribution.

When studying protein phosphorylation, one of the first questions to ask is which kinase acts on the protein, and then to determine which signal transduction pathway regulates the protein. A simple way to propose a candidate kinase is to find a temporal correlation of phosphorylation with known active kinases. This study carefully examines when and where the phosphorylation of NuMA occurs to try to find a pattern that correlates with the activity of a known mitotic kinase (such as cdc2 kinase at the mitotic spindle). By examining known substrates for kinases such as lamin B for cdc2 kinase while

examining NuMA's phosphorylation pattern may provide clues to the identity of the kinase that regulates NuMA at mitosis.

Another important question to address has to do with the functional consequence of this mitotic phosphorylation. Does the phosphorylation correlate to changes in the protein's subcellular distribution? Does it change NuMA's binding partners? Do properties such as solubility of the protein change in response to these events? Answers to these questions will contribute to understanding of how NuMA interacts with the nucleus and mitotic spindle as well as how proteins are regulated at mitosis.

The work in this chapter demonstrates that NuMA undergoes multiple phosphorylation events with similar timing to lamin B phosphorylation. The mitotic phosphorylation did not require spindle formation or correlate with a change in the protein's solubility. Dephosphorylation of NuMA occurred in two distinct steps, after lamin B assembled into the nuclear lamina in early G_1 and at the end of G_1. Based on the timing of the phosphorylation and dephosphorylation observed in this study, it is proposed that these events may play a role in aspects of the nucleus such as nuclear organization, transcription, or initiation of DNA replication at G_1/S.

RESULTS

A. Relationship of phosphorylation to spindle association.

The timing of NuMA's mitotic phosphorylation was consistent with its release from the nucleus as cells entered mitosis. In fact, it was strikingly similar to the phosphorylation-dependent disassembly of lamin B from the nuclear lamina [65]. However, it was also possible that the phosphorylation of NuMA occurred when it

redistributed to the mitotic spindle. To determine whether NuMA's mitotic phosphorylation was the result of its association with the spindle apparatus, the phosphorylation state of the protein was examined in nocodazole-treated cells in which microtubule spindle formation was prevented and cells were arrested cells in prometaphase [80]. NuMA was phosphorylated (Figure 20, lane N) to the same level as in metaphase cells with intact spindles (lane M) indicated by the consistent presence of bands with equivalent electrophoretic mobilities. In addition, a previously undetected doublet was resolved in both cases indicating that multiple phosphorylation events had occurred. These data demonstrated that NuMA did not require spindle formation to undergo these mitotic phosphorylation events and indicated that the phosphorylation occurred prior to spindle assembly in metaphase, while NuMA was still in the nucleus.

To ensure that the mitotic spindles were disrupted by nocodazole treatment and to determine where NuMA was located under these conditions, immunofluorescence microscopy was performed with NuMA and pericentrin antibodies. In non-drug treated mitotic cells, normal microtubule spindles were observed (shown in Figure 24B). NuMA and pericentrin were located at the spindle poles, and chromosomes were aligned on the metaphase plate (Figure 21A). In nocodazole-treated mitotic cells, the majority of NuMA was dispersed throughout the cell (Figure 21B), and no microtubule spindles were detected (Figure 21C). NuMA was also found in a variable number of foci randomly arranged in the cytoplasm and near chromosomes and centrosomes (Figure 21B, [37, 45]). Taken together, the biochemical and morphological data demonstrated that phosphorylation of NuMA occurred independently of its association with the spindle apparatus.

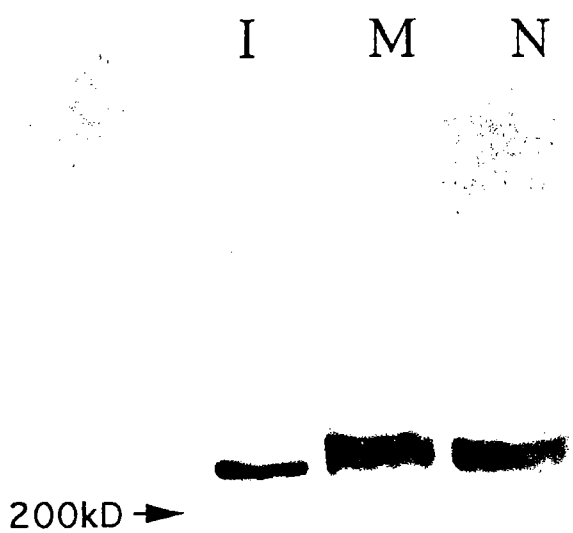

FIG. 20. NuMA phosphorylation in the absence of spindles. NuMA was immunoprecipitated from extracts prepared from interphase CHO cells (I), cells prepared by mitotic shake-off (M) and nocodazole-treated mitotic cells (N). Samples were blotted and probed. Molecular mass standards are indicated in kDa.

FIG. 21. NuMA localization in the absence of spindles. Cells were triple stained with a monoclonal antibody to pericentrin or tubulin (red), a polyclonal antibody to NuMA (green), and with DAPI (DNA, blue). In nondrug-treated mitotic cells (A) NuMA is centrosomal, partially overlapping with pericentrin (indicated by yellow signal). In nocodazole-treated mitotic cells (B), NuMA is largely cytoplasmic (green) with several foci near centrosomes (defined by pericentrin-red) and chromosomes. In nocodazole-treated mitotic cells stained with a tubulin antibody (red, panel C), no microtubule spindle is formed and NuMA is overlapping tubulin signal throughout the cell. Bar 5um.

B. Cell cycle profile of phosphorylation

To better understand the role of phosphorylation in NuMA localization and function, the changes in the phosphorylation state of NuMA were carefully examined through the cell cycle. To precisely correlate morphological and biochemical events during mitosis, synchronized cell populations were used (Figure 22A). Quantitative analysis demonstrated that a highly enriched population of mitotic cells (85%, Figure 22B) progressed synchronously through telophase and into G1 (98%). These synchronous populations were used to determine the phosphorylation state of NuMA (Figure 23) in relation to its intracellular distribution (Figure 24).

The results from Figure 20 demonstrated that NuMA was phosphorylated prior to its assembly onto the mitotic spindle suggesting that it had undergone phosphorylation before metaphase. This implies that phosphorylation occurs at prophase. It could, however, have been a gradual event beginning in G_2. To determine if NuMA underwent this phosphorylation event in G_2, NuMA from two different populations of G_2 cells were subjected to electrophoretic analysis for detection of shifted forms of the protein. In Figure 23A, both G_2 populations contained NuMA that migrated at the same position as NuMA from interphase cells. Therefore, NuMA was phosphorylated after G_2, in the G_2/M transition.

The synchronous cell populations described in Figure 22 were used to determine the dephosphorylation of NuMA in relation to its intracellular distribution. NuMA's metaphase phosphorylation state (Figure 23B, lane M) persisted through telophase (Figure 23B, lane T) even though the protein redistributed from the spindle poles (metaphase, Figure 24B) to the reforming nucleus at this time (Figure 24C), seen with the exact same cells used in Figure 23. With NuMA still present in reforming

A.

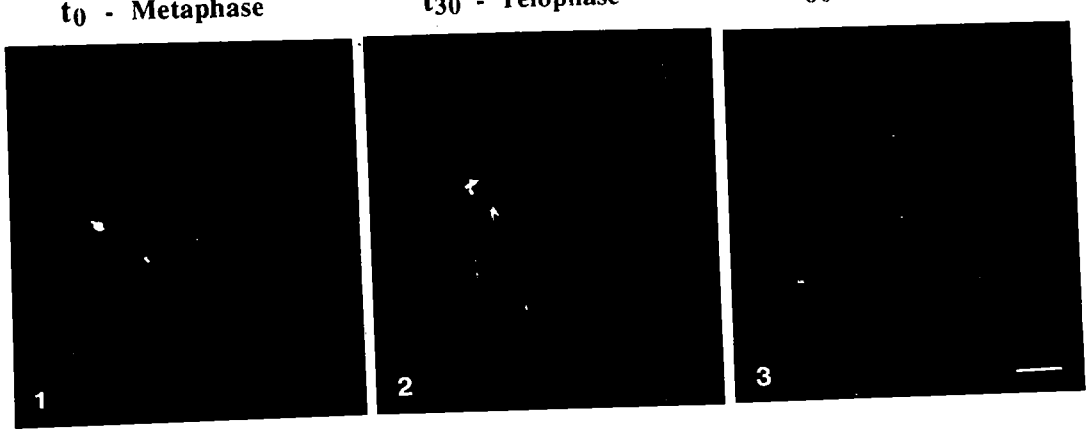

B.

Phase	0 minutes	60 minutes
Metaphase	85.7%	1.0%
Anaphase	10.2%	0.1%
Telophase	2.7%	0.3%
G1	1.4%	98.6%

FIG. 22. Preparation of highly synchronized mitotic cells. (A) Fluorescence micrographs of metaphase cells incubated in media for 0, 30, or 60 minutes (panels 1, 2, 3 respectively) at 37^{0}C. Cells were stained with a tubulin monoclonal antibody (red), and DAPI (blue). Bar, 20 mm. (B) Quantitation of the synchrony. More than 2000 cells were counted in five separate experiments and results are summarized as the percent of cell population in each phase.

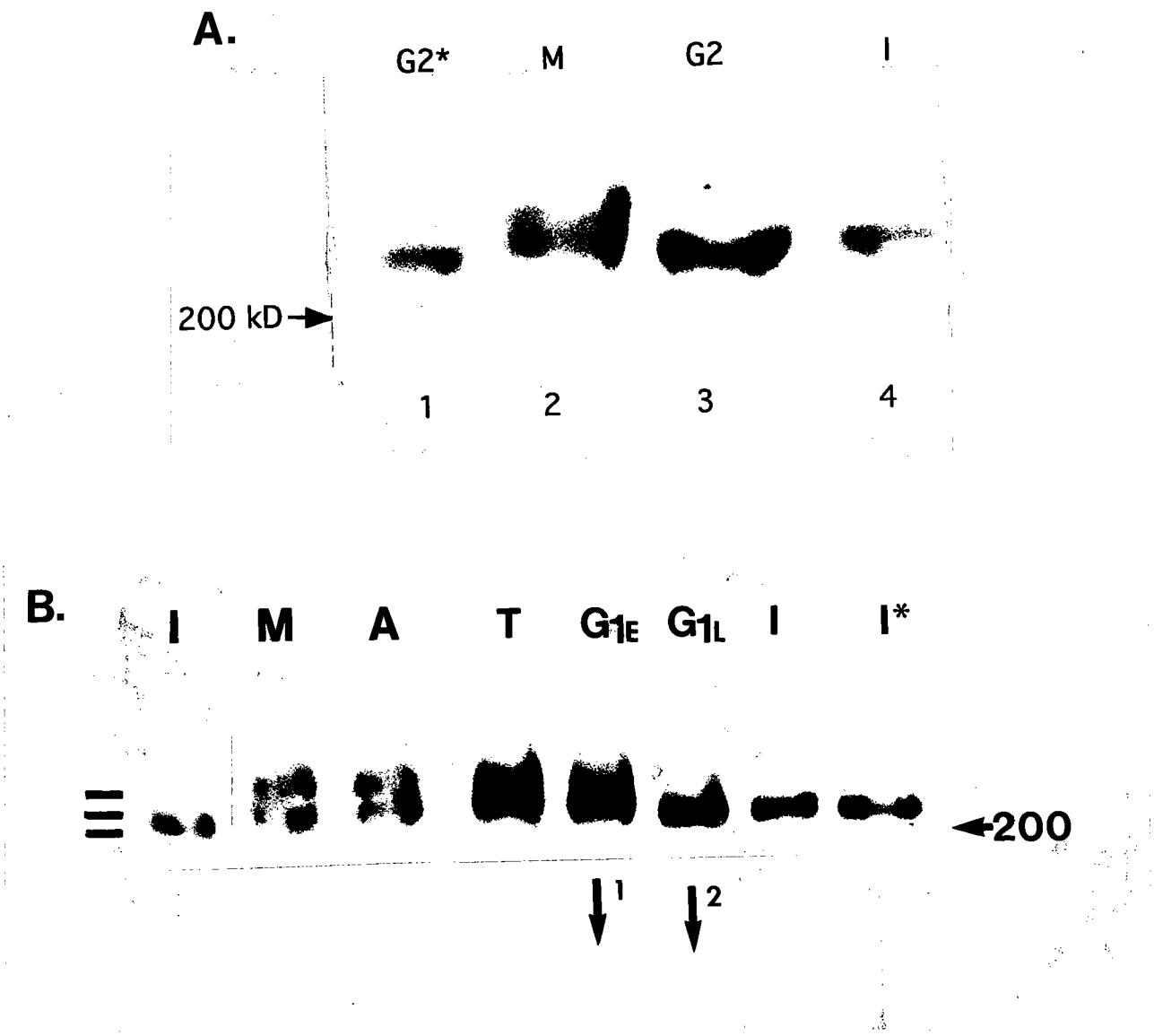

FIG. 23. Phosphorylation profile of NuMA during the cell cycle. NuMA was immunoprecipitated from cells at various stages of the cell cycle and Western blotted. (A) Total protein extracts were prepared from chinese hamster cells enriched for the G2 stage of the cell cycle. Lane 1. G2 cells(*) obtained from populations double blocked with mimosine and VM26. Lane 2 - mitotic (nocodazole blocked) cells; Lane 3 -G2 cells obtained after 8 hour release from mimosine block; Lane 4 - interphase cells. (B). Cell cycle stages: (I), interphase cells in log phase, (*I), previously frozen interphase cells, anaphase (t-10, A), telophase-t30 (T), early G_1-t_{60} (G_1E), and late G_1-t_{240}(G_1L). NuMA's downward shift in G_1E and G_1L is indicated by arrows 1 and 2. Three forms of NuMA were detected (three dashes).Molecular mass standards are indicated in kDa.

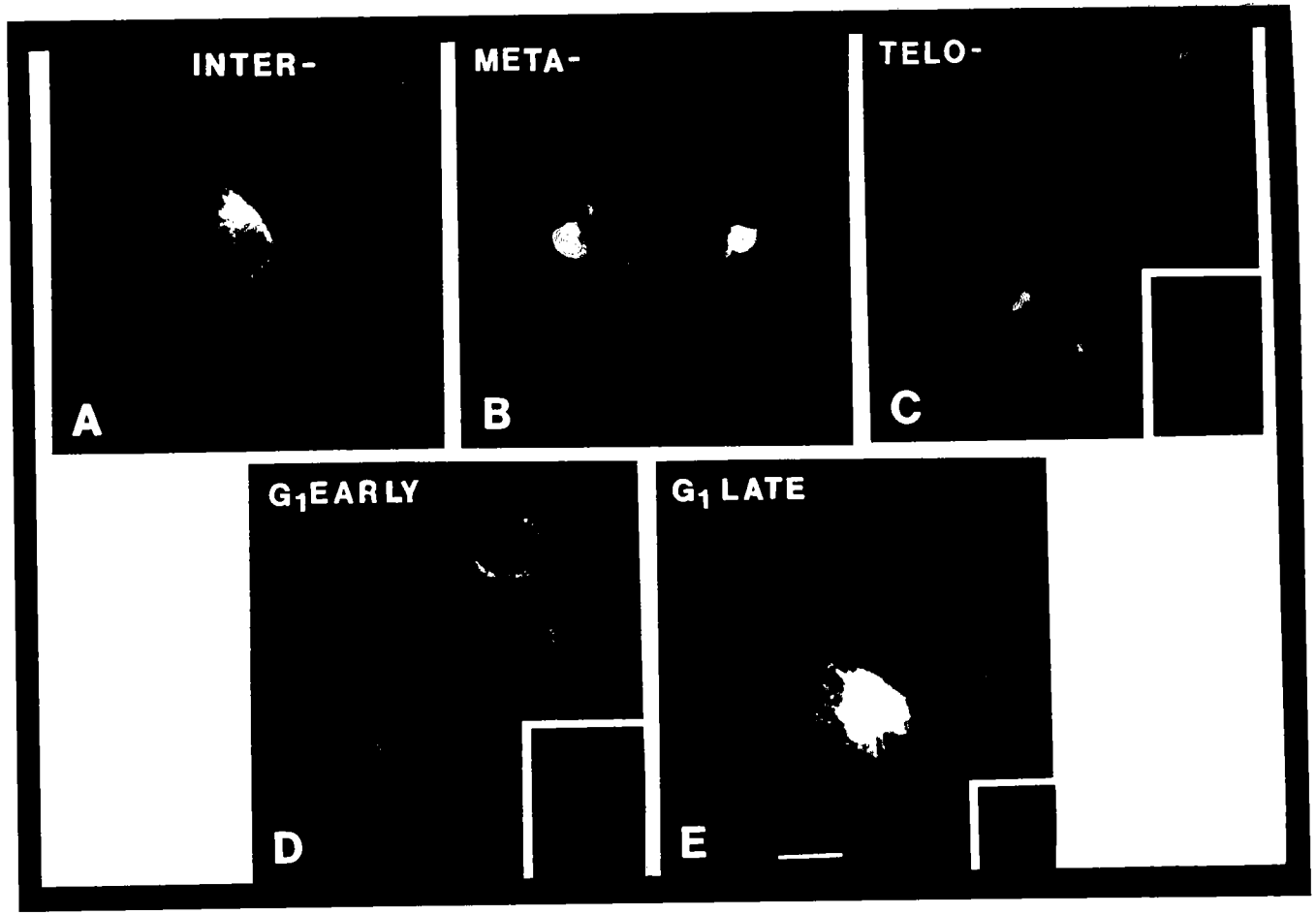

FIG. 24. NuMA distribution through the mitotic cell cycle. Immunofluorescence microscopy was used to localize NuMA (green), microtubules (red) and DNA (DAPI, blue) in synchronized cells as described in Fig. 5. NuMA is nuclear in interphase (A), relocates to the poles of the mitotic spindle at metaphase (B, yellow-green), and reassembles back into the reforming nucleus in telophase (C). Throughout G_1 (D,E), NuMA remains in the nucleus and does not undergo any detectable morphological changes. Inset (C,D,E) shows NuMA stain alone for each group of cells. Bar, 5μm.

nuclei at early G_1 (Figure 24D), the higher of the shifted bands became undetectable (Figure 23B, lane G_{1E}), apparently shifting down to the intermediate mobility as a result of dephosphorylation. Indeed, results from several experiments suggested that the intermediate band increases in intensity as the upper band is lost. The disappearance of the intermediate form occurred three hours later (Figure 23B, lane G_{1L}) and did not correlate with any changes in NuMA distribution or nuclear morphology (Figure 24E).

Since the timing of NuMA phosphorylation and disassembly from the nucleus were similar to lamin B [65], it seemed reasonable that the timing of dephosphorylation and reassembly of the two proteins would also be similar. Using the synchronized cell system (Figure 22), lamin B was distributed from the nucleus in interphase (Figure 25A), to the cytoplasm in mitosis (Figure 25B) and reassembled into the reforming nuclear lamina starting at telophase (Figure 25C), an event previously shown to require dephosphorylation [65, 67]. Thus, lamin B and NuMA both assemble into reforming nuclei at the same time. However, lamin B dephosphorylation correlated with its reassembly while NuMA dephosphorylation did not. Instead, dephosphorylation occurred in two separate events in G_1.

C. Relationship of mitotic phosphorylation and solubility.

NuMA was originally identified based on its presence in the nuclear matrix. Therefore, it should be an insoluble component of the nuclear fraction of a cell. Several previous studies concluded that NuMA was not sensitive to extraction with Triton-X100 [39, 41]. However, immunofluorescence studies through the cell cycle showed that the protein relocalized to the mitotic spindle in the G_2/M transition and back to the nucleus

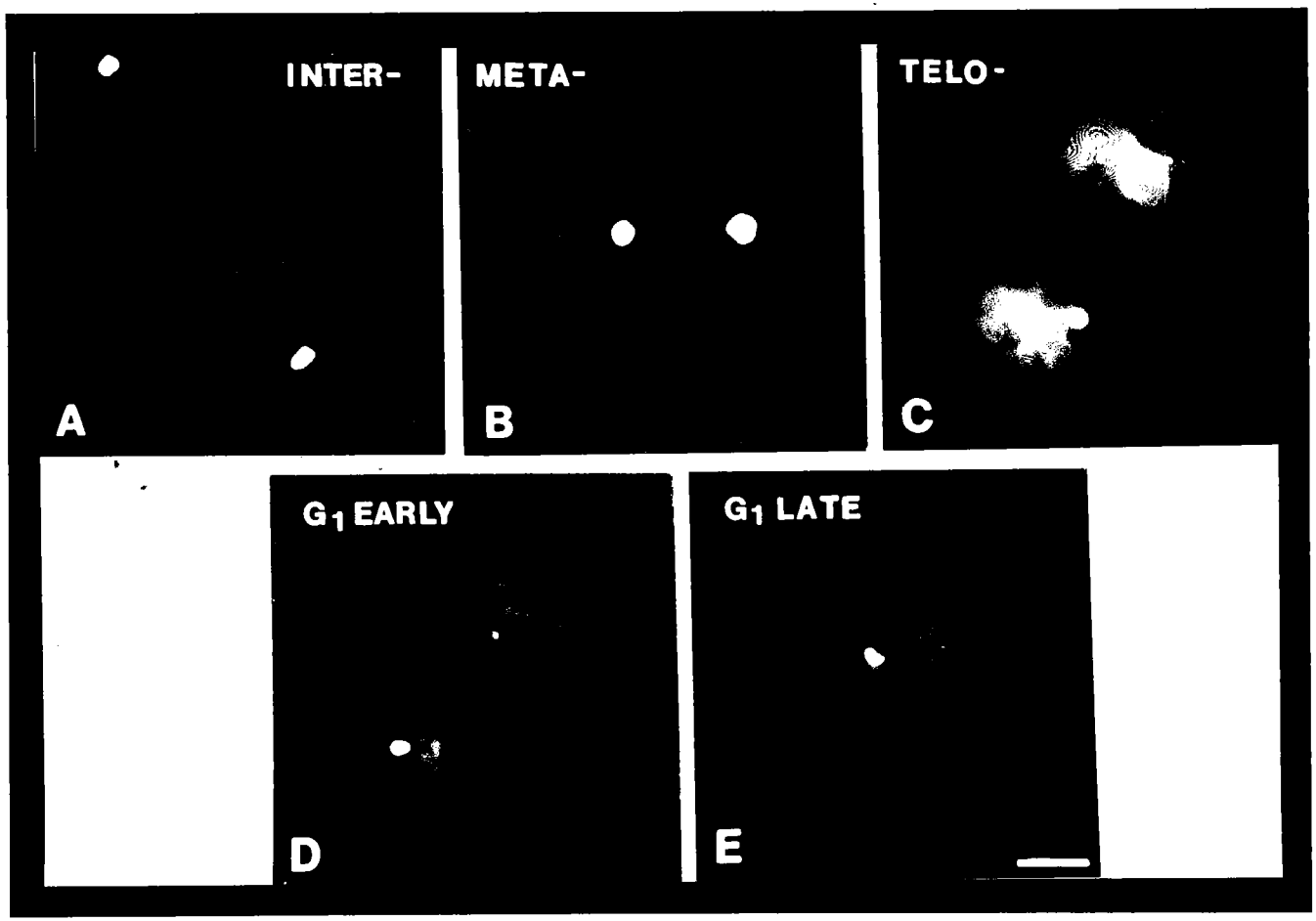

FIG. 25. Lamin B distribution through the cell cycle. Synchronized cells were stained for pericentrin (red), lamin B (green) and DNA (blue). Lamin B is in the nuclear lamina in interphase (A), redistributes to the cytoplasm in metaphase (B) and reassembles into the newly forming nuclear envelope (green rim) at telophase through G_1 (C,D,E). Pericentrin and DNA define the spindle area in metaphase cells. Bar, 5μm.

protein relocalized to the mitotic spindle in the G_2/M transition and back to the nucleus at telophase. This change in distribution suggests that NuMA may become soluble during specific transitions. There is precedent for other nuclear proteins becoming soluble during changes in their intracellular distribution. Lamin B undergoes mitotic-specific phosphorylation that affects the protein's solubility upon entry into mitosis [65]. One study found a soluble fraction of NuMA in mitotic cells [37]. Thus, it seemed reasonable that there would be a soluble form of NuMA at specific phases of the cell cycle.

To examine the solubility changes in NuMA, total protein from cells synchronized at telophase (T), early G_1, and interphase (I) were separated into a Triton-soluble and Triton-insoluble fractions. Cell equivalents of each extract were slot-blotted onto nylon membrane and probed with NuMA antibodies. There was a striking increase in the soluble fraction in telophase cells (Figure 26A). The change in solubility was quantitated in Table 3. At the beginning of telophase, when NuMA appears to leave the spindle, the majority of the protein was Triton-soluble (54.7%). This result suggested that NuMA was released from the spindle into the cytoplasm before reassembling into nuclei. Support for this idea is shown in the insoluble fractions (Figure 26A) where NuMA becomes increasingly insoluble as cells progress into G_1 and later in interphase.

Since there was soluble NuMA at telophase, it became of interest to see if the soluble form of the protein correlated with the phosphorylated forms (see Figure 23). Soluble and insoluble fractions were Western blotted to examine solubility of the shifted formsof NuMA. It was immediately apparent that the uppermost form (with slower electrophoretic mobility) was completely segregated to the insoluble fraction while the lower band was split between the soluble and insoluble fractions in telophase (Figure

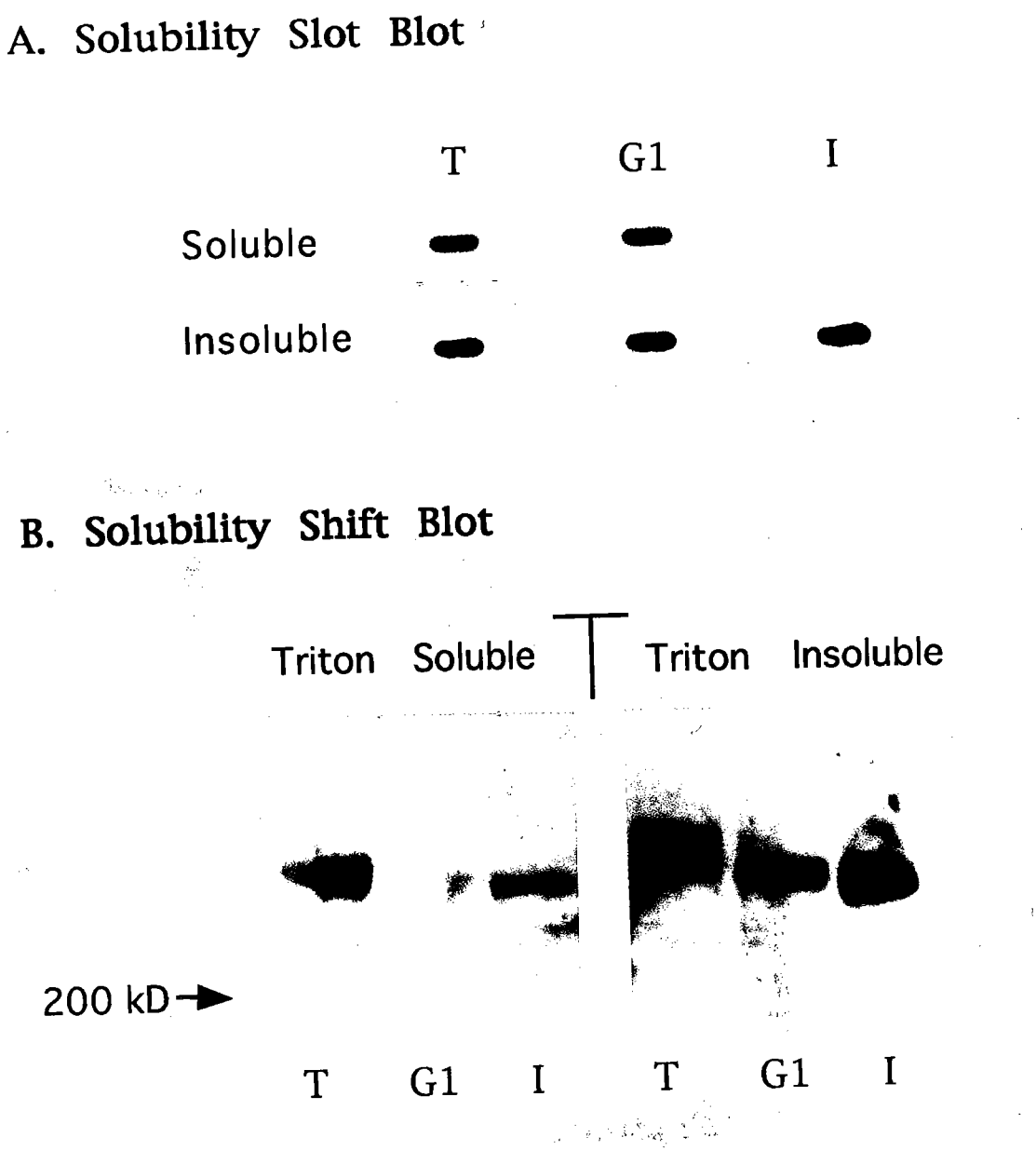

FIG. 26. NuMA has a soluble fraction. (A) Total CHO cell protein was slotted onto immobilon-P at equal cell number amounts, through the cell cycle. Membranes were analyzed by Western blot with the 204.41 NuMA monoclonal antibody and chemiluminescent detection. (B) Total soluble and insoluble fractions were subjected to analysis for the shifted forms of phosphorylated NuMA. Molecular weight markers are in kDa.

TABLE 3 - Quantitation of Soluble NuMA. A) Western blots of NuMA's soluble and insoluble fractions from 15 experiments were scanned into Photoshop and subjected to densitometric analysis with Scan Analysis software. Relative amounts are expressed as percentage of total NuMA at each stage of the cell cycle. B) graph illustrating changes in NuMA's solubility.

Table 3 - Quantitation of Soluble NuMA in the Reforming Nucleus

A)

Fraction	Telophase	G1	Interphase
Soluble	54.7%$^{+/-16.7}$	33.9%$^{+/-16.1}$	25.3%$^{+/-18.9}$
Insoluble	45.3%$^{+/-16.7}$	66.1%$^{+/-16.1}$	74.7%$^{+/-18.9}$

B)

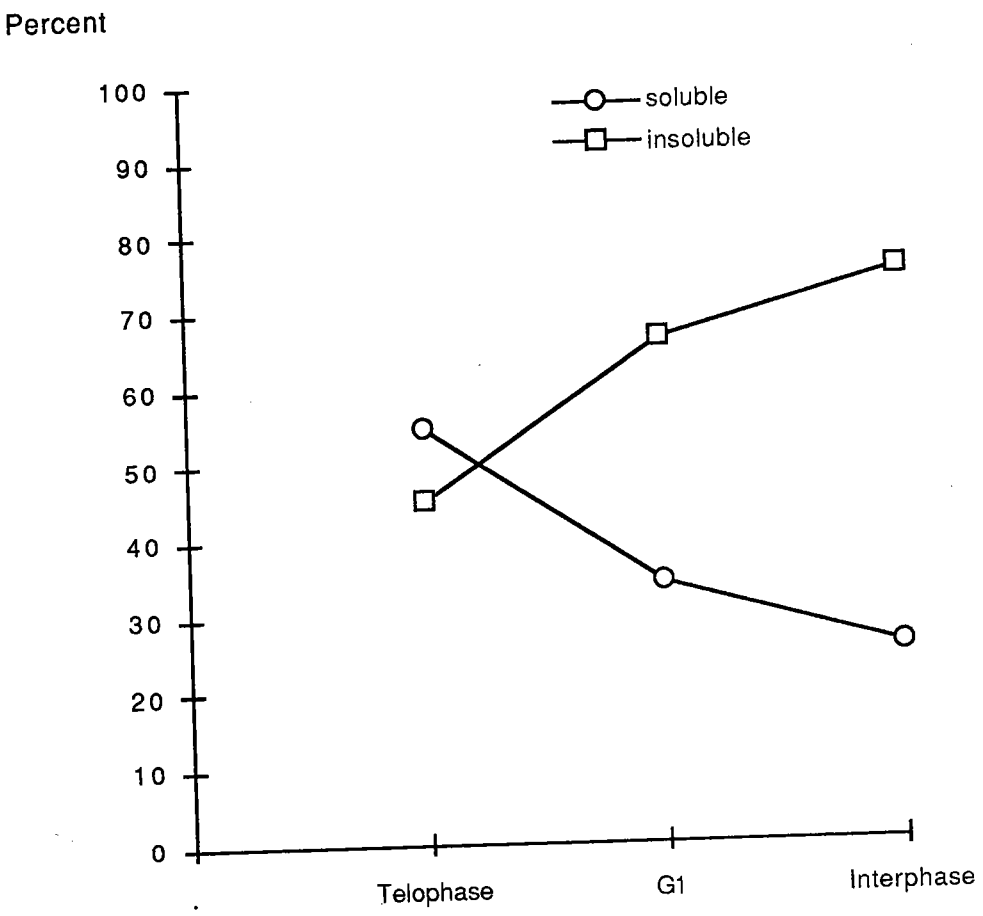

n=15

26B). This result demonstrated that there is no correlation between the mitosis-specific phosphorylation events and changes in NuMA solubility at mitosis.

NuMA became increasingly insoluble in cells from telophase to G_1 (45.5 to 66.1%) and G_1 to later interphase (66.1 to 74.7%, Figure 26 and Table 3). This insoluble fraction contained both phosphorylated forms of NuMA (Figure 26B, Triton-insoluble lane T), thus showing no correlation to phosphorylation state. The final question addressed in this study was whether NuMA had begun to reassociate with the reforming nuclear matrix at these stages of the cell cycle. Nuclear matrix proteins were examined from telophase (T), early G_1, and interphase (I) cells by Western blot analysis (Figure 27A) and NuMA was found in all three stages. Thus, a fraction of insoluble NuMA was part of the nuclear matrix as early as telophase. There was a formal possibility that the telophase cells contained up to 14% G_1 cell contaminants (Figure 22) which could have provided the nuclear matrix signal. Therefore, as a control, the telophase cells were spun onto coverslips and subjected to a nuclear matrix extraction procedure. These cells were fixed and stained with NuMA and tubulin antibodies. The image in Figure 27B demonstrates by immunofluorescence microscopy that NuMA was present in the reforming nuclear matrix in telophase. The results of the solubility study demonstrated that in telophase when nuclear reformation begins, NuMA has both soluble and insoluble forms that do not correspond to phosphorylated forms. The results of all cell cycle analyses have been compiled in Table 4.

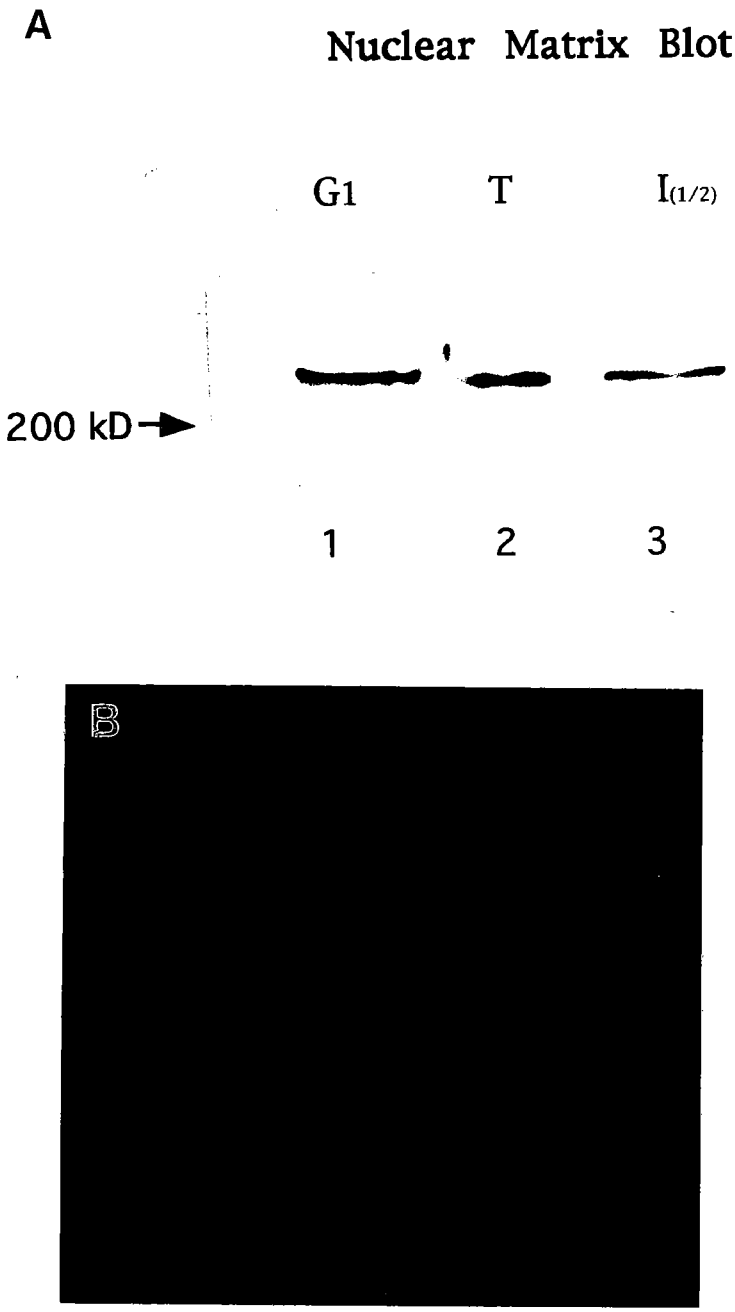

FIG. 27. NuMA in the reforming nuclear matrix. (A) Cells from telophase, early G1 and total interphase were used to prepare nuclear matrix fractions and analyzed for the presence of NuMA by Western blot. (B) CHO cells were subjected to a nuclear matrix extraction then fixed and stained with antibodies to NuMA (green) and tubulin (red).

NuMA Characteristics Through the Cell Cycle

	G_2	M	T	G_{1E}	G_{1L}	I_T
Distribution	nuclear	spindle pole	nuclear	nuclear	nuclear	nuclear
Phosphorylation State*						
Form 3		———	———			
Form 2		———	———	———	———	———
Form 1	———					
Total Solubility						
Soluble	NA	NA	54.7%	33.9%	NA	25.3%
Insoluble			45.5%	66.1%		74.7%
Solubility of Phosphorylated Forms**						
Form 3			____ i only			
Form 2			____ s and i	____ s and i		____ s and i
Form 1						

*Form 1 - interphase - lowest mobility form
Form 2 - mitotic - intermediate mobility form
Form 3 - mitotic - highest mobility form

**s - soluble
i - insoluble

NA - not available

Table 4. Summary. NuMA changes though the cell cycle. NuMA's distribution, phosphorylation, and solubility states represented schematically.

D. Discussion

NuMA phosphorylation.

These studies demonstrate that NuMA is a phosphoprotein in interphase that undergoes additional phosphorylation events at the G_2/M transition and is dephosphorylated post-mitotically in several steps. These phosphorylation events are believed to demarcate specific points in the 'life cycle' of NuMA that are important for its localization and/or function. Importantly, this work shows that the mitosis-specific phosphorylation is not a consequence of the protein's redistribution to the mitotic spindle and that dephosphorylation is not required for its release from the spindle. In fact, since both phosphorylation and dephosphorylation of NuMA seem to occur while the protein is in the nucleus, it appears that these post-translational modifications may regulate nuclear events.

Prior to its molecular identification, NuMA's distribution pattern was analyzed by many groups (reviewed in [38]). Most observations were the same as those in this study. One exception is an observation by one group that NuMA may not move from the spindle pole to the reforming nucleus until late telophase via transition through reformed nuclear pores [44]. This was clearly not the case in this and other studies, as NuMA was detected on condensed chromosomes in early telophase (Figure 24C, [32, 34, 42]), well before the nuclear envelope reformation was complete (Figure 25C, [65]). This precise cell cycle analysis was possible using highly synchronized cells (Figure 22).

NuMA phosphorylation and spindle pole association.

NuMA interacts with both microtubules and centrosomes at the mitotic spindle. For example, intact microtubules are required for the observed cell cycle specific distribution pattern [32, 34, 37, 39]. Drug-induced depolymerization of spindle microtubules results in the redistribution of NuMA throughout the cytoplasm and into heterogeneously-sized cytoplasmic foci (Figure 21B, [32 , 37, 39]). In addition, NuMA is found at the center of taxol-induced microtubule asters [40, 50], and in purified microtubule fractions [40, 50]. NuMA's association with centrosomes is discussed in Chapter 6. Many NuMA antibody microinjection and overexpression studies have resulted in aberrant spindle formation and function (reviewed in [38]). These data suggest that NuMA plays a role in the formation and stability of the mitotic spindle. A natural assumption from these observations is that the mitotic phosphorylation events that we describe here affect NuMA's ability to associate with the mitotic spindle.

Although this study examines only a specific set of mitotic phosphorylation events, NuMA may undergo many other phosphorylation events not detected in these assays. The results in this chapter do not support a role for the mitotic phosphorylation events defined by altered electrophoretic mobility of NuMA, in spindle association for several reasons. First, phosphorylation occurs at the time of nuclear disassembly, between G_2 and prometaphase, prior to spindle assembly. Second, in mitotic cells lacking spindles, phosphorylation still occurs. Third, if phosphorylation is required for spindle association then one would expect that dephosphorylation would be required for dissociation of NuMA in telophase. However, dephosphorylation of NuMA occurs much later, in G_1. Thus, it is unlikely that the phosphorylation and dephosphorylation events observed in this study are involved in NuMA's spindle association and dissociation.

However, it is formally possible that other phosphorylation events, not detected by these analyses, play a role in spindle association, assembly, or stabilization.

NuMA phosphorylation and nuclear function.

NuMA's phosphorylation occurs at roughly the same time that it disassembles from the nucleus. These events are mechanistically and temporally analogous to the phosphorylation-driven disassembly of lamin B from the nuclear lamina [65]. Thus, it is possible that NuMA's disassembly from the nucleus at mitosis is also driven by phosphorylation. Assembly of lamin B into the reforming nuclear lamina occurs concomitantly with its dephosphorylation [65, 69, 70]. In contrast, reassembly of NuMA into the nucleus does not correlate with its dephosphorylation. In fact, the first dephosphorylation event occurs after NuMA is already nuclear (Figure 24D) and partially associated with the nuclear matrix (Figure 27). The dephosphorylation is complete within 10 minutes (data not shown). This rapid dephosphorylation does not correlate with NuMA's localization, its detergent-solubility (Figure 26B) or with changes in nuclear morphology.

The second dephosphorylation event takes place near the G_1/S boundary as demonstrated by the rapid (not shown) and quantitative shift in electrophoretic mobility (Figure 23B). It is possible that dephosphorylation of NuMA plays a role in the activation of DNA replication which occurs at this time. In support of this idea are recent data demonstrating that NuMA binds to matrix attachment regions (MARs) [96], which are DNA sequences believed to be responsible for organizing chromatin into constrained loops. MARs have been implicated in the regulation of DNA replication and transcription [23, 97, 98].

Based on these results, the dephosphorylation events described in this study may play a role in the assembly of NuMA into higher order structures in the nucleus or in other nuclear events not detectable in this analysis. Dephosphorylation drives the assembly of other coiled-coil proteins such as lamin B [66], vimentin [99], and others [100, 101]. NuMA is predicted to form a 200 nm filament based on the amino acid sequence [42]. Indeed, a recent ultrastructural study provides evidence that recombinant full-length protein forms a 207 nm parallel double-stranded coiled-coil [84]. This study did not find evidence for filament assembly, however. There is some debate over whether NuMA will form filamentous structures via the coiled coil domain since the sequence lacks periodicity in acidic and basic residues [85]. However, the complex phosphorylation pattern of NuMA in both mitosis and interphase described here may contribute to changes in charge distribution and tertiary structure of the molecule which would enable the protein to form filaments.

Regulation of NuMA phosphorylation and dephosphorylation.

The kinases and phosphatases that act on NuMA at different stages of the cell cycle have not been identified. The mitosis-specific cdc2 kinase may regulate the disassembly of NuMA from the nucleus as it does the disassembly of lamin B from the nuclear lamina [67]. Although site-directed mutagenesis of the consensus sites for cdc2 kinase in NuMA affects its subcellular distribution [53], there has been no direct demonstration that NuMA is a substrate for cdc2 kinase. This will require the careful identification of the specific amino acids on NuMA that are phosphorylated at mitosis. There are other cell cycle-specific phosphoproteins such as DNA topoisomerase II that have been mis-identified as in vivo substrates for cdc2 kinase [102-105]. While this protein is capable of being phosphorylated by cdc2 in vitro, activation of the enzymatic activity in vivo was regulated by protein kinase c and casein kinase II phosphorylation events.

CHAPTER 6

CONCLUSIONS AND FUTURE DIRECTIONS

This dissertation is a study of the nuclear matrix and mitotic spindle protein NuMA. In this work, the partial cDNA for NuMA was cloned and sequenced using nuclear matrix-specific antibodies and molecular biological methodologies. The cDNAs and antibodies were used to characterize the gene, mRNA, and protein. NuMA was found to be a single copy gene located on human chromosome 11q13. The mRNA profile consisted of a major 7.2 kb species and a minor 8.0 kb species with alternatively spliced exons suggesting that one or more RNA isoforms were produced from the NuMA gene. A single phosphoprotein of 250 kDa was detected by immunoprecipitation and Western blot analysis on interphase mammalian cells. Immunofluorescence microscopy demonstrated that NuMA oscillated between the nucleus and the mitotic spindle pole during the cell cycle.

The nature and distribution of NuMA through mitosis was studied in greater detail. Highly synchronized cell populations were used to demonstrate that the protein was released from the nucleus at the G_2/M transition concomitant with a phosphorylation event. The mitotic-specific phosphorylation state of NuMA did not change as the protein transiently associated with the mitotic spindle (metaphase) or as it became a partially insoluble nuclear component (telophase). NuMA was dephosphorylated in two steps, in early G_1 and in late G_1. These changes in phosphorylation state did not correlate with changes in the protein's localization or solubility but may reflect changes in the function of NuMA in the G_1 nucleus. This work contributes to the validation of the nuclear matrix and opens avenues to identify other nuclear matrix proteins based on interactions with NuMA. Through these studies, we can begin to understand the cell

cycle regulation of structural proteins and mechanisms of nuclear spindle organization.

There are at least three pivotal observations from this study that provide the basis for exciting future studies: 1. the cell cycle specific phosphorylation of NuMA (Figure 23), 2. the identification of a phosphorylated NuMA binding protein (Figure 17), and 3. the localization of NuMA to the interphase centrosomes (see below, Figure 28). These potential studies will be addressed individually below.

The observation that NuMA is phosphorylated in a cell cycle-dependent manner (Figure 23) opens several lines of investigation. Phosphoamino acid analysis and tryptic peptide mapping should be done to characterize the two mitosis-specific phosphorylation states. Identification of the specific amino acids that are phosphorylated may prove useful in the identification of the kinases and phosphatases that act on NuMA. Future investigations designed to elucidate the mechanism of phosphorylation and dephosphorylation of NuMA will, in turn, lead to an understanding of the regulation of NuMA function. Finally, identification of enzymes that regulate NuMA function may provide valuable insights into how the protein is coupled to other cell cycle events which could also lead to information about its role in spindle and nuclear organization.

The second intriguing observation is that NuMA coprecipitates another phosphorylated protein of approximately 180 kDa (Figure 17). The identity of the 180 kDa protein is unknown, but it is not related to NuMA by Western analysis with polyclonal antibodies. Interestingly, the 180 kDa protein co-precipitates with pericentrin, another centrosome protein but not with TPR, a nuclear pore protein. If the same 180 kDa

protein is co-precipitated by both NuMA and pericentrin, it may be a highly phosphorylated centrosomal component that interacts with both proteins. It could be a kinase that phosphorylates NuMA and pericentrin to target them to the centrosome or regulate common functional activities. Surprisingly, the 180 kDa phosphoprotein is not present in the mitotic NuMA immunoprecipitation (Figure 18, lane M). It is well known that NuMA redistributes to the centrosome at mitosis (Figures 12, 21, and 24), so it is surprising that the 180 kDa band is not present in these immunoprecipitations. However, it has been suggested that there is a fraction of NuMA at the centrosome throughout the cell cycle (see below). Tryptic peptide analysis of the 180 kDa band from both NuMA and pericentrin immunoprecipitations may provide the necessary information to determine whether they are the same or different proteins. Future studies could then involve identification of this protein through purification and microsequencing. Finally, identification of the 180 kDa protein by ^{32}P-labeling and immunoprecipitation suggests that this approach could be used in identifying other NuMA-interacting proteins in both the nucleus and centrosomes.

The final future direction is derived from preliminary observations suggesting that a fraction of NuMA is always present in isolated centrosomes (Figure 28). During the examination of nocodazole-treated cells (Figure 21), foci of NuMA staining were often observed near or on the centrosome. To further analyze this potential association, centrosomes were isolated from log-phase CHO cells and co-stained for NuMA, tubulin, and pericentrin. NuMA was detected in each centrosome (Figure 28B) stained with pericentrin (Figure 28A). The centrosome localization of NuMA was more striking in preparations where microtubules were regrown from isolated centrosomes and then fixed and co-stained with tubulin (Figure 28C) and NuMA antibodies (Figure 28D).

FIG. 28. A portion of NuMA is present in centrosomes at all cell cycle stages. Centrosome isolated from log-phase CHO cells (Doxsey, 1994) were spun onto coverslips and costained with pericentrin (A) and NuMA (B). Isolated centrosomes from which microtubules were regrown (Doxsey, 1994), were stained for tubulin (C) and NuMA (D). The images in panels C and D were merged in panel E to show overlap (yellow) with tubulin (Red) and NuMA (Green). Bar 5um.

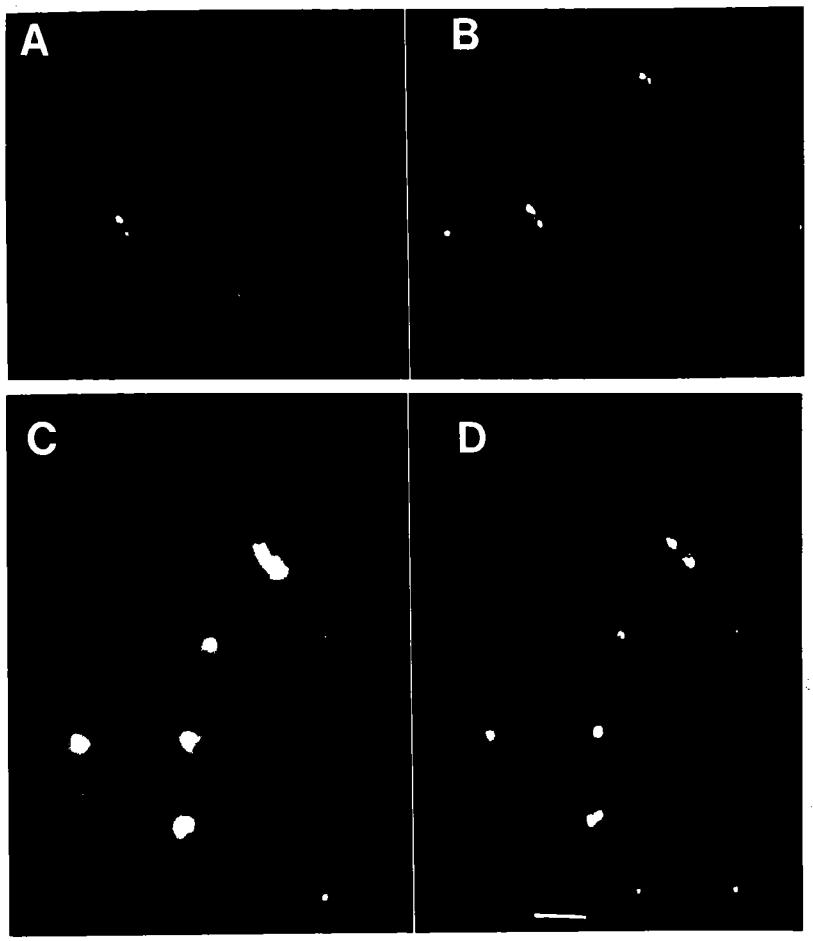
A
B
C
D
E

Under these conditions, NuMA was located at the center of each microtubule aster (overlap seen in Figure 28E).

This and other data suggests that a fraction of NuMA is associated with the centrosomes throughout the cell cycle for the following reasons. First, the centrosome isolation protocol involves depolymerizing actin and microtubules and releasing centrosomes into a Triton-soluble fraction [106] separated from the insoluble fraction of NuMA in the nuclear matrix, which remains on the dish. The cells were rapidly lysed in a large volume to minimize interactions with non-centrosomal components. Thus, it is unlikely that nuclear NuMA would contact the centrosomes during the isolation procedure, and even less likely that NuMA would contact every centrosome (Figure 28). Finally, there have been other localization studies identifying NuMA at the centrosome throughout the cell cycle [39, 40, 47] and at the minus end of taxol-stabilized microtubule asters [40].

Results from a recent study suggest that there are NuMA isoforms that exist as resident centrosome components. It is possible that our antibody crossreacts with this form as it is a polyclonal serum raised against three separate parts of the protein independently and pooled together. Two alternatively spliced cDNA constructs that are C-terminal variants of NuMA mRNA, when expressed in mammalian cells localized specifically to the centrosome [47]. This result suggests that these isoforms of NuMA reside in the centrosome in small amounts in vivo. There may be specific fixation conditions necessary to preserve their association or antigenicity. Or they may need to be unmasked by removing cytoplasmic microtubules or other proteins. Consistent with this idea is the increased accessibility of antibodies to centrosome antigens after microtubule depolymerization, treatment with millimolar amounts of calcium [39], or

treatment with reducing agents [107]. This would also explain why some images of NuMA at the mitotic centrosome have negatively stained centers (Figure 12H). Resident centrosomal NuMA may not be accessible at intact mitotic spindles Future studies such as Western analysis of purified centrosomes should contribute to our understanding of the relationship of NuMA with the centrosome.

NuMA is an unusual and intriguing molecule with a complex intracellular distribution and cell cycle phosphorylation pattern. Results from these and other future studies may provide crucial information about NuMA's contribution to nuclear, spindle, and centrosome function.

CHAPTER 7

REFERENCES

1. Berezney, R., and Coffey, D.S., Identification of a nuclear protein matrix. *Biochem. Biophys. Res. Comm.*, 1974. **60**: p. 1410-1417.

2. Peters, K.E., Okada, T.A., and Comings, D.E., *Eur. J. Biochem.*, 1982. **129**: p. 221-232.

3. Hodge, L.D., Mancini, P., Davis, F.M., and Heywood, P., Nuclear matrix of Hela S3 cells. Polypeptide composition durring adenovirus infection and in phases of the cell cycle. *J. Cell Biol.*, 1977. **72**: p. 194-208.

4. Capco, D.G., Wan, K.M., and Penman, S., The nuclear matrix: three-dimensional architecture and protein composition. *Cell*, 1982. **29**: p. 847-858.

5. Fey, E.G., Wan, K., and Penman, S., Epithelial cytoskeletal framework and nuclear matrix-intermediate filament scaffold: three-dimensional organization and protein composition. *J. Cell Biol.*, 1984. **98**: p. 1973-1984.

6. Fey, E.G., Krochmalnic, G., and Penman, S., The non-chromatin substructures of the nucleus: The ribonucleoprotein (RNP)-containing and RNP-depleted matrices analyzed by sequential fractionation and resinless electron microscopy. *J. Cell Biol.*, 1986. **102**: p. 1654-1665.

7. Kaufman, S.H., and Shaper, J.H., A subset of non-histone nuclear proteins reversibly stabilized by the sulfhydryl cross-linking reagent tetrathionate: polypeptides of the internal nuclear matrix. *Exp. Cell Res.*, 1984. **155**: p. 477-495.

8. Pieck, A.C.M., van der Velden, H.M.W., Rijken, A.A.M., Neis, J.M., and Wanka, F., Protein composition of the chromosomal scaffold and interphase nuclear matrix. *Chromosoma*, 1985. **91**: p. 137-144.

9. He, D., Nickerson, J.A., and Penman, S., Core filaments of the nuclear matrix. *J. Cell Biol.*, 1990. **110**: p. 569-580.

10. Berezney, R., and Coffey, D.S., Nuclear matrix isolation and characization of a framework structure from rat liver nuclei. *J. Cell Biol.*, 1977. **73**: p. 616-637.

11. Mirkovitch, J.M., M-.E., amd Laemmli, U.K., Organization of the higher-order chromatin loop: Specific DNA attachment sites on nuclear scaffold. *Cell*, 1984. **39**: p. 223-232.

12. Jackson, D.A., and Cook, P.R., Transcription occurs at the nucleoskeleton. *EMBO J.*, 1985. **4**: p. 919-925.

13. Fey, E.G., Bangs, P., Sparks, C., and Odgren, P., The nuclear matrix: defining structural and functional roles. *Crit. Rev. Euk. Gene Exp.*, 1991. **1**: p. 127-143.

14. Nelson, W.G., Pienta, K.J., Barrack, E.R., and Coffey, D.S., The role of the nuclear matrix in the organization and function of DNA. *Annu. Rev. Biophys. Chem.*, 1986. **15**: p. 457-475.

15. Schroder, H.C., Trolltsch, D., Friese, U., Bachmann, M., and Mullerrr, W.E.G., Mature mRNA is selectively released from the nuclear matrix by an ATP/dATP-dependent mechanism sensitive to topoisomerase inhibitors. *J. Biol. Chem.*, 1987. **262**: p. 8917.

16. Verheijen, R., van Venrooji, W., and Raemaekers, F., The nuclear matrix: structure and composition. *J. Cell Sci.*, 1988. **90**: p. 11-36.

17. Cook, P.R., The nucleoskeleton: artefact, passive framework, or active site? *J. Cell Sci.*, 1988. **90**: p. 1-6.

18. Berezney, The nuclear matrix: A heuristic model for investigating genomic organization and function in the cell nucleus. *J. Cell. Biochem.*, 1991. **47**: p. 109-123.

19. van Driel, R., Humbel, B., and de Jong, L., The nucleus: A black box being opened. *J. Cell. Biochem.*, 1991. **47**: p. 311-316.

20. von Kries, J.P., Buhrmester, H., and Stratling, W.H., A matrix/scaffold attachment region binding protein: identification, purification, and mode of binding. *Cell*, 1991. **64**: p. 123-35.

21. Pardoll, D.M., Vogelstein, B. and Coffey, D.S., A fixed site of DNA replication in eucaryotic cells. *Cell*, 1980. **19**: p. 527-536.

22. Berezney, R., and Coffey, D.S., Nuclear protein matrix: association with newly synthesized DNA. *Science*, 1975. **189**: p. 291-292.

23. Razin, S.V., Vassetsky, Y.S., and Hancock, R., Nuclear matrix attachment regions and topoisomerase II binding and reaction sites in the vicinity of a chicken DNA replication origin. *Biochem. Biophys. Res. Commun.*, 1991. **177**: p. 265-270.

24. Jackson, D.A., and Cook, P.R., Replication occurs at a nucleoskeleton. *EMBO J.*, 1 986. **5**: p. 1403-1410.

25. Nakayasu, H., and Berezney, R., Mapping replication sites in the eucaryotic cell nucleus. *J. Cell Biol.*, 1989. **108**: p. 1-11.

26. Hozak, P., Bassim Hassan, A., Jackson, D.A., and Cook, P.R., Visualization of replication factories attached to a nucleoskeleton. *Cell*, 1993. **73**: p. 361-373.

27. Herman, R., Weymouth, L., and Penman, S., Heterogeneous nuclear RNA-protein fibers in chromatin-depleted nuclei. *J. Cell Biol.*, 1978. **78**: p. 663-674.

28. Xing, Y., and Lawrence, J.B., Preservation of specific RNA distribution within chromatin-depleted nucllear substructure demonstrated by in situ hybridization coupled with biochemical fraction. *J. Cell Biol.*, 1991. **112**: p. 1055-1063.

29. Zeitlin, S., Parent, A., Silverstein, S., and Efstratiadis, A., Pe-mRNA splicing and the nuclear matrix. *Moll. Cell. Biol.*, 1987. **7**: p. 111-120.

30. Roberge, M., Dahmus, M.E., and Bradbury, E.M., Chromosomal loops: Nuclear matrix organization of transcriptionally active and inactive RNA polymerases in Hela nuclei. *J. Mol. Bio.*, 1988. **201**: p. 545-555.

31. Berezney, R., *Organization and functions of the nuclear matrix*, in *Nonhistone Chromosomal Proteins: Structural Associations*. 1984, CRC Press: Boca Raton, FL. p. 119-180.

32. Lydersen, B.K., and Pettijohn, D.E., Human-specific nuclear protein that associates with the polar region of the mitotic apparatus: Distribution in a human/hamster hybrid cell. *Cell*, 1980. **22**: p. 489-499.

33. Price, C.M., McCarty, G.A., and Pettijohn, D.E., NuMA protein is a human autoantigen. *Arthritis Rheum.*, 1984. **27**: p. 774-779.

34. Price, C.M., and Pettijohn, D.E., Redistribution of the nuclear mitotic apparatus protein (NuMA) during mitosis and nuclear assembly. *Exp. Cell Res.*, 1986. **166**: p. 295-311.

35. Pettijohn, D.E., M. Henzel, and Price, C., Nuclear proteins that become part of the mitotic apparatus: A role in nuclear assembly. *J. Cell Sci. Suppl.*, 1984. **1**: p. 187-201.

36. Van Ness, J., and Pettijohn, D.E., Specific attachment of Nuclear Mitotic Apparatus protein to metaphase chromosomes and mitotic spindle poles: Possible function in nuclear reassembly. *J. Mol. Biol.*, 1983. **171**: p. 175-205.

37. Kallajoki, M., Weber, K., and Osborn, M., A 210 kDa nuclear matrix protein is a functional part of the mitotic spindle; a microinjection study using SPN monoclonal antibodies. *Embo J.*, 1991. **10**(11): p. 3351-62.

38. Compton, D.A., and Cleveland, D.W., NuMA, a nuclear protein involved in mitosis and nuclear reformation. *Curr. Opin. Cell Biol.*, 1994. **6**(3): p. 343-346.

39. Tousson, A., Zeng, C., Brinkley, B. R., and Valdivia, M. M., Centrophilin: a novel mitotic spindle protein involved in microtubule nucleation. *J. Cell Biol.*, 1991. **112**(3): p. 427-40.

40. Maekawa, T., Leslie, R., Kuriyama, R, Identification of a minus end-specific microtubule-associated protein located at the mitotic poles in cultured mammalian cells. *Eur.J. Cell Biol.*, 1991. **54**: p. 255-267.

41. Compton, D.A., Yen, T.J., and Cleveland, D.W., Identification of novel centromere/kinetochore-associated proteins using monoclonal antibodies generated against Human mitotic chromosome scaffolds. *J. Cell Biol.*, 1991. **112**: p. 1083-1097.

42. Yang, C.H., Lambie, E. J., and Snyder, M., NuMA: an unusually long coiled-coil related protein in the mammalian nucleus. *J. Cell Biol.*, 1992. **116**(6): p. 1303-17.

43. Tang, T.K., Tang, C. J., Chen, Y. L., and Wu, C. W., Nuclear proteins of the bovine esophageal epithelium. II. The NuMA gene gives rise to multiple mRNAs and gene products reactive with monoclonal antibody W1. *J. Cell Sci.*, 1993. **104**(Pt 2): p. 249-60.

44. Compton, D.A., Szilak, J., and Cleveland, D.W., Primary structure of NuMA, an intranuclear protein that defines a novel pathway for segregation of proteins at mitosis. *J. Cell Biol.*, 1992. **116**: p. 1395-1408.

45. Maekawa, T., and Kuriyama, R., Primary structure and microtubule-interacting domain of the SP-H antigen: a mitotic map located at the spindle pole and characterized as a homologous protein to NuMA. *J. Cell Sci.*, 1993. **105**: p. 589-600.

46. Auer-Grumbach, P., Achleitner, B., Epidemiology and clinical associations of NuMA (nuclear mitotic apparatus protein) autoantibodies. *J.Rheumato.*, 1994. **21**: p. 1779-1781.

47. Tang, T.K., Tang, C.C., Chao, Y., and Wu, C., Nuclear mitotic apparatus protein (NuMA): spindle association, nuclear targeting and differential subcellular localization of various NuMA isoforms. *J. Cell Sci.*, 1994. **107**: p. 1389-1402.

48. Zeng, C., He, D., Berget, S., and Brinkley, B., Nuclear-Mitotic Apparatus Protein: A Structural Protein Interface Between the Nucleoskeleton and RNA Splicing. *PNAS USA*, 1994. **91**: p. 1505-1509.

49. Compton, D.A. and D.W. Cleveland, NuMA is required for the proper completion of mitosis. *Journal of Cell Biology*, 1993. **120**(4): p. 947-57.

50. Kallajoki, M., Weber, K., and Osborn, M., Ability to organize microtubules in taxol-treated mitotic PtK2 cells goes with the SPN antigen and not with the centrosome. *J. Cell Sci.*, 1992. **102**(Pt 1): p. 91-102.

51. Yang, C.H., and Snyder, M., The nuclear-mitotic apparatus protein is important in the establishment and maintenance of the bipolar mitotic spindle apparatus. *Mol. Biol. Cell*, 1992. **3**(11): p. 1259-67.

52. Kallajoki, M., Herborth, J., Weber, K., and Osborn, M., Microinjection of a Monoclonal Antibody against SPN Antigen, Now Identified by Peptide Sequences as the NuMA Protein, Induces Micronuclei in Ptk2 Cells. *J. Cell Sci.*, 1993. **104**: p. 139-150.

53. Compton, D.A., and Luo, C., Mutation of the predicted $p34^{cdc2}$ phosphorylation sites in NuMA impair the assembly of the mitotic spindle and block mitosis. *J. Cell Sci.*, 1995. **108**: p. in press.

54. Zeng, C., He, D., and Brinkley, B.R., Localization of NuMA Protein Isoforms in the nuclear matrix of mammalian cells. *Cell Mot. Cyto.*, 1994. **29**: p. 167-176.

55. McIntosh, J.R., and Koonce, M.P., Mitosis. *Science*, 1989. **246**: p. 622-628.

56. Earnshaw, W.C., and Pluto, A.F., Mitosis. *Bioessays*, 1994. **16**: p. 639-643.

57. Alberts, B., Bray, D., Lewis, J., Raff, M., Roberts, K., and Watson, J.D., *Mitosis*, in *Molecular biology of the cell*. 1994, Garland Publishing, Inc: New York. p. 919-926.

58. Adolph, K.W., Cheng, S.M., and Laemmli, U.K., Role of nonhistone proteins in metaphase chromosome structure. *Cell*, 1977. **12**: p. 805-816.

59. King, R., Jackson, P.K., and Kirschner, M.W., Mitosis in transition. *Cell*, 1994. **79**: p. 563-571.

60. Murray, A.W., Solomon, M.J., Kirschner, M.W., The role of cyclin synthesis and degradation in the control of MPF activity. *Nature*, 1989. **339**: p. 275-280.

61. Halleck, M.S., Reed, J.A., Lumley-Sapanski, K., Schlegel, R.A., Injected mitotic extracts induce condensation of interphase chromatin. *Exp.Cell Res.*, 1984. **153**: p. 561-569.

62. Gerhart, J., Wu, M., Kirschner, M., Cell cycle dynamics of an m-phase-specific cytoplasmic factor in Xenopus laevis oocytes and eggs. *J.Cell Biol.*, 1984. **98**: p. 1247-1255.

63. Masui, Y., Markert, C.L., Cytoplasmic control of nuclear behavior during meiotic maturation of frog oocytes. *J.Exp.Zool.*, 1971. **177**: p. 129-146.

64. Sunkara, P.S., Wright, D.A., Rao, P.N., Mitotic factors frrom mammaian cells: a preliminary study. *PNAS USA*, 1979. **76**: p. 2799-2802.

65. Gerace, L., and Blobel, G., The nuclear envelope lamina is reversibly depolymerized during mitosis. *Cell*, 1980. **19**: p. 277-287.

66. Heald, R., and McKeon, F., Mutations of phosphorylation sites in lamin A that prevent nuclear lamina disassembly in mitosis. *Cell*, 1990. **61**: p. 579-589.

67. Peter, M., Nakagawa, J., Doree, M., Labbe, J.C., and Nigg, E.A., In vitro disassembly of the nuclear lamina and M phase-specific phosphorylation of lamins by cdc2 kinase. *Cell*, 1990. **61**: p. 591-602.

68. Ward, G.E., Kirschner, M.W., Identification of cell cycle-regulated phosphorylation sites on nuclear lamin C. *Cell*, 1990. **61**: p. 561-577.

69. Gerace, L., and Burke, B., Functional organization of the nuclear envelope. *Ann. Rev. Cell Biol.*, 1988. **4**: p. 335-373.

70. Nigg, E.A., Assembly and dynamics of the nuclear lamina. *Sem. Cell Bio.*, 1992. **3**: p. 245-53.

71. Cance, W.G., Chaudhary, N., Worman, H.J., Blobel, G., and Cordon-Cardo, C., Expression of the nuclear lamins in normal and neoplastic human tissues. *J. Exp. Clin. Cancer Res.*, 1992. **11**: p. 233-246.

72. Doxsey, S.J., Stein, P., Evans, L., Calarco, P.D., and Kirschner, M., Pericentrin, a highly conserved centrosome protein involved in microtubule organization. *Cell*, 1994. **76**: p. 639-650.

73. Sambrook, J., Fritsch, E.F., and Maniatis, T., *Molecular Cloning: A Laboratory Manual* . 1989, Cold Spring Harbor, NY: Cold Spring Harbor Laboratory Press.

74. Taylor, G.R., *Polymerase chain reaction: basic principles and automation*, in *PCR, a practical approach*, M.J. McPherson Quirke, P., and Taylor, G.R., Editor^Editors. 1993, Oxford University Press: New York.

75. Pearson, W.R., Rapid and sensitive sequence comparison with FASTP and FASTA. *Meth. Enzymol.*, 1990. **183**: p. 63-98.

76. Lawrence, J.B., Singer, R.H., and McNeil, J.A., Interphase and metaphase resolution of different distances within the human dystrophin gene. *Science*, 1990. **249**: p. 928-932.

77. Harlow, E., and Lane, D., *Antibodies: A Laboratory Manual.* 1988, Cold Spring Harbor, New York: Cold Spring Harbor Laboratory Press.

78. Jostes, R.F., Bushnell, K.M., and Dewey, W.D., X-ray induction of 8-azaguanine-resistant mutants in synchronous Chinese Hamster Ovary cells. *Radiation Res.*, 1980. **83**: p. 146-161.

79. Borrelli, M.J., Mackey, M.A., and Dewey, W.C., A Method for freezing synchronous mitotic and G1 cells. *Exp. Cell Res.*, 1987. **170**: p. 363-368.

80. Zieve, G.W., Turnbull, D., Mullins, J.M., and McIntosh, J.R., Production of large numbers of mitotic mammalian cells by use of the reversible microtubule inhibitor nocodazole. *Exp. Cell Res.*, 1980. **126**: p. 397-405.

81. Laemmli, U.K., Cleavage of structural proteins during the assembly of the head of bacteriophage T4. *Nature*, 1970. **227**: p. 680-685.

82. Cherniack, A.D., Klarland, J.K., Conway, B.R., and Czech, M.P., Disassembly of son-of-sevenless proteins from Grb2 during p21ras desensitization by insulin. *J. Biol. Chem.*, 1995. **270**(4): p. 1485-8.

83. Sparks, C.A., Bangs, P.L., McNeil, G.P., Lawrence, J.B., and Fey, E.G., Assignment of the nuclear mitotic apparatus protein (NuMA) gene to human chromosome 11q13. *Genomics*, 1993. **17**: p. 222-224.

84. Harborth, J., Weber, K. and Osborn, M, Epitope mapping and direct visualization of the parallel, in-register arrangement of the double-stranded coiled-coil in the NuMA protein. *EMBO J.*, 1995. **14**: p. 2447-2460.

85. Parry, D.A.D., NuMA/Centrophilin: Sequence analysis of the coiled-coil rod domain. *Biophysical J.*, 1994. **67**: p. 1203-1206.

86. Bloomfield, C.D., Trent, J.M., and van der Berghe, Report of the committee on structural chromosome changes in neoplasia. *Cytogen. Cell Genet.*, 1987. **46**: p. 344-66.

87. Sutherland, G.R., and Mattei, J.F., Report of the committee on cytogenetic markers. *Cytogen. Cell Genet.*, 1987. **46**: p. 316-24.

88. Hinds, P.W., Dowdy, S.F., Eaton, E.N., Arnold, A., and Weinberg, R.A., Function of a human cyclin gene as an oncogene. *PNAS*, 1994. **91**: p. 709-13.

89. Marx, J., How cells cycle toward cancer. *Science*, 1994. **263**: p. 319-321.

90. Hardie, D.G., Campbell, D.G., Caudwell, F.B., and Haystead, T.A., *Analysis of sites phosphorylated in vivo and in vitro*, in *Protein phosphorylation*, D.R.a.B.D. Hames, Editor^Editors. 1993, Oxford press: New York. p. 62.

91. Wintrobe, M.M., Lee, G.R., Boggs, D.R., Bithell, T.C., Foerster, J., Athens, J.W., and Lukens, J.N., *Clinical Hematology*, . 1981, Lea and Febiger: Philadelphia. p. 35-74.

92. Collins, S.J., Ruscetti, F.W., Ruscetti, R.E., Gallager, R., and Gallo, R.C., Terminall differentiation of human premyelocytic leukemia cells induced by dimethyl sulfoxide and other polar compounds. *PNAS*, 1978. **755**: p. 2458-2462.

93. Kempf, T., Bischoff, F.R., Kalies, I., and Posting, H, Isolation of human NuMA protein. *FEBS Lett.*, 1994. **354**: p. 307-310.

94. Cooper, J.A., *Estimation of phosphorylation stoichiometry by separation of phosphorylated isoforms*, in *Meth. in Enzymology*, S. Hunter T. B.M., Editor^Editors. 1991, Academic Press, Inc.: San Diego, CA. p. 251-260.

95. Buchkovich, K., Duffy, L., and Harlow, E., The retinoblastoma protein in phosphorylated during specific phases of the cell cycle. *Cell*, 1989. **58**: p. 1097-1105.

96. Luderus, M.E., den Blaauwen, J.L., de Smit, O., Compton, D.A., and van Driel, R., Binding of matrix attachment regions to lamin polymers involves single-stranded regions and the minor groove. *Mol. Cell. Biol.*, 1994. **14**: p. 6297-6305.

97. Getzenberg, R.H., Pienta, K.J., Ward, W.S., amd Coffey, D.S., Nuclear structure and the three-dimensional organization of DNA. *J. Cell. Biochem.*, 1991. **47**: p. 289-299.

98. Phi-van, L., von Kries, J.P., Ostertag, W., and Stratling, W.H., The chicken lysozyme 5' matrix attachment region increases transcription from a heterologous promoter in heterologous cells and dampens position effects on the expression of transfected genes. *Mol. Cell. Biol.*, 1990. **10**: p. 2302-2307.

99. Evans, R., Cyclic AMP-dependent protein kinase-induced vimentin disassembly involves modification of the n-terminal domain of intermediate filament subunits. *FEBS Lett.*, 1988. **234**: p. 73-78.

100. Pasternak, C., Flicker, P.F., Ravid, S., and Spudich, J.A., Intermolecular verses intramolecular interactions of Dictostelium myosin: possible regulation by heavy chain phosphorylation. *J. Cell Biol.*, 1989. **109**: p. 203-210.

101. Inagaki, M., Gonda, Y., Matsuyama, M., Nishizawa,K., Nishi, Y., and Sato, C., Intermediate filament reconstitution in vitro: the role of phosphorylation on the assembly-disassembly of desmin. *J. Biol. Chem.*, 1988. **263**: p. 5970-5978.

102. Holm, C., Goto, T., Wang, J.C., and Botstein, D., DNA topoisomerase II is required at the time of mitosis in yeast. *Cell*, 1985. **41**: p. 553-563.

103. Uemura, T., Ohkura, H., Adachi, Y., Morino, K., Shiozaki, K., and Yanagida, M., DNA topoisomerase II is required for condensation and separation of mitotic chromosomes in S. pombe. *Cell*, 1987. **50**: p. 917-925.

104. Uemura, T., and Yanagida, M., Isolation of type I and II DNA topoisomerase mutants from fission yeast: single and double mutants show different phenotypes in cell growth and chromatin organization. *EMBO J.*, 1984. **3**: p. 1737-1744.

105. DiNardo, S., Voelkel, K., and Sternglanz, R., DNA topoisomerase II mutant of Saccharomyces cerevisiae: topoisomerase II is required for segregation of daughter molecules at the termination of DNA replication. *Proc. Natl. Acad. Sci. USA*, 1984. **81**: p. 2616-2620.

106. Mitchison, T., and Kirschner,M., Microtubule assembly nucleated by isolated centrosomes. *Nature*, 1984. **312**: p. 232-237.

107. Stearns, T., The form and the substance. *Nature Medicine*, 1995. **1**: p. 19-52.